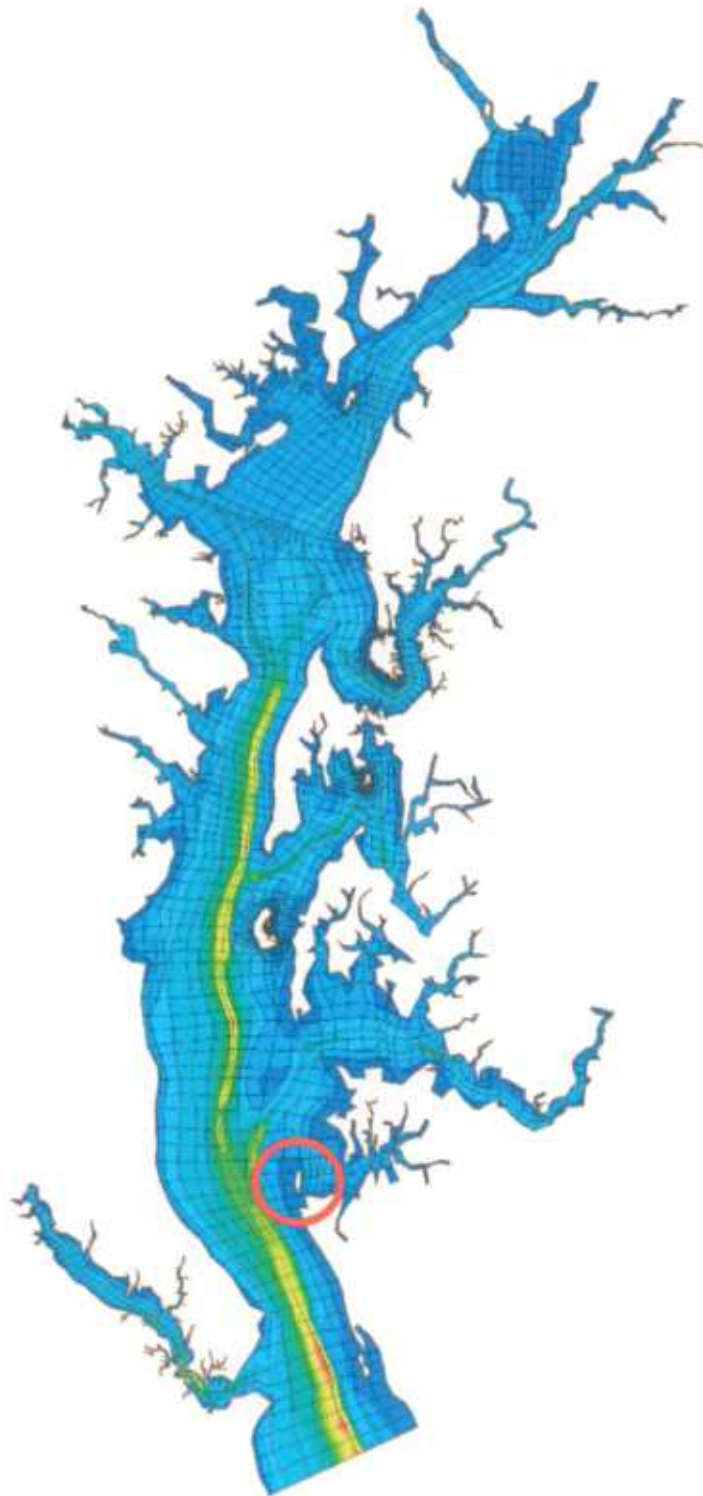# JAMES ISLAND RECONNAISSANCE STUDY

HYDRODYNAMICS AND SEDIMENTATION MODELING

FINAL REPORT
NOVEMBER 15, 2002

Maryland Port Administration
MPA Contract Number: 500912
MPA Pin Number: 600105-P

Maryland Environmental Services
MES Contract Number: 02-07-49

Prepared by

Moffatt & Nichol Engineers
2700 Lighthouse Point East
Suite 501
Baltimore, MD 21224

EXECUTIVE SUMMARY

The purpose of this Hydrodynamics and Sedimentation Modeling Reconnaissance Study is to evaluate the projected impacts due to construction of a Beneficial Use Habitat Restoration Site at James Island. Moffatt & Nichol Engineers' (MNE) Upper Chesapeake Bay – Finite Element Model (UCB-FEM) (MNE, 2000) was used to predict existing conditions and with- and without-project hydrodynamics and sedimentation. This report summarizes the calibration and implementation of the UCB-FEM two-dimensional numerical model of the Chesapeake Bay and evaluation of hydrodynamic and sedimentation output including time-varying flow velocity, water surface elevations, and patterns of erosion and accretion.

A summary of site conditions that are relevant to the project is provided below:

- **Bathymetry and Topography.** Water depths in the area where the dikes would be located range from –2 to –12 ft Mean Lower Low Water (MLLW), with an average depth along the exterior dikes ranging from –3 to –12 MLLW. Water depths in the deeper main stem portions of the Bay west of James Island are as great as –93 ft MLLW.

- **Freshwater Inflow.** The drainage area of the Chesapeake Bay is approximately 64,000 square miles and includes portions of Maryland, Virginia, West Virginia, Pennsylvania, New York and the District of Columbia. Freshwater enters the Chesapeake Bay via approximately 150 major rivers and streams at approximately 80,000 cubic ft per second (Schubel and Pritchard, 1987).

- **Tides.** Water levels in the Chesapeake Bay are dominated by a semidiurnal lunar tide. Tides enter the Bay via the Chesapeake Bay entrance and the Chesapeake and Delaware (C&D) Canal. The mean range of tides throughout the entire Chesapeake Bay is generally 1 to 3 ft (NOS, 1988). In the project vicinity, the mean tide level is 0.9 ft above MLLW; the mean tidal range is 1.3 ft and the spring tidal range is 1.8 ft (NOS 1997).

- **Currents.** In the project vicinity, approximately 2.5 miles west of James Island, peak flood currents are about 1.0 ft/sec, and peak ebb currents are about 0.8 ft/sec (NOS,

1996). Currents are not considered important for shore protection design at this project site.

- **Wind and Wave Conditions.** Design winds for the site were developed on the basis of data collected at Baltimore-Washington International (BWI) airport. These winds, which can exceed 90 miles per hour during a 100-year storm event, were used to develop design wave conditions. James Island is exposed to wind-generated waves approaching from all directions.

- **Site Soil Characteristics.** Results of the separate geotechnical preliminary study indicate that the underlying soil consists of silty sand, suitable for supporting the dike. Areas with soft silty clays at the mud line, however, would need to be undercut and backfilled with sand.

The numerical modeling system used in this study consists of the US Army Corps of Engineers finite element hydrodynamics (RMA-2) and sedimentation (SED-2D) models – collectively known as TABS-2 (Thomas, McAnally and Ademac, 1985). The numerical modeling system uses a bathymetric mesh of water depths, represented by nodes located in the horizontal plane that are interconnected to create elements.

Correlation of the hydrodynamic model calibration results to NOAA predicted data for tidal elevations and current velocities is generally better than 90%. Predicted percent error is typically less than 10% for tidal elevations and less than 15% for current velocity.

The non-cohesive sediment model was run using 0.1mm (.004 inch) sediment under no-wind conditions. Analysis of results shows negligible sand transport due to tidal currents. Modeled non-cohesive sediment transport for existing conditions is negligible for 4- and 13-mph winds for all directions. Sixteen-mph winds, when taken cumulatively with lower wind speeds, account for nearly 90% of the yearly wind occurrences and cause significant sediment transport for winds from the NNW and SSE directions with less sediment transport for winds from other directions.

The cohesive sediment model was run for a 6-month simulation period at which point the model achieved a dynamic equilibrium (average values and rates remain steady over time). The cohesive sediment model was then run for each of 16 wind directions for wind speeds of 4- and

13-mph.

Hydrodynamics and sedimentation numerical modeling for the James Island Reconnaissance Study show minimal impacts on local tidal elevations, which are essentially unchanged. Current velocities are impacted following island construction, with maximum increase or decrease in current velocity of about 0.4 ft/sec. Construction at James Island also would have beneficial effects on sedimentation rates and patterns, with less erosion of the James Island shoreline and the shallow areas surrounding the remnant James Islands. Some protection would also be afforded to the shoreline of Taylors Island from wind and waves coming from the N, NNW, and NW directions. This reduction in erosion would likely cause reduced suspended sediment and improved water quality.

TABLE OF CONTENTS

MOFFATT & NICHOL
E N G I N E E R S

LIST OF TABLES

LIST OF FIGURES

ACRONYMS AND SYMBOLS

CDF	–	Confined Disposal Facility
DEM	–	Digital Elevation Map
E	–	Erosion rate constant
H_s	–	Nearshore Significant Wave Height
MCY	–	Million Cubic Yards
Mi	–	Statute Mile (5,280 Feet)
MLLW	–	Mean Lower Low Water
MPH	–	Miles Per Hour
NGVD	–	National Geodetic Vertical Datum
Nmi	–	Nautical Mile (6,076 Feet)
NCDC	–	National Climatic Data Center
NOS	–	National Ocean Service
NOAA	–	National Oceanic and Atmospheric Administration
ρ	–	Bulk Density
RMA-2	–	Hydrodynamic Model (by United States Army Corps of Engineers)
RMS	–	Root Mean Square
SED-2D	–	Sediment Transport Model (by United States Army Corps of Engineers)
SPM	–	Shore Protection Manual
T_p	–	Peak Spectral Wave Period
τ_{cd}	–	Critical Shear Stresses of Deposition
τ_{ce}	–	Critical Shear Stresses of Erosion
UCB-FEM	–	Upper Chesapeake Bay Finite Element Model (by Moffatt & Nichol Engineers)
USACE	–	United States Army Corps of Engineers
USGS	–	United States Geological Survey
w_s	–	Settling Velocity
WES	–	Waterways Experiment Station (of the United States Army Corps of Engineers)

1. INTRODUCTION

1.1   STUDY PURPOSE AND OBJECTIVES

The purpose of this Hydrodynamics and Sedimentation Numerical Modeling Reconnaissance Study report is to analyze the projected impacts due to construction of a Beneficial Use and Habitat Restoration Site at James Island as regards hydrodynamics and sedimentation in the site vicinity. Moffatt & Nichol Engineers' (MNE) Upper Chesapeake Bay – Finite Element Model (UCB-FEM) (MNE, 2000) was modified to include James Island and used to predict with- and without-project hydrodynamics and sedimentation.

Study objectives include the following:

> ➢ Comparison of with- and without-project tidal elevations

> ➢ Comparison of with- and without-project current velocities

> ➢ Comparison of with- and without-project relative sedimentation rates and patterns for non-cohesive and cohesive sediments

The proposed five alignments are compared to existing conditions, both graphically and numerically, to determine both specific and relative impacts.

1.2   PROJECT SCOPE

James Island is being studied as a potential site for beneficial use of dredged material. Benefits of this project include:

> ➢ Protection of the remnant James Island and Taylors Island shorelines from additional erosion

> ➢ Protection of the shallow water surrounding James Island to provide improved water quality and subsequently promote the re-establishment of subaquatic vegetation

---

MOFFATT & NICHOL ENGINEERS

To accomplish these objectives, the project consists of the construction of armored dikes that would serve to contain clean sediments dredged from the Baltimore Harbor approach channels located within the Chesapeake Bay.

1.3   STUDY DESCRIPTION

This report summarizes the calibration and implementation of a two-dimensional numerical model of the Chesapeake Bay to evaluate the impacts of construction at the James Island Restoration Site on tidal elevations, current velocity conditions, and sedimentation patterns.

The existing UCB-FEM model was modified to provide additional detail near James Island and was re-calibrated with published data, including astronomical tidal information, tidal current velocity information, and streamflow discharge for existing conditions. The calibrated model was used to compare hydrodynamic and sedimentation conditions within the model domain for the proposed construction alignment.

The UCB-FEM model was developed based on the following U.S. Army Corps of Engineers (USACE) numerical models:

> RMA-2: A depth-averaged finite element model for the simulation of velocities and water elevations for river systems, estuaries and other shallow water bodies. The model can be applied in either a one- or two-dimensional mode.

> SED-2D: A two-dimensional flow model for sediment transport related to unsteady flows. The model is based on the solution of the depth-averaged convection-diffusion equations of sediment with bed source terms. SED-2D is capable of modeling cohesive and non-cohesive sediment transport.

Assumptions critical to these numerical modeling efforts include:

> Calibration and application of the UCB-FEM hydrodynamic model was performed based on available data for normal tide and freshwater discharge conditions for existing conditions.

> Hydrodynamic conditions are analyzed to ascertain potential changes arising from

construction of the James Island project.

➤ Sedimentation modeling was performed to estimate the change in bay sedimentation and scouring patterns and relative rates if the James Island project was constructed.

➤ All results are subject to limitations of existing data, modeling capabilities and existing information regarding environmental resources and historical records. Hence, results depicted herein may be subject to modification in any additional future study stages as additional information is made available.

UCB-FEM hydrodynamic output includes time-varying flow velocity and water surface elevation fields. The UCB-FEM model also evaluates and predicts areas where erosion and accretion are likely to occur.

2.   PROJECT SITE PHYSICAL CONDITIONS

2.1   GENERAL

James Island is located in the Chesapeake Bay at the mouth of the Little Choptank River. It is located in Dorchester County at approximately 38° 31' N latitude and 76° 20' W longitude (Maryland State Plane Coordinates N 310,000 E 1,503,000) as shown in Figure 2-1. Figure 2-2 is an aerial photograph of James Island taken in August 2002. Figure 2-3 shows the proposed five alignments for James Island.

Site conditions germane to project design include bathymetry and topography, water levels, currents, wind and wave conditions, and site soil characteristics. A discussion of each of these factors is presented in the following paragraphs.

2.2   BATHYMETRY AND TOPOGRAPHY

The Chesapeake Bay is the largest estuary in the United States, extending over 200 miles from its seaward end at Cape Charles and Cape Henry in Virginia to the mouth of the Susquehanna River at Havre de Grace, Maryland. The Chesapeake Bay (including tributaries) has a surface area of approximately 4,500 square miles. Water depths in the Bay, including all of its tidal tributaries, average approximately 21 feet (ft) with a few deep troughs reaching a maximum depth of 174 ft (Schubel and Pritchard, 1987).

Chesapeake Bay bathymetric data was obtained from the National Ocean Service (NOS) Digital Elevation Models (NOS, 2000) and Charts 12230, 12263, 12264, 12266, 12268, 12270, 12272, 12273, 12274, and 12278. Vertical and horizontal data in this report are referenced to mean lower low water (MLLW) based on the 1960 to 1978 tidal epoch, and the Maryland State Plane, North American Datum 1983, respectively.

The bathymetry surrounding James Island is shown in Figure 2-3. Water depths within the project vicinity vary from -2 ft to -12 ft MLLW; maximum water depths in which the new containment dikes would be constructed is -12 ft MLLW. Water depths approximately one mile west of James Island are as great as -93 ft MLLW.

MOFFATT & NICHOL
E N G I N E E R S

2.3   FRESHWATER INFLOW

The drainage area of the Chesapeake Bay is approximately 64,000 square miles and includes portions of Maryland, Virginia, West Virginia, Pennsylvania, New York and the District of Columbia. Freshwater enters the Chesapeake Bay via approximately one-hundred and fifty major rivers and streams at approximately 80,000 cubic ft per second (Schubel and Pritchard, 1987). The primary rivers within the Chesapeake Bay drainage basin are the Susquehanna, Chester, Severn, Choptank, Patuxent, Nanticoke, Potomac, Rappahannock, York, and James Rivers. The Susquehanna River provides approximately 48.2% of the total freshwater inflow into the bay. Additional rivers on the western shore of the Bay, which contribute significant flows are the Potomac, James, Rappahannock, York, and Patuxent, contributing 13.6%, 12.5%, 3.1% 3.0% and 1.2%, respectively. Two significant sources of freshwater flow on the eastern shore of Maryland and Virginia are the Choptank (1.2%) and Nanticoke (1.1%) Rivers (Schubel and Pritchard, 1987).

2.4   TIDES

Water levels in the Chesapeake Bay are dominated by a semidiurnal lunar tide. Tides enter the Bay via the Chesapeake Bay Entrance and the Chesapeake and Delaware (C&D) Canal. The Bay is sufficiently long to contain one complete wavelength of the semidiurnal tide (NOS, 1988). The combination of tides and freshwater inflow creates a spring tide approximately 30-40% larger than mean tide and a neap tide approximately 30-40% smaller than the mean tide (Schubel and Pritchard, 1987).

The mean range of tides throughout the entire Chesapeake Bay is generally 1 to 3 ft (NOS, 1988). Tides are amplified in some tributaries as the tide progresses from the mouth of the tributary to the limit of the tide.

Average and spring tidal ranges, as published by NOS for the Bay north of the Potomac River (NOS Chart Nos. 12263, 12266, 12268, 12270, 12272), are listed in Table 2-1.

Table 2-1: Chesapeake Bay Tidal Ranges		
Location	**Mean Tidal Range (ft)**	**Spring Tidal Range (ft)**
Main Chesapeake Bay		
Cove Point	1.3	2.0
Bloody Point Bar Light	1.3	1.6
Pooles Island	1.2	1.8
Sevenfoot Knoll Light	0.9	1.3
Western Chesapeake Bay		
Fairhaven, Herring Bay	0.9	1.3
Thomas Point Shoal Light	0.9	1.4
Annapolis	0.9	1.4
Sandy Point	0.8	1.2
Baltimore (Ft. McHenry)	1.2	1.7
Pond Point	1.4	2.1
Choptank River		
Cambridge	1.7	2.4
Chesapeake Beach	1.0	1.5
Eastern Bay		
St. Michaels, Miles River	1.2	1.8
Kent Island Narrows	1.2	1.8
Chester River		
Love Point	1.2	1.7
Queenstown	1.3	2.0
Cliffs Wharf	1.5	2.2
Chestertown	1.8	2.7
Sassafras River		
Betterton	1.6	2.4
C & D Canal		
Chesapeake City	2.8	2.9
Susquehanna River		
Havre de Grace	1.8	2.6

Average tides range from 0.8 ft in various locations on the western shore to 2.8 ft in the C & D Canal. Spring tides (tides occurring at or near the time of new or full moon which rise highest and fall lowest from the mean sea level) range from 1.3 ft at Fairhaven on Herring Bay to 2.9 ft in the C & D Canal. Near James Island, mean tide range is approximately 1.3 ft (NOS, 1996).

Additionally, tides in the Chesapeake Bay are influenced by Coriolis forces (momentum forces due to the rotation of the Earth). Browne and Fisher (NOS, 1988) found a significant west to east tide range differential due to Coriolis forces throughout the bay with peak differences of 1.0 foot in the region between Smith Point (1 foot range, western shore) and Tangier Sound (2 foot range, eastern shore).

2.5   CURRENTS

Currents in the Chesapeake Bay are tidally driven and range in values up to a maximum velocity of over 3 ft/sec near the Bay entrance (NOS, 1988). Peak current velocities in the Bay north of Kent Island approach 1.5 ft/sec and average 1.2 ft/sec. Phasing of current velocity is influenced by bottom friction. Browne and Fisher (NOS, 1988) determined that during a given tidal cycle the peak current velocity occurs first in the center of the bay over the deepest channels, whereas peak velocity occurs later closer to shore in shallower water.

In the project vicinity, approximately 2.5 miles west of James Island, peak tidal current velocities are approximately 1.0 ft/sec for flood currents and 0.8 ft/sec for ebb currents (NOS, 1996).

2.6   WIND AND WAVE CONDITIONS

The frictional force of air on water as wind blows generates waves. Higher winds, deeper water, and longer distances over which the wind travels result in larger waves. Wind and wave conditions representative of the James Island vicinity are discussed in the following paragraphs.

2.6.1   Wind Conditions

Average annual wind speeds at James Island are represented by the wind rose shown in Figure 2-4. The wind rose represents percent occurrence of wind speeds and directions at Baltimore-Washington International (BWI) Airport as reported by the National Oceanic and Atmospheric Administration (NOAA), National Climatic Data Center (NOS, 1982 and NCDC, 1994). Table 2-2 shows the data used to generate the wind rose.

In Table 2-2, 0 to 3 mph winds are considered "calm" with indeterminate direction, resulting in these winds being grouped together for all directions. On average, nearly 90% of the yearly

wind occurrences are less than 16 mph and only 1-2% of wind occurrences are greater than 25 mph.

Table 2-2: Wind Speed (% Occurrence) By Direction for BWI Airport, 1951-1982							
Direction	0-3 MPH	4-13 MPH	13-16 MPH	16-19 MPH	19-25 MPH	25-32 MPH	>32 MPH
N		3.6	0.6	0.3	0.1	0	0
NNE		2.1	0.4	0.2	0.1	0	0
NE		3.3	0.5	0.2	0.1	0	0
ENE		3.3	0.6	0.3	0.1	0	0
E		4.3	0.5	0.2	0	0	0
ESE		2.3	0.2	0.1	0	0	0
SE		3.1	0.4	0.2	0.1	0	0
SSE		3.2	0.5	0.2	0.1	0	0
S		5.2	0.6	0.3	0.1	0	0
SSW		3.5	0.7	0.3	0.2	0	0
SW		4.7	0.8	0.4	0.2	0	0
WSW		4.7	0.6	0.3	0.1	0	0
W		9.4	1.4	1.0	0.7	0.2	0
WNW		5.9	1.8	1.5	1.3	0.4	0
NW		4.4	1.6	1.2	0.7	0.2	0
NNW		3.0	0.8	0.5	0.2	0	0
ALL	10.2						

Annual extreme wind speed data from the NOAA, NCDC for BWI Airport for the period 1951 through 1982 (NOS, 1982 and NCDC, 1994) are presented in Table 2-3 as fastest mile winds. Fastest mile winds are defined as the highest recorded wind speeds that last long enough to travel one mile during a 24-hour recording period. For example, a fastest mile wind speed of 60 miles per hour would have a duration of 60 seconds, a fastest mile wind speed of 50 miles per hour would have a duration of 72 seconds, etc.

Table 2-3: Annual Extreme Wind Speed (mph) Per Direction for BWI Airport, 1951-1982								
Year	North	Northeast	East	Southeast	South	Southwest	West	Northwest
1951	24	41	27	34	39	29	42	46
1952	66	25	47	66	41	66	46	43
1953	20	28	22	27	34	39	47	43
1954	31	27	22	60	28	39	57	44
1955	21	43	29	28	43	53	40	43
1956	29	34	25	24	28	34	56	40
1957	29	53	35	33	33	30	46	46
1958	30	52	25	33	37	43	40	43
1959	28	26	20	27	23	38	46	43
1960	26	38	28	27	25	35	40	53
1961	45	28	28	29	24	70	41	54
1962	56	41	28	17	25	36	42	61
1963	38	32	18	34	25	28	44	60
1964	34	31	23	24	47	23	48	61
1965	36	26	28	34	36	54	44	44
1966	32	25	29	24	47	43	50	48
1967	30	29	25	39	27	46	53	43
1968	45	30	36	26	19	45	48	50
1969	28	21	20	34	26	45	45	53
1970	28	28	18	21	39	34	48	60
1971	31	45	26	18	21	41	39	58
1972	28	25	35	26	20	41	41	41
1973	40	26	26	38	26	35	49	33
1974	32	23	46	29	33	33	45	41
1975	40	26	21	24	25	38	54	45
1976	31	18	20	28	32	28	45	54
1977	32	31	19	28	26	25	49	48
1978	39	28	36	28	19	52	33	45
1979	32	25	27	36	32	32	45	47
1980	33	27	18	32	20	32	45	50
1981	24	24	19	26	23	28	41	42
1982	31	20	23	23	29	34	40	48

Note: Data adjusted to 10 meter height.

2.6.2 Wave Conditions

James Island is exposed to wind-generated waves approaching from all directions. In accordance with procedures recommended by the USACE, Shore Protection Manual (SPM) (USACE, 1984),

a radially averaged fetch distance was computed for the eight directions, namely N, NE, E, SE, S, SW, W and NW. The radially averaged fetch distances for these directions are shown in Table 2-4 and Figure 2-5.

Table 2-4: Radial Fetch Distance and Mean Water Depth at James Island		
Direction	Mean Distance (Miles)	Mean Water Depth (ft, MLLW)
North	26.9	34.2
Northeast	5.3	9.6
East	5.3	12.2
Southeast	2.4	3.7
South	29.5	43.1
Southwest	6.9	39.8
West	8.3	35.4
Northwest	8.0	28.5

Wave conditions were hindcast along each fetch direction for the design winds presented in Table 2-3 (adjusted appropriately for duration) and the mean water depths along the fetch directions as shown in Table 2-4 using methods published in the SPM (1984). Wave hindcast results are presented in Figure 2-6 (Significant Wave Height, H_s) and Figure 2-7 (Peak Wave Period, T_p). These figures present a summary of H_s and T_p showing the directions from which the highest waves and longest periods approach the site.

2.7 SITE SOIL CHARACTERISTICS

An evaluation of the soil characteristics at the project site was performed by Engineering

Consultation Construction Remediation, Inc. (E2CR, 2002). The evaluation included performing soil borings, preparing soil boring profiles, identifying soil strata thickness, location and characteristics, and conducting a preliminary slope stability analysis. Results of the preliminary study indicate that the underlying soil consists of silty sand suitable for supporting a dike. Areas with soft silty clays at the mud line, however, would need to be undercut and backfilled with sand.
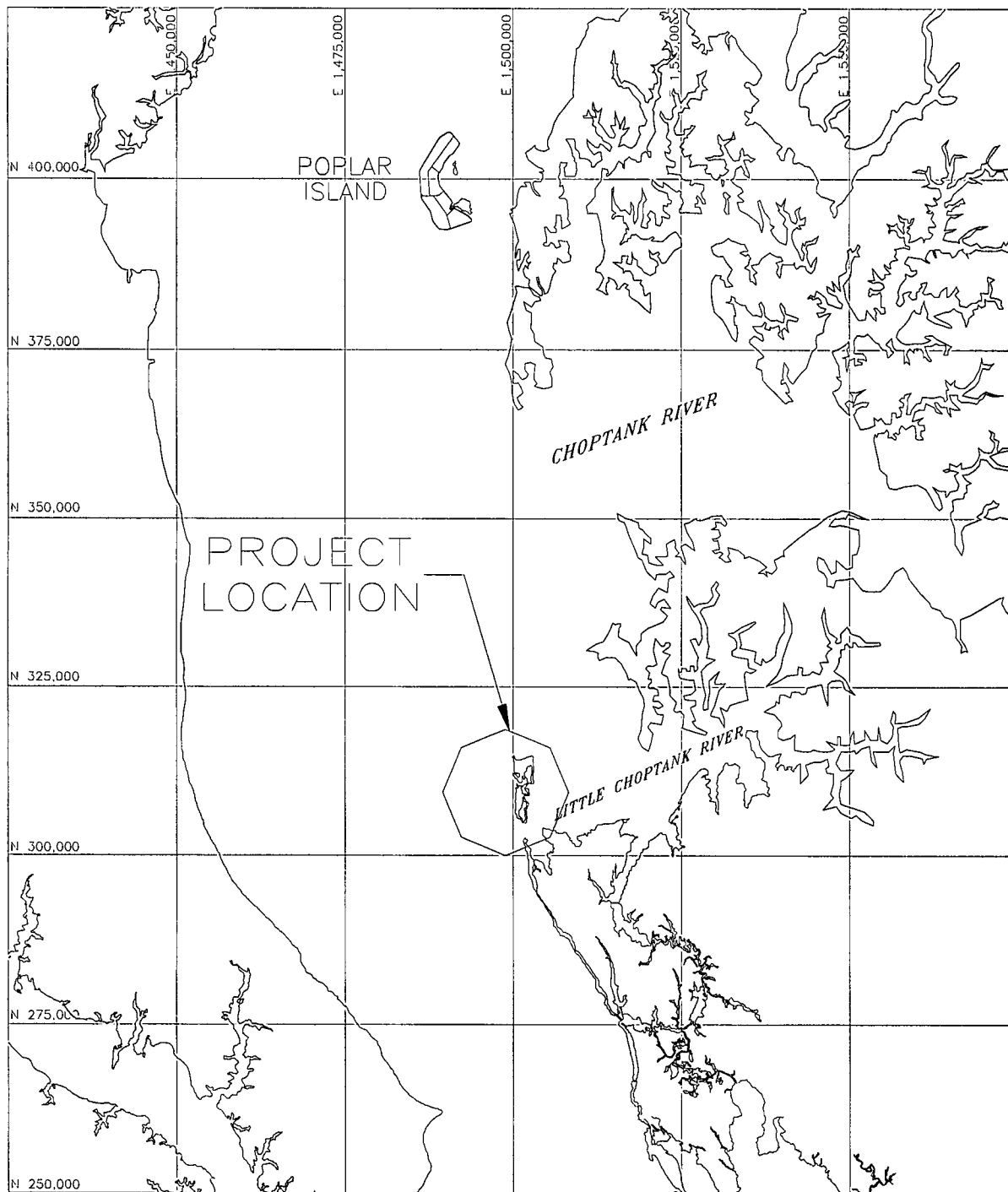
Figure 2-1:   James Island Location Map

Figure 2-2:   James Island August 2002 Aerial Photograph Looking Southeast
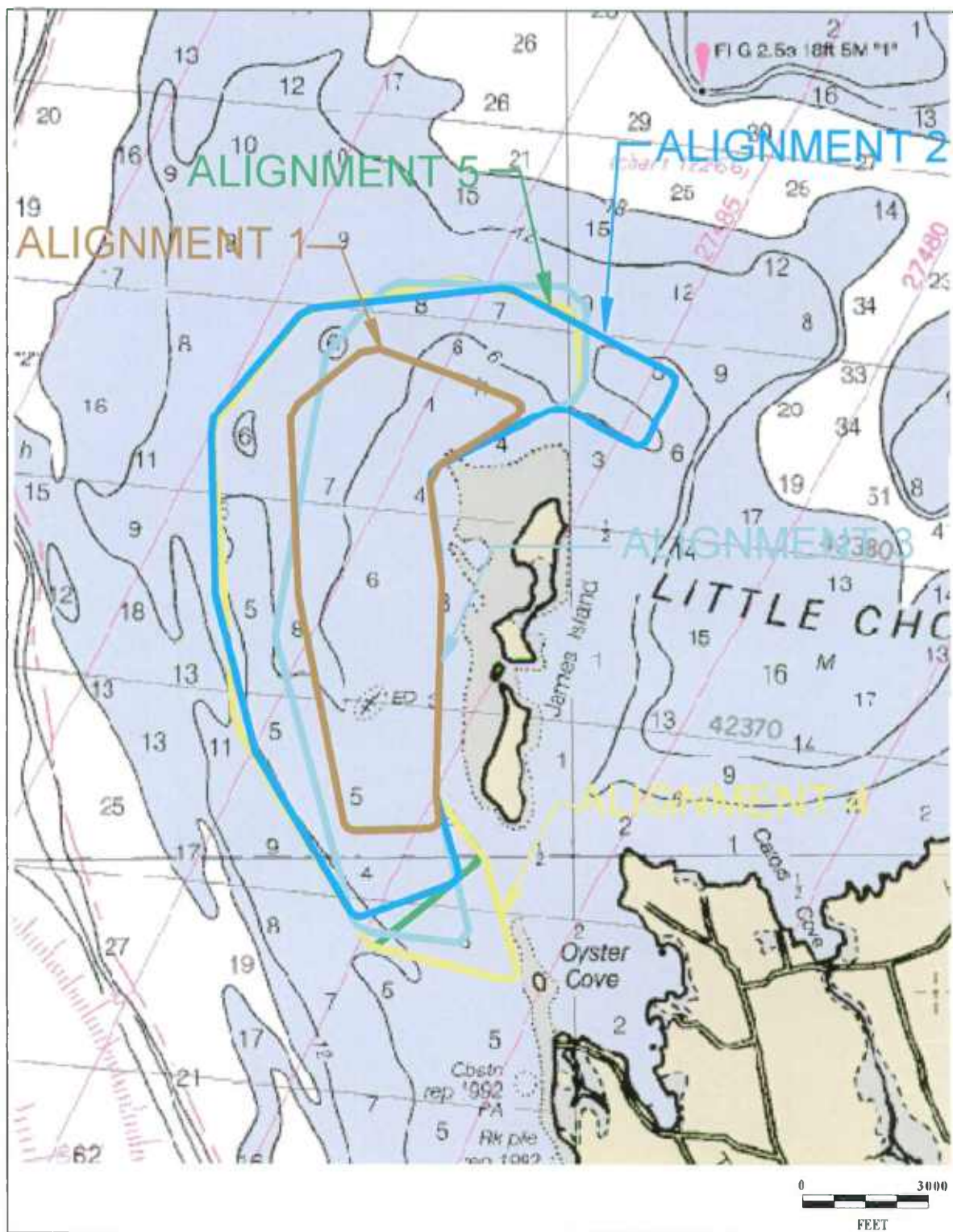
Figure 2-3:   James Island Five Alignments and Surrounding Bathymetry
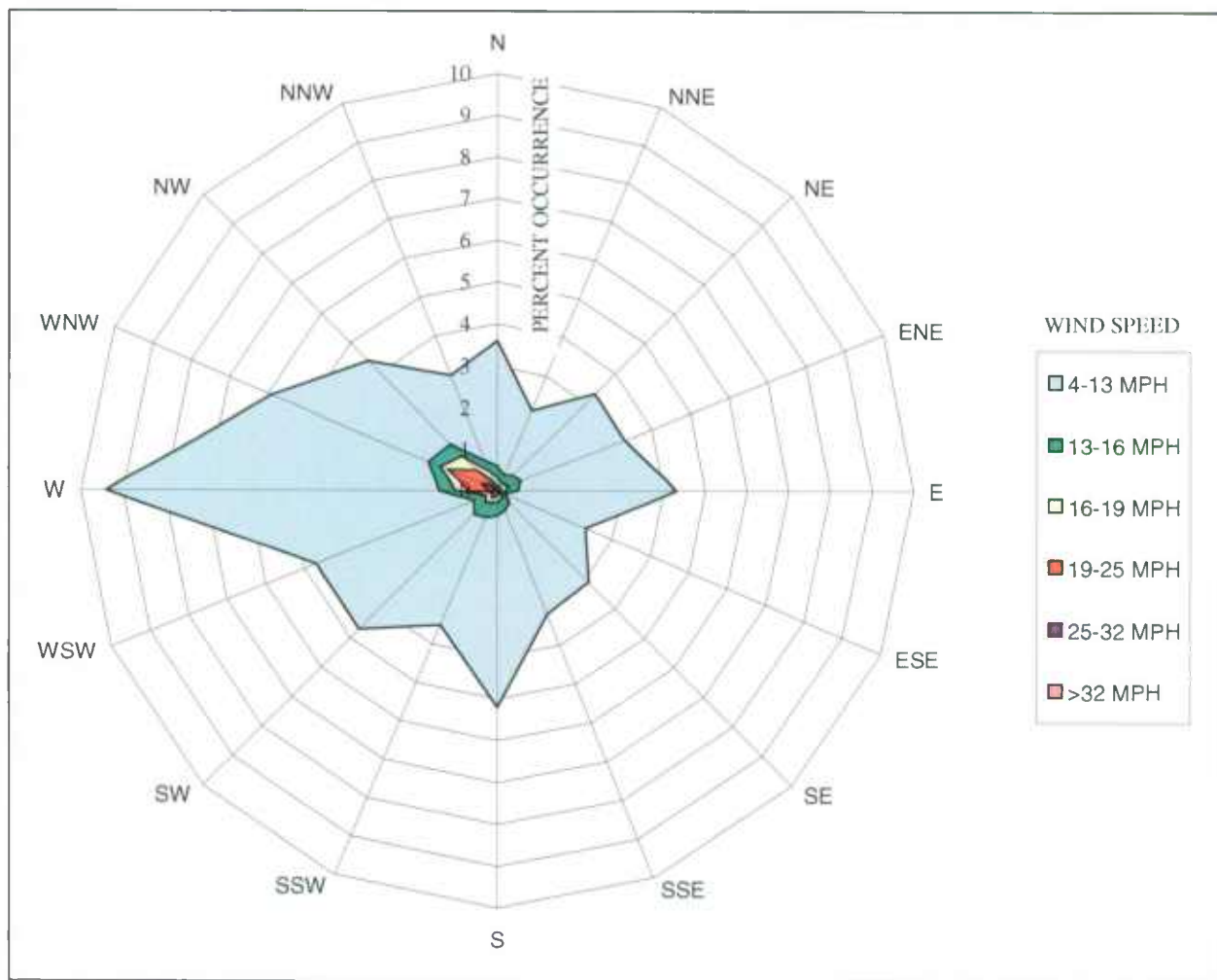
Figure 2-4:   Baltimore-Washington International Airport (BWI) Wind Rose
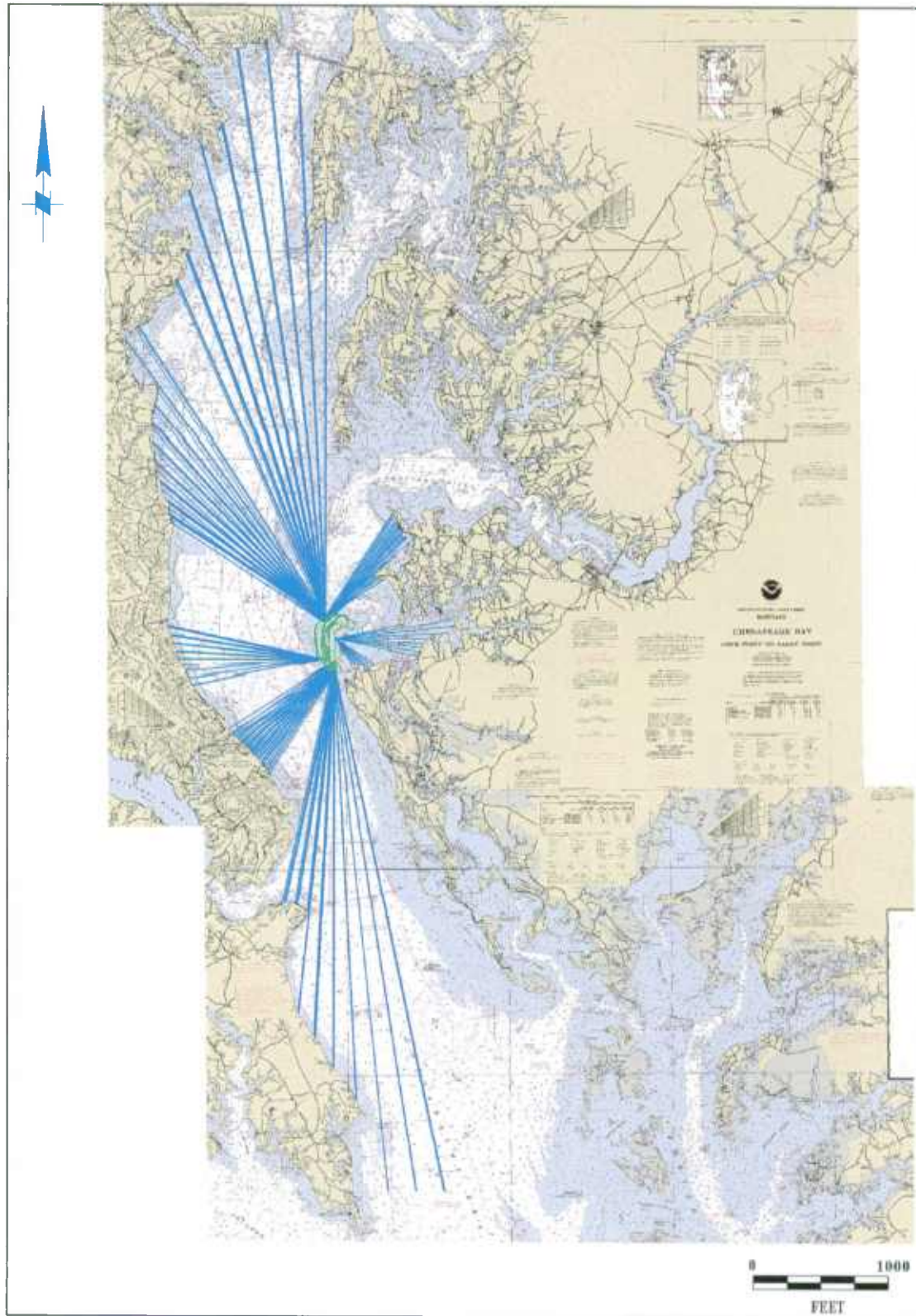
Figure 2-5:   James Island Radially-Averaged Fetch Distances
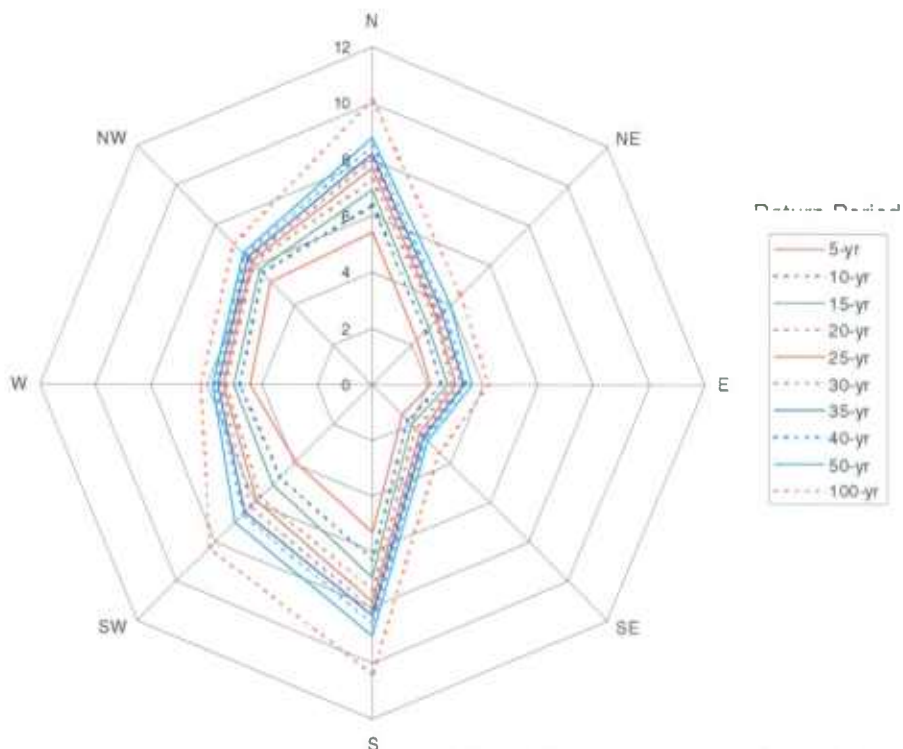
Figure 2-6:   **Offshore Significant Wave Heights (ft) for James Island**
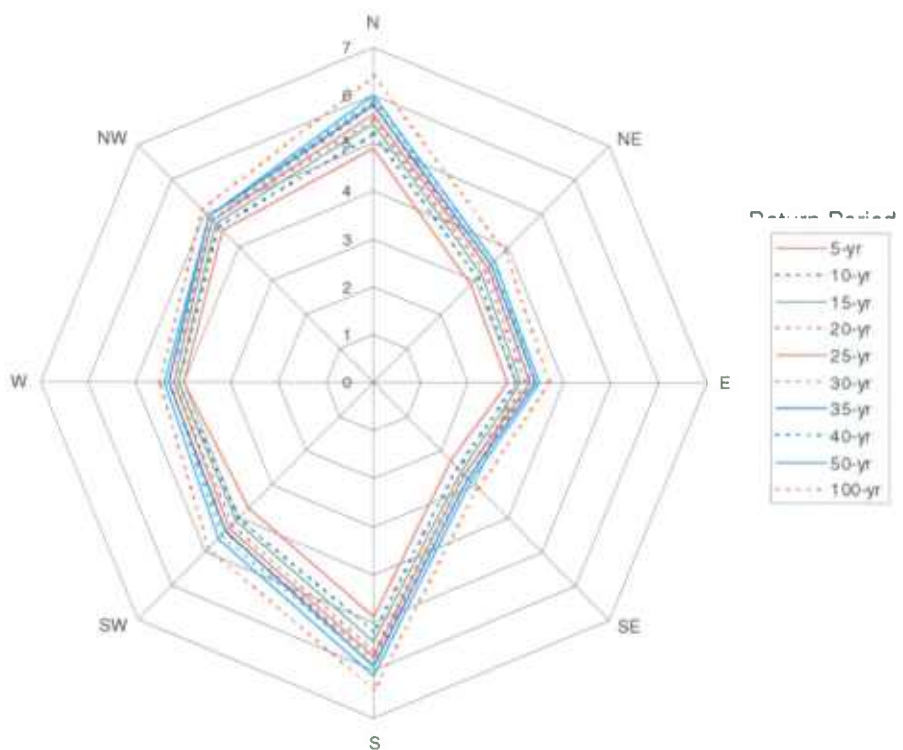
Figure 2-7:   **Peak Spectral Wave Periods (sec) for James Island**

3. SIMULATION MODELS

3.1 GENERAL

The numerical modeling system used in this study is the USACE, Waterways Experiment Station (WES) finite element hydrodynamics (RMA-2) and sedimentation (SED-2D) models – collectively known as TABS-2 (Thomas et al., 1985). TABS-2 is a collection of generalized computer programs and pre- and post-processor utility codes integrated into a numerical modeling system for studying two-dimensional depth-averaged hydrodynamics, constituent transport, and sedimentation problems in rivers, reservoirs, bays, and estuaries. The finite element method provides a means of obtaining an approximate solution to a system of governing equations by dividing the area of interest into smaller sub-areas called elements.

Time-varying partial differential equations are transformed into finite element form and then solved in a global matrix system for the modeled area of interest. The solution is smooth across each element and continuous over the computational area. This modeling system is capable of simulating wetting and drying of marsh and intertidal areas of the estuarine system.

A schematic representation of the system is shown in Figure 3-1. It can be used either as a stand-alone solution technique or as a step in the hybrid modeling approach. The model calculates water surface elevations, current patterns, constituent transport, sediment erosion and deposition, the resulting bed surface elevations, and the feedback to hydraulics. Existing conditions can be analyzed to determine the impacts of project construction at James Island on flow circulation and sedimentation. All models are depth-averaged and are solved by the finite element method using Galerkin weighted residuals.
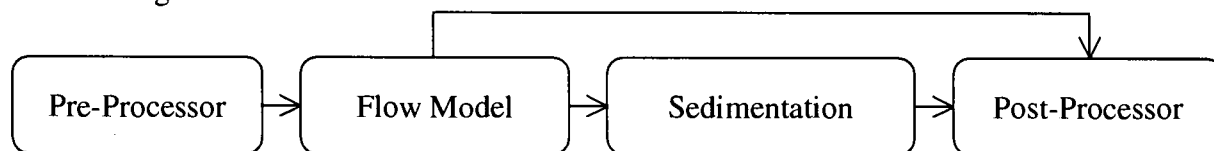
Figure 3-1: TABS-2 Schematic

3.2   HYDRODYNAMIC MODEL

RMA-2 is a two-dimensional, depth-averaged, finite element, hydrodynamic numerical model. It computes water surface elevations and horizontal velocity components for subcritical, free-surface flow in two dimensional flow fields. RMA-2 computes a finite element solution of the Reynolds form of the Navier-Stokes equations for turbulent flows. Friction is calculated with the Manning's or Chezy equation, and eddy viscosity coefficients are used to define turbulence characteristics. The equations also account for Coriolis forces and surface wind stresses. Both steady and unsteady state (dynamic) problems can be analyzed. The general governing equations are:

$$h\frac{\partial u}{\partial t} + hu\frac{\partial u}{\partial x} + hv\frac{\partial u}{\partial y} - \frac{h}{\rho}\left(E_{xx}\frac{\partial^2 u}{\partial x^2} + E_{xy}\frac{\partial^2 u}{\partial y^2}\right) + gh\left(\frac{\partial a}{\partial x} + \frac{\partial h}{\partial x}\right) + \frac{gun^2}{\left(1.486h^{1/6}\right)^2} +$$

$$(u^2 + v^2)^{1/2} - \zeta V_a^2 \cos\psi - 2h\omega v \sin\phi = 0$$

$$h\frac{\partial v}{\partial t} + hu\frac{\partial v}{\partial x} + hv\frac{\partial v}{\partial y} - \frac{h}{\rho}\left(E_{yx}\frac{\partial^2 v}{\partial x^2} + E_{yy}\frac{\partial^2 v}{\partial y^2}\right) + gh\left(\frac{\partial a}{\partial y} + \frac{\partial h}{\partial y}\right) + \frac{gvn^2}{\left(1.486h^{1/6}\right)^2} +$$

$$(u^2 + v^2)^{1/2} - \zeta V_a^2 \sin\psi - 2h\omega v \sin\phi = 0$$

$$\frac{\partial h}{\partial t} + h\left(\frac{\partial u}{\partial x} + \frac{\partial v}{\partial y}\right) + u\frac{\partial h}{\partial x} + v\frac{\partial h}{\partial y} = 0$$

where:

h = Depth

u,v = Velocities in Cartesian directions

x,y,t = Cartesian coordinates and time

ρ = Density of fluid

E = Eddy viscosity coefficient

for xx = normal direction on x-axis surface

for yy = normal direction on y-axis surface

for xy and yx = shear direction on each surface

g = Acceleration due to gravity

a = Elevation of Bottom

n = Manning's roughness n-value

1.486   = Conversion from SI (metric) to non-SI units

ζ = Empirical wind shear coefficient

V_a = Wind speed

Ψ = Wind direction

ω = Rate of Earth's angular rotation

ϕ = Local latitude

RMA-2 operates under the hydrostatic assumption, meaning accelerations in the vertical direction are negligible. RMA-2 is two dimensional in the horizontal plane and is not intended for use in near-field problems where vortices, vibrations, or vertical accelerations are of primary interest. Vertically stratified flow effects are beyond the capabilities of RMA-2.

3.3 SEDIMENTATION MODEL

The sedimentation model, SED-2D, can be applied to sediments where flow velocities can be considered two-dimensional in the horizontal plane (i.e., the speed and direction can be satisfactorily represented as a depth-averaged velocity). It is useful for both deposition and erosion studies. The program treats two categories of sediment: 1) noncohesive, which is referred to as sand herein; and 2) cohesive, which is referred to as clay.

Both clay and sand may be analyzed, but the model considers a single, effective grain size during each simulation. Therefore, a separate model run is required for each effective grain size. Settling velocity must be prescribed along with the water surface elevations, x-velocity, y-velocity, diffusion coefficients bed density, critical shear stresses for erosion, erosion rate constants, and critical shear stress for deposition.

The derivation of the basic finite element formulation is presented in Ariathurai (1974) and Ariathurai, MacArthur, and Krone (1977) and is summarized below.

There are four major computations.

1. Convection-Diffusion Governing Equation

2. Bed Shear Stress Calculation

3. The Bed Source/Sink Term

4. The Bed Strata Discretization

3.3.1 Convection-Diffusion Governing Equation

The mesh employed for the hydrodynamic model is used for the sedimentation model. The convection-dispersion equation in two horizontal dimensions for a single sediment constitute solved by the model is:

$$\frac{\partial C}{\partial t} + u\frac{\partial C}{\partial x} + v\frac{\partial C}{\partial y} = D_x\frac{\partial^2 C}{\partial x^2} + D_y\frac{\partial^2}{\partial y^2} + \alpha_1^C + \alpha_2$$

where:

u,v = depth-averaged sediment velocity components

C = suspended sediment concentration

D_x = effective diffusion coefficient in X-direction

D_y = effective diffusion coefficient in Y-direction

α_1 = concentration-dependent source/sink term

α_2 = coefficient of source/sink term

The source/sink terms in the above equation are computed in routines that pertain to the interaction of the flow and the bed. Separate sections of the code handle computations for clay bed and sand bed problems as described below.

3.3.2 Bed Shear Stress

Bed shear stresses are calculated from the flow speed according to one of four optional equations: the smooth-wall log velocity profile or Manning equation for flows alone; and a smooth bed or rippled bed equation for combined currents and wind waves. Shear stresses are calculated using the shear velocity concept where

$$\tau_b = \rho u_*^2$$

where:

τ_b = bed shear stress

u_* = shear velocity

and the shear velocity is calculated by one of four methods:

a.   Smooth-wall log velocity profiles

$$\frac{\bar{u}}{u_*} = 5.75 \log\left(3.32 \frac{u_* h}{\nu}\right)$$

which is applicable to the lower 15 percent of the boundary layer when

$$\frac{u_* h}{\nu} > 30$$

where $\bar{u}$ is the mean flow velocity (resultant of u and v components)

b.   The Manning shear stress equation

$$u_* = \frac{(\bar{u} n)\sqrt{g}}{CME(h)^{1/6}}$$

where CME is a coefficient of 1 for SI (metric units) and 1.486 for non-SI units of measurement.

c.   A Jonsson-type equation for surface shear stress (plane beds) caused by waves and currents

$$u_* = \sqrt{\frac{1}{2}\left(\frac{f_w u_{om} + f_c \overline{u}}{u_{om} + u}\right)\left(\overline{u} + \frac{u_{om}}{2}\right)}$$

where

f_w = shear stress coefficient for waves

u_{om} = maximum orbital velocity of waves

f_c = shear stress coefficient for currents

d.   A Bijker-type equation for total shear stress caused by waves and current

$$u_* = \sqrt{\frac{1}{2} f_c \overline{u}^2 + \frac{1}{4} f_w u_{om}^2}$$

3.3.3   Source/Sink Terms

The Ackers-White (1973) procedure is used to calculate a sediment transport potential for sand from which actual sand transport is calculated based on sediment availability. Model clay erosion is based on formulas by Partheniades (1962) and Ariathurai while the deposition of clay utilizes Krone's equations (Ariathurai, MacArthur, and Krone, 1977).

3.3.3.1   Sand Transport

For sand transport, the transport potential of the flow and availability of material in the bed control the supply of sediment from the bed. The bed source term is

$$S = \frac{C_{eq} - C}{t_c}$$

where:

S = source term

C_{eq} = equilibrium concentration (transport potential)

C =   sediment concentration in the water column

t_c =   characteristic time for effecting the transition

There are many transport relations for calculating C_{eq} for sand size material. The Ackers-White (1973) formula performed satisfactorily in tests by WES and others (White, Milli, and Crabbe 1975; Swart1976) and was thus adopted for this model. The transport potential is related to sediment and flow parameters by the expressions in the following paragraphs. The Ackers-White formula computes the total load, including suspended load and bed load, and was developed originally for fine sand. The formulation was later updated to include coarser sands and these revised coefficients are included in the current model formulation. However, the appropriateness of the use of SED-2D with the Ackers-White formula diminishes with coarsening of the sediment. The Ackers-White procedure is as follows:

$$P_{ei} g_s = P_{bi} G_{gri} \gamma_s U \frac{(U)^b}{u_*} D_i$$

$$g_s = G_{gri} \gamma_s U \left(\frac{U}{u_*}\right)^b D_m$$

$$G_{ri} = \left\{ a\left(\frac{F}{A} - 1\right)^m \right\} \; for \quad D_m = D_i$$

$$F = \left(\frac{u_*^{\,b}}{\sqrt{gD_m(\gamma_g - 1)}}\right)\left(\frac{U^{1-b}}{\sqrt{32}\log\left(\frac{10R}{D_m}\right)}\right)$$

$$D_g = D_m \frac{[g(\gamma_g - 1)]^{\frac{1}{3}}}{\nu^2}$$

Value of a:

$$a = 0.025 \ for \ D_g > 60$$

$$\log a = 2.86 \log D_g - \left(\log D_g\right)^2 - 3.53 \ for \ 60 \geq D_g > 1$$

Value of b:

$$b = 0.0 \ for \ D_g > 60$$

$$b = 1 - 0.56 \log D_g \ \ for \ 60 \geq D_g > 1$$

Value of A:

$$A = 0.17 \ for \ D_g > 60$$

$$A = \frac{0.23}{\sqrt{D_g}} + 0.14 \ for \ 60 \geq D_g > 1$$

Value of m:

$$m = 1.50 \ for \ D_g > 60$$

$$m = \frac{9.66}{\sqrt{D_g}} + 1.34 \ for \ 60 \geq D_g > 1$$

where:

P_{ei} =   Percentage of grain-size D_i transported

g_s =   transport rate for uniform sediment of size D_m

P_{bi} =   Percentage of grain-size D_i for bed materials

γ_s =   Specific gravity of sediment particle

U =   Average flow velocity

$\mathbf{u}_*$ = Shear velocity on riverbed

D_g = Dimensionless grain-size

D_m = Sediment particle-size

R = Hydraulic radius

The characteristic time, t_c, is somewhat subjective. It should be the amount of time required for the concentration in the flow field to change from C to C_{eq}. In the case of deposition, t_c is related to fall velocity. The following expression was adopted.

$$t_c = \text{the larger of} \begin{cases} C_d \dfrac{h}{V_s} \\ or \\ DT \end{cases}$$

where:

t_c = Characteristic time

C_d = Coefficient for deposition

V_s = Fall velocity of a sediment particle

DT = Computational time interval

In the case of scour, there are no simple parameters to employ. The following expression is used.

$$t_c = \text{the larger of} \begin{cases} C_e \dfrac{h}{u} \\ or \\ DT \end{cases}$$

where:

C_e = Coefficient for entrainment

V = Flow speed

3.3.3.2   Clay Transport

Cohesive sediments (usually clays and some silts) are considered to be depositional if the bed shear stress exerted by the flow is less than a critical value τ_d. When that value occurs, the deposition rate is given by Krone's (1962) equation:

$$S = \begin{cases} -\dfrac{2V_s}{h}C\left(1-\dfrac{\tau}{\tau_d}\right) \text{ for } C < C_c \\[4mm] -\dfrac{2V_s}{hC_c^{4/3}}C^{5/3}\left(1-\dfrac{\tau}{\tau_d}\right) \text{ for } C > C_c \end{cases}$$

where:

S =   source term

V_s =   fall velocity of a sediment particle

h =   flow depth

C =   sediment concentration in water column

τ =   bed shear stress

τ_d =   critical shear stress for deposition

C_c =   critical concentration = 300 mg/ℓ

If the bed shear stress is greater than the critical value for particle erosion τ_e, material is removed from the bed. The source term is then computed by Ariathuarai's (Ariathurai, MacArthur, and Krone 1977) adaptation of Partheniades' (1962) findings:

$$S = \frac{P}{h}\left(\frac{\tau}{\tau_e}-1\right) \text{ for } \tau > \tau_e$$

where P is the erosion rate constant, unless the shear stress is also greater than the critical value for mass erosion. When this value is exceeded, mass failure of a sediment layer occurs and

$$S = \frac{T_L \rho_L}{h \Delta t} \text{ for } \tau > \tau_s$$

MOFFATT & NICHOL E N G I N E E R S

where:

T_L =   thickness of the failed layer

ρ_L =   density of the failed layer

Δt =   time interval over which failure occurs

τ_s =   bulk shear strength of the layer

3.3.4   Bed Strata Discretization

The source-sink term in convection-diffusion equation becomes a source-sink term for the bed model, which keeps track of the elevation, composition, and character of the bed.

3.3.4.1   Sand Beds

Sand beds are considered to consist of a sediment reservoir of finite thickness, below which is a nonerodible surface. Sediment is added to or removed from the bed at rate determined by the value of the source-sink term at the previous and present time-steps. The mass rate of exchange with the bed is converted to a volumetric rate of change by the bed porosity parameter.

3.3.4.2   Clay Beds

Clay beds are treated as a sequence of layers. Each layer has its own characteristics as follows:

- Thickness.
- Density.
- Age.
- Bulk shear strength.
- Type.

In addition, the layer type specifies a second list of characteristics.

- Critical shear stress for erosion.
- Erosion rate constant.
- Initial and 1-year densities.
- Initial and 1-year bulk shear strengths.

- Consolidation coefficient.

- Clay or sand.

New clay deposits form layers up to a specified initial thickness and then increase in density and strength with increasing overburden pressure and age. Variation with overburden occurs by increasing the layer type value by one for each additional layer deposited above it.

4. FINITE ELEMENT MESH

4.1 GENERAL

The numerical modeling system implemented herein requires that a database of water depths and bottom material properties represent the estuarial system. Water depths are represented by nodes located in the horizontal plane, which are interconnected to create elements. Two, three, or four nodes can be connected to form elements. The resulting nodal/element network is commonly called a finite element mesh and provides a computerized representation of the estuarial geometry and bathymetry.

4.2 ELEMENTS

RMA-2 is capable of supporting different types of elements within the same computational finite element mesh. The types of elements fit into three basic categories:

- Two Dimensional Elements
- One Dimensional Elements
- Special Elements

These element types are discussed briefly in the following sections.

4.2.1 Two Dimensional Elements

Two-dimensional elements are the customary type used with RMA-2 and may be either triangular or quadrilateral in shape, as shown in Figure 4-1. A two dimensional element possesses a length and a width, determined by the positions of the corner nodes which define the element. The depth at any location within a two dimensional element is obtained by interpolating among the depths of the corner nodes which define the element.

Quadrilateral Element   **Triangular Element**
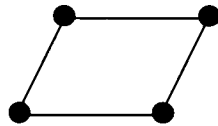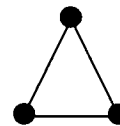
Figure 4-1:   Finite Element Shapes

4.2.2   One Dimensional Elements

A one-dimensional element is a simplified element which is composed of two corner nodes and one midside node. The Finite Element Governing Equations for one-dimensional elements are based on a trapezoidal cross section with side slopes, and an off channel storage area. The depth at any location along a one-dimensional element is obtained by interpolating between the depths of the two corner nodes defining the element.

4.2.3   Special Elements

Special elements are one-dimensional elements that serve special purposes including transition from one- to two-dimensional elements, junctions between multiple one-dimensional elements, and flow control structures.

4.3   MODEL EXTENTS

The areal extent and the level of detail necessary to represent the project area are the parameters that define a finite element mesh. The TABS-2 system, described in Section 3.0, is numerically robust and capable of simulating tidal elevations, flows, and sediment transport over a mesh with widely varying boundaries and levels of detail. Accordingly, the incorporation of significant bathymetric features of the estuary generally dictates the level of detail for the mesh. However, there are several factors used to guide decisions regarding the extents of the mesh. First, it is desirable to extend the mesh to areas sufficiently distant from the project site such that the boundary conditions do not directly influence the hydrodynamics at the site. Secondly, the terminus of the mesh should be in a location where conditions can be reasonably measured and described to the model. Additionally, it is preferable to locate boundaries in locations where flow characteristics have been measured or are known and can be accurately specified.

Geometric information for the UCB-FEM model was obtained from NOAA Digital Elevation Models (DEMs), nautical charts, and recently performed bathymetric surveys. NOAA DEM's are electronic maps of bathymetric elevations imposed on a 30-meter grid and are based on many years of hydrographic survey data acquired for production of navigational charts. For the areas not covered by the DEM, navigation charts were used to complete the mesh. The resulting mesh geometry was checked and alterations were made as deemed necessary to improve physical representation of the estuary and to improve model stability in areas of large depth gradients.

The UCB-FEM model finite element mesh used herein is shown in Figure 4-2. Quadrilateral and triangular 2-dimensional elements were used to represent the estuarial system. The southern boundary of the mesh is located in the Chesapeake Bay near the Hooper Island Light from which it extends north to its terminus at the Conowingo Dam on the Susquehanna River and Chesapeake City on the C & D Canal resulting in total mesh length of roughly 90 nautical miles. A dense mesh was created around James Island to provide a more accurate simulation of conditions at the project site.

Water depths were adjusted to represent both existing and with-project conditions. Figure 4-3 depicts the finite element mesh developed for existing conditions in the vicinity of James Island. Figures 4-4 through 4-8 depict the finite element meshes developed for Alignments 1 through 5, respectively.
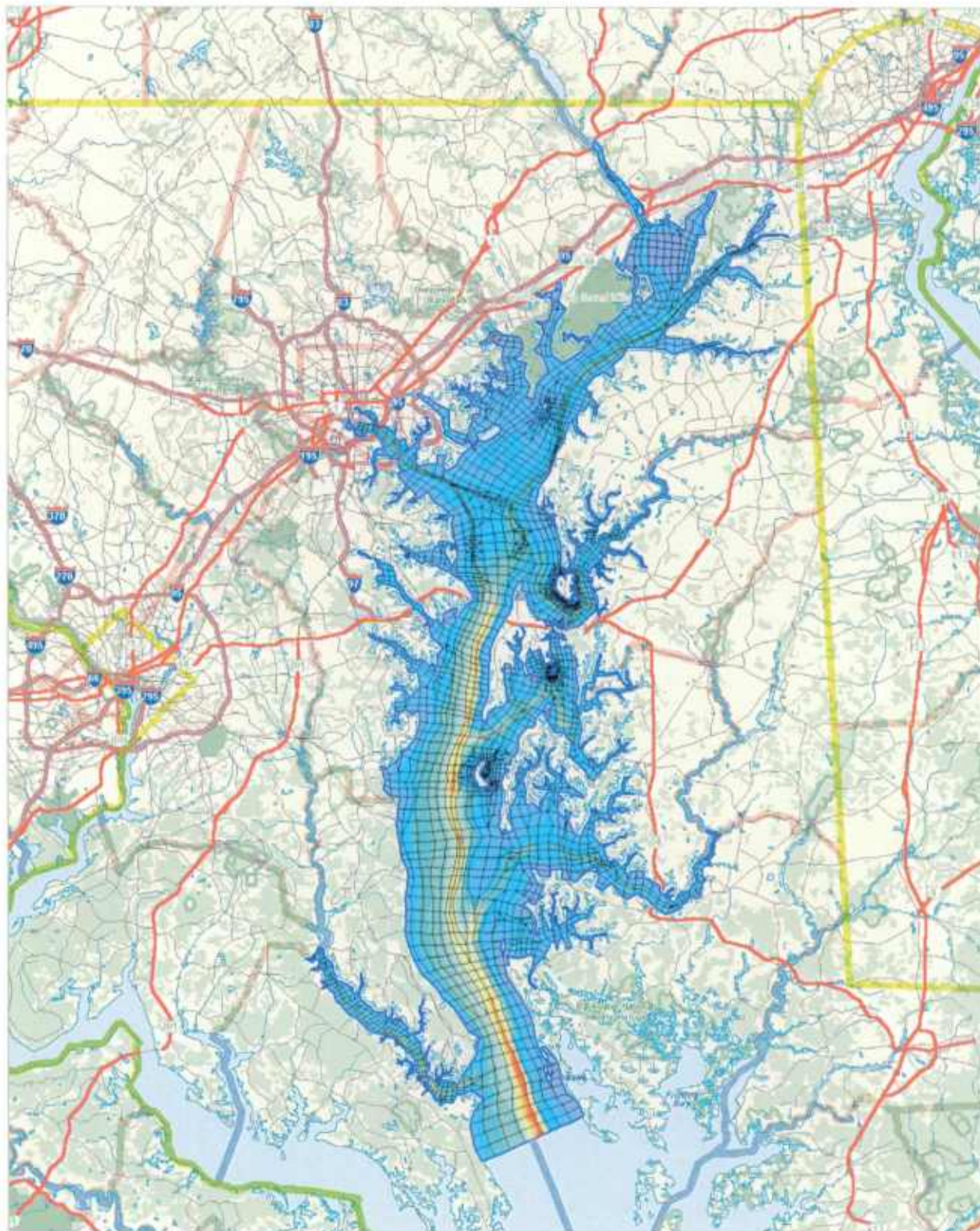
Figure 4-2:   Upper Chesapeake Bay Finite Element Model (UCB-FEM)
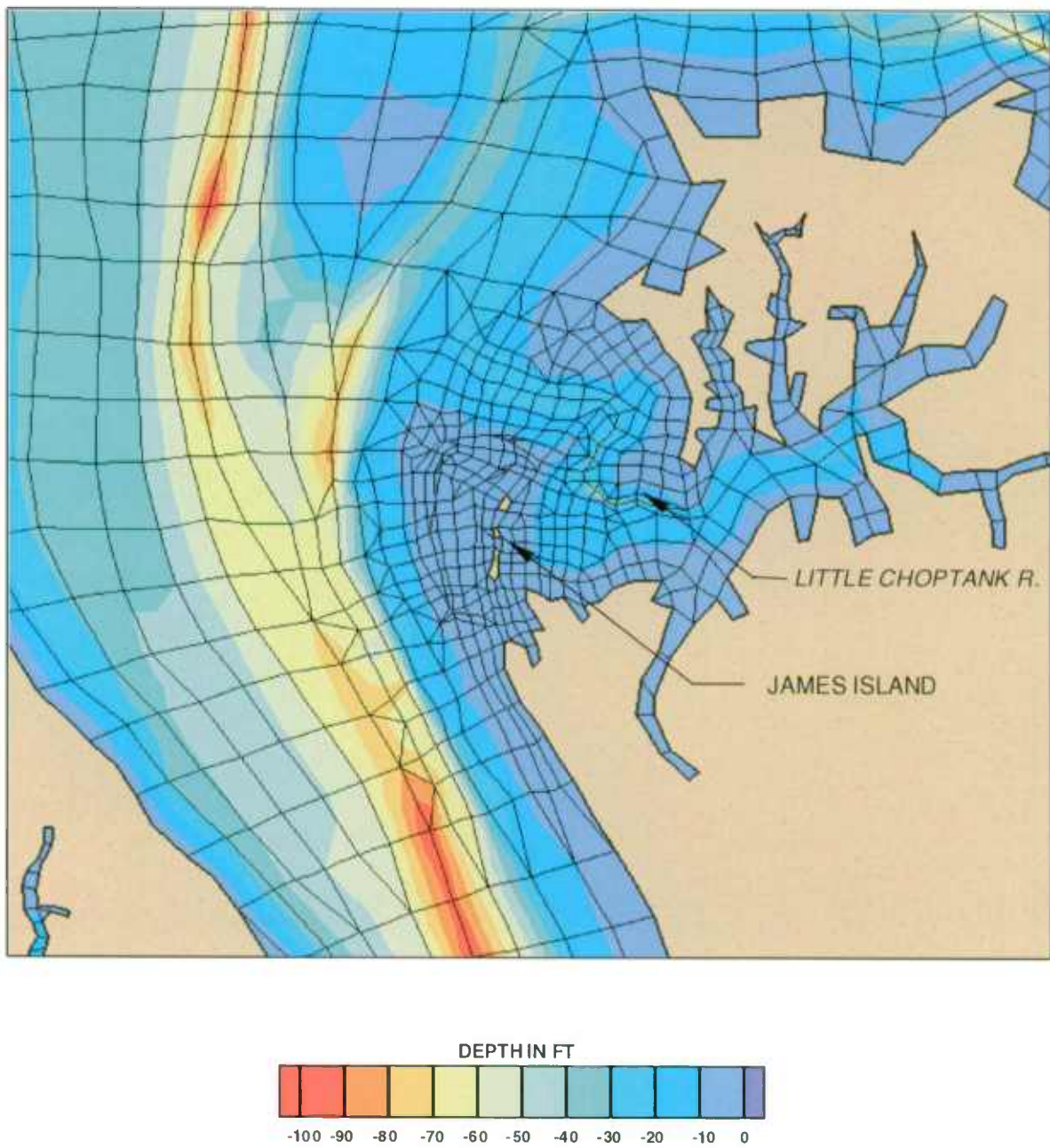
Figure 4-3:   UCB-FEM – James Island Existing Conditions

DEPTH IN FT

-100 -90 -80 -70 -60 -50 -40 -30 -20 -10 0
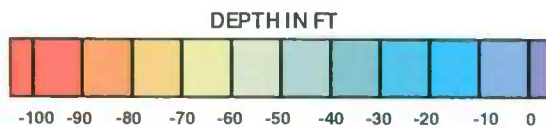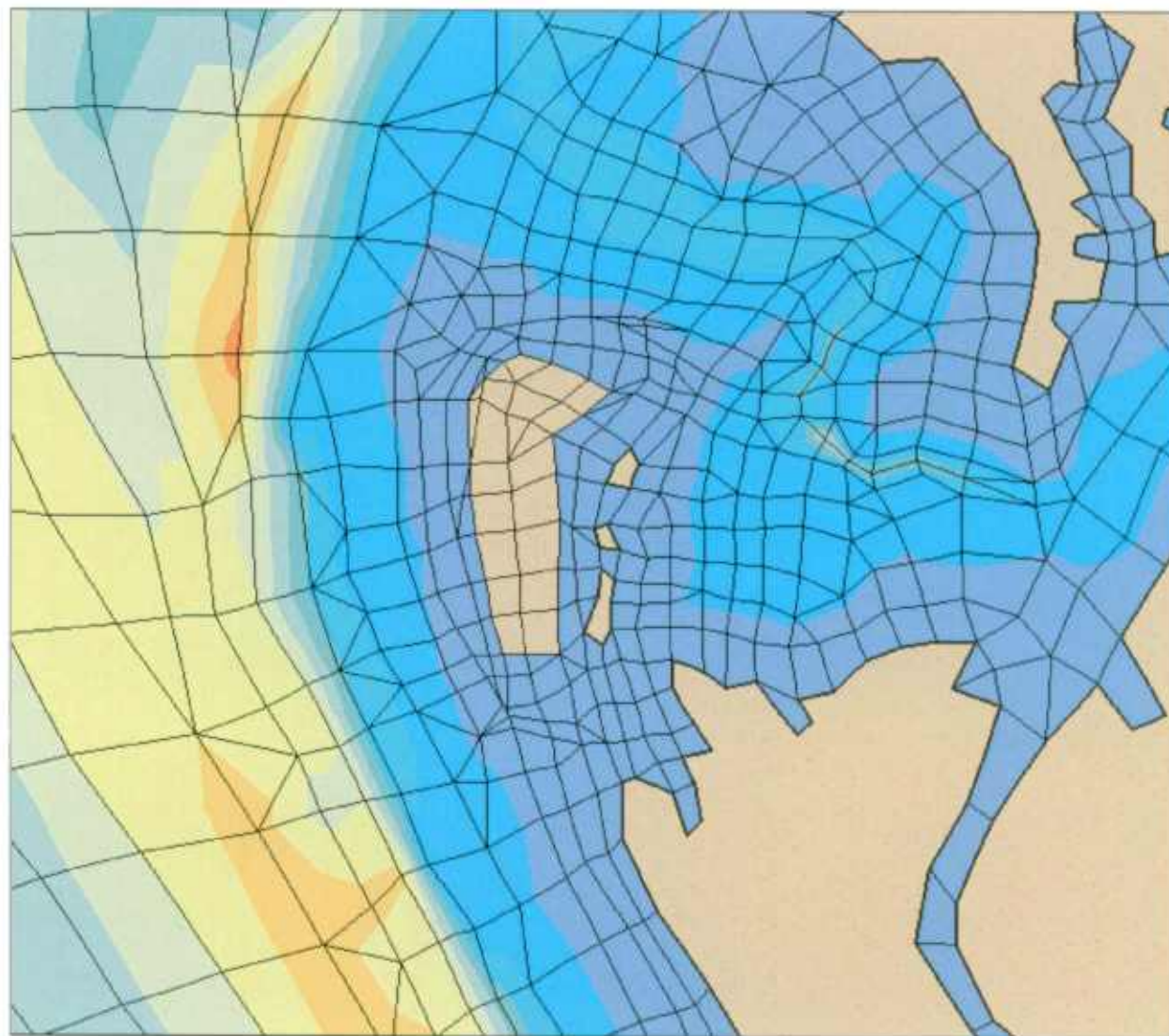
Figure 4-4:   UCB-FEM – James Island Alignment 1
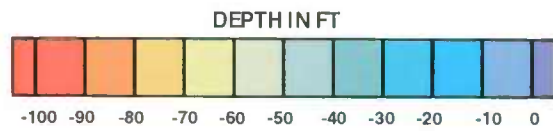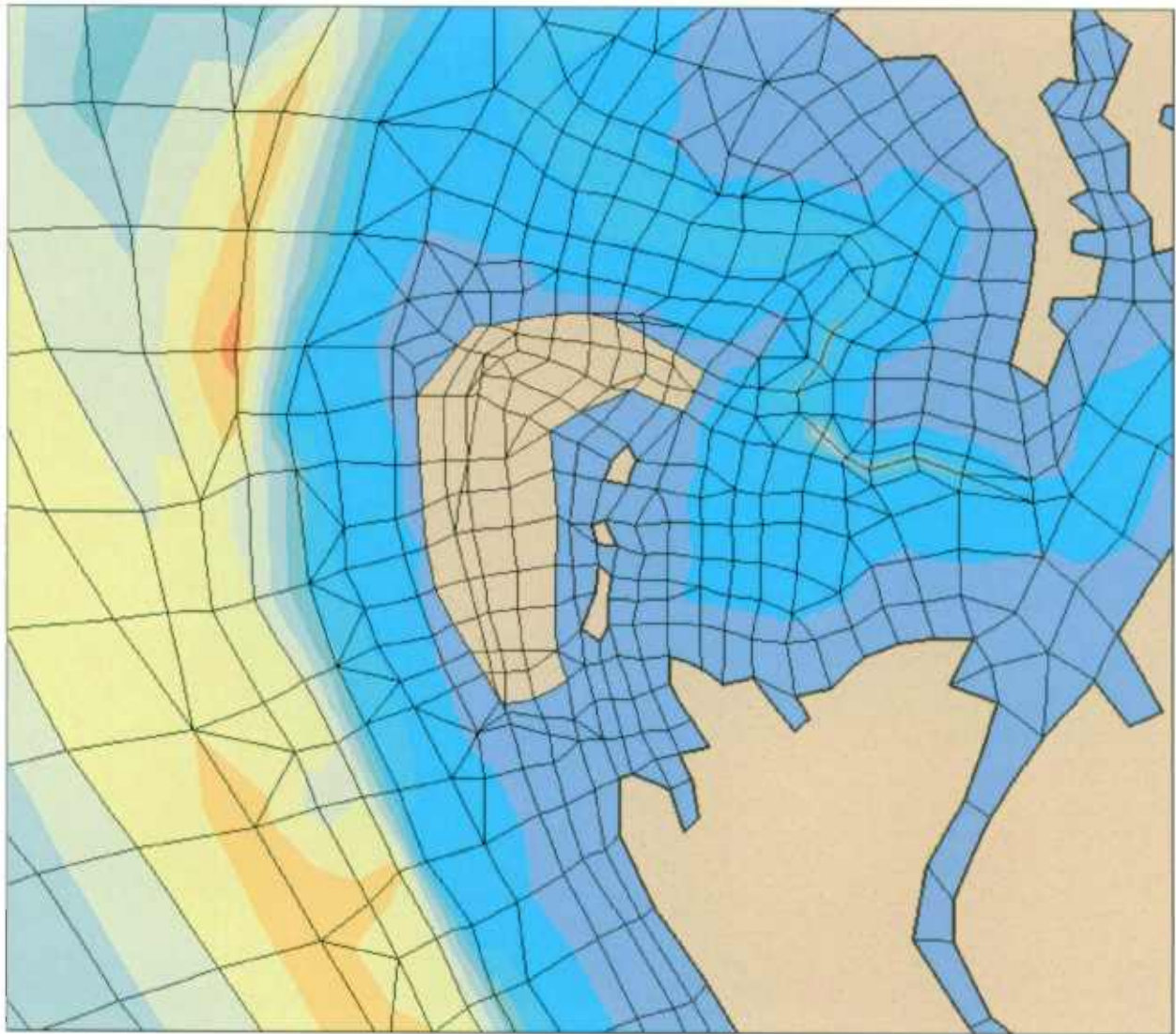
Figure 4-5:   UCB-FEM – James Island Alignment 2
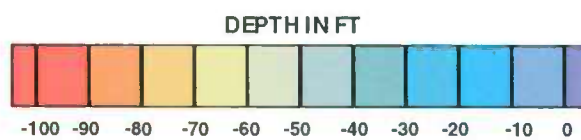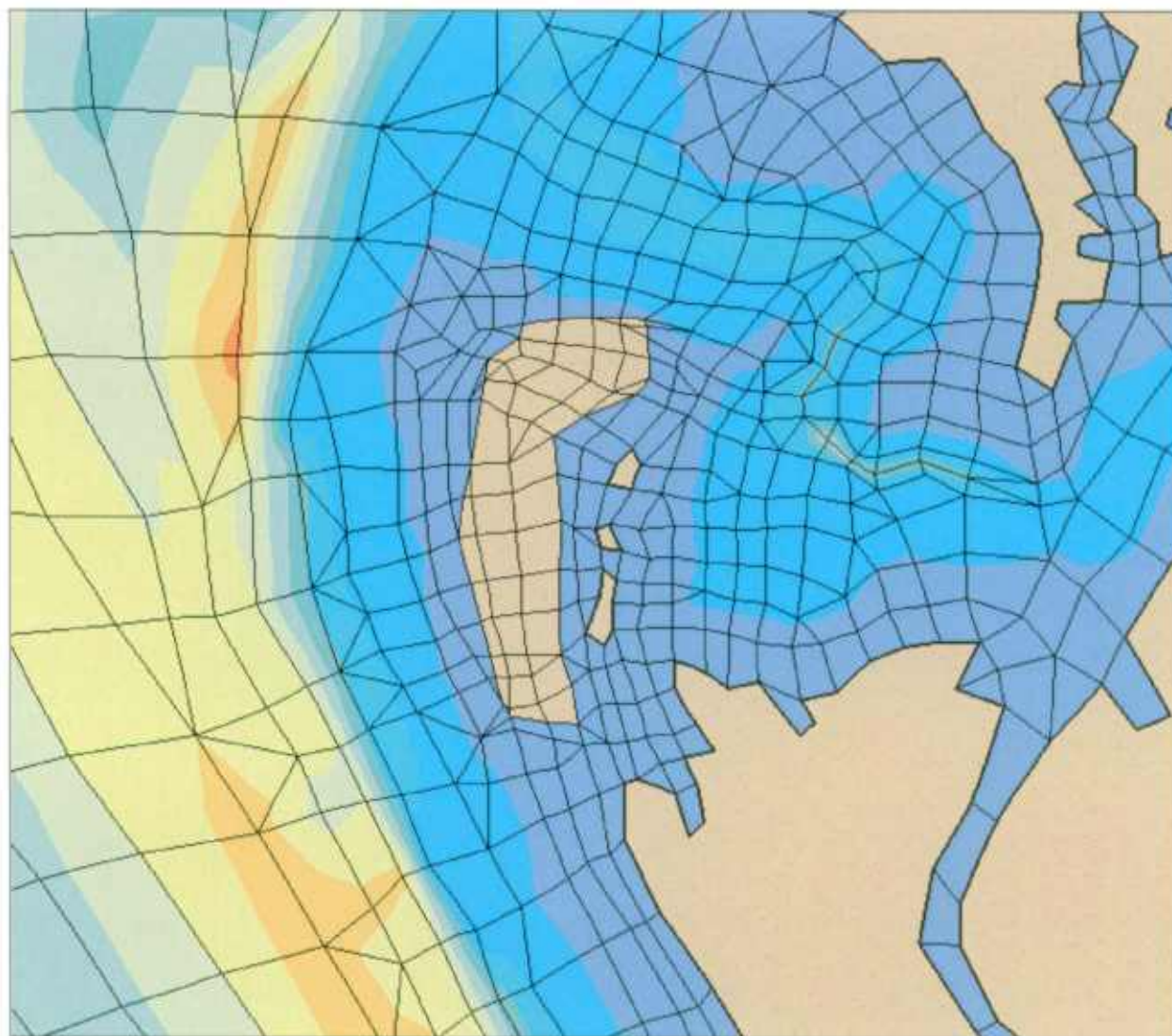
Figure 4-6:   UCB-FEM – James Island Alignment 3
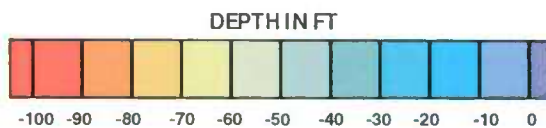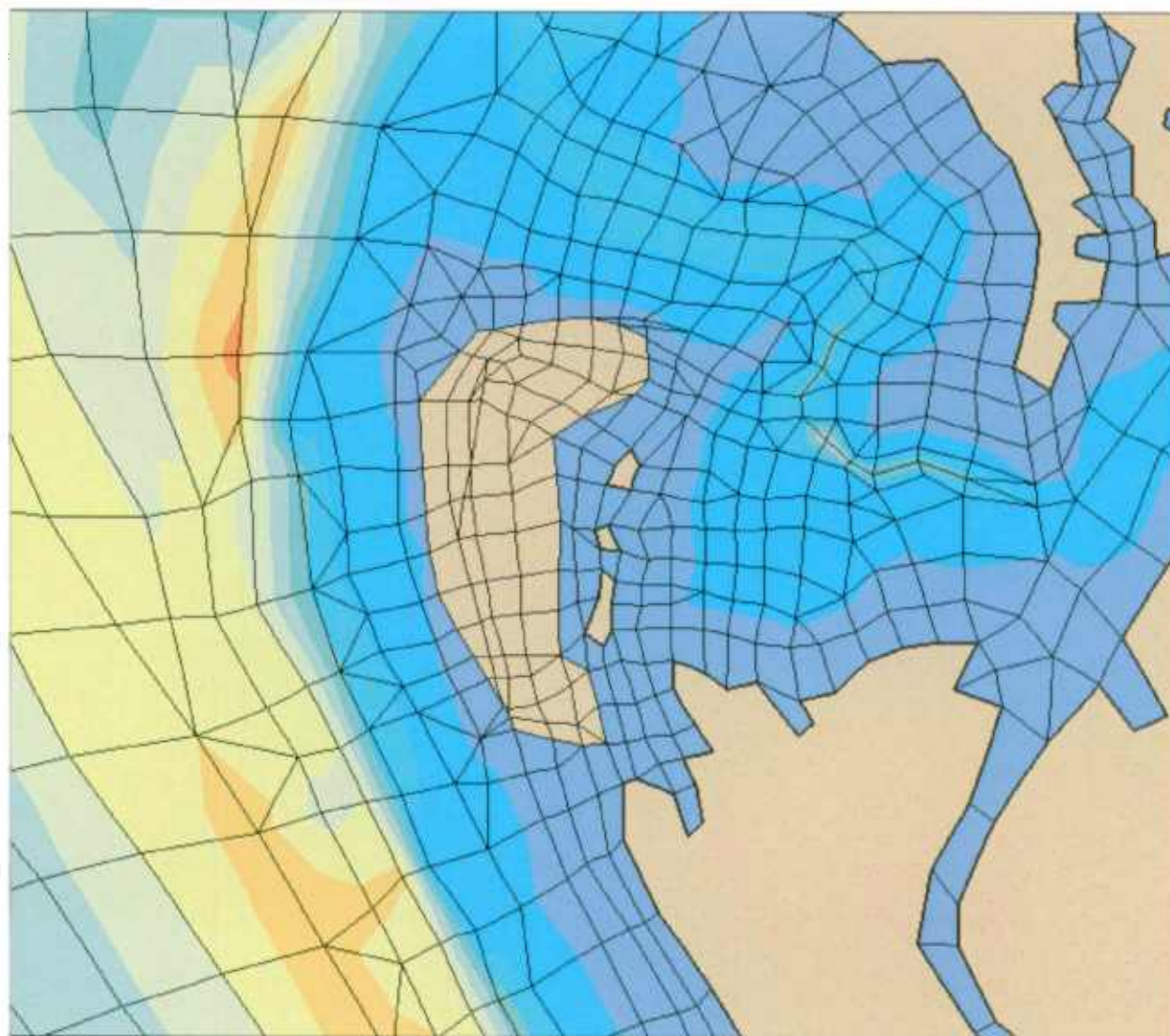
Figure 4-7:　UCB-FEM – James Island Alignment 4

DEPTH IN FT

-100 -90 -80 -70 -60 -50 -40 -30 -20 -10 0
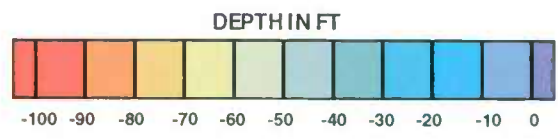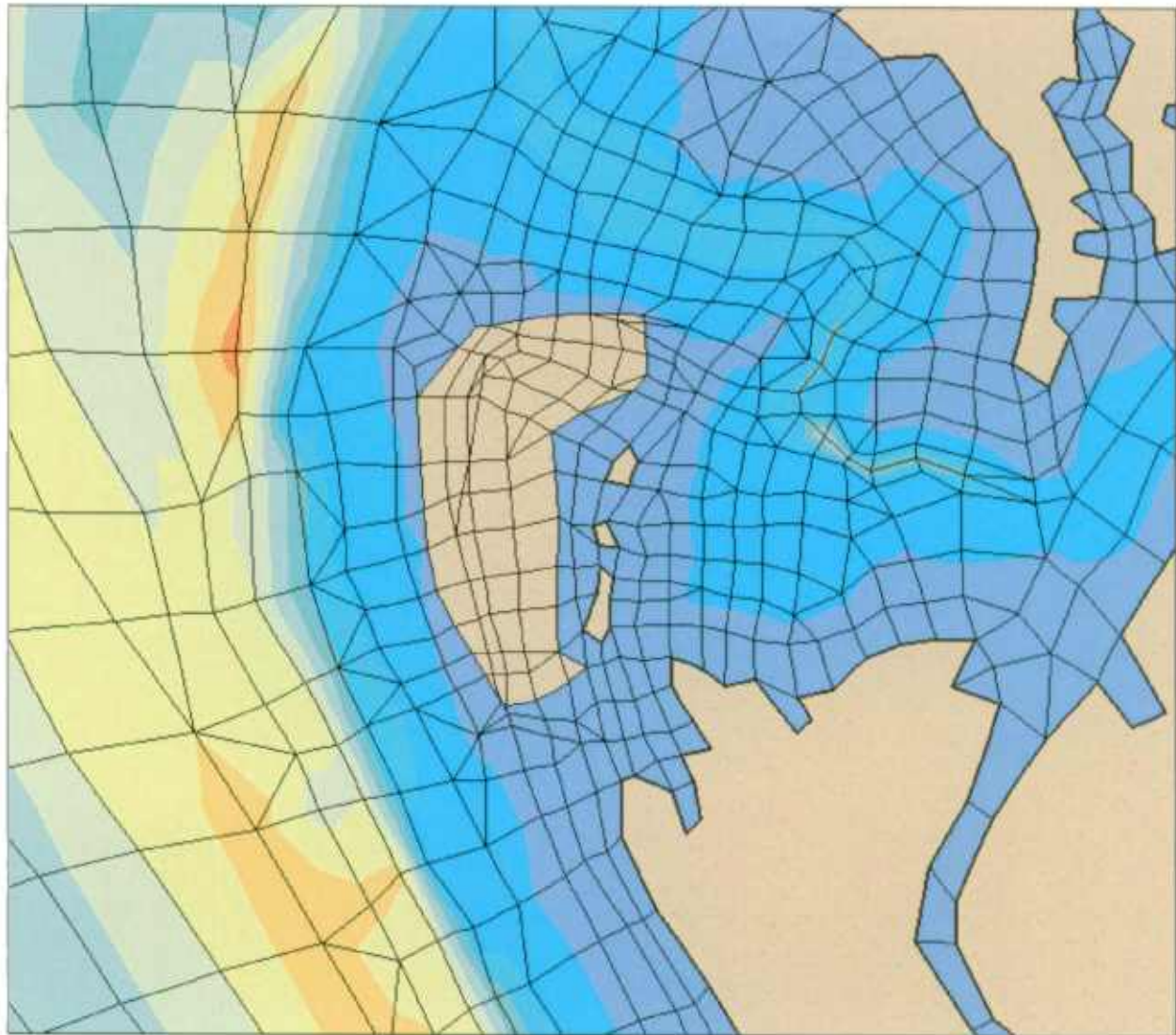
Figure 4-8:   UCB-FEM – James Island Alignment 5

5.　MODEL CALIBRATION

5.1　GENERAL

A measure of a finite element model's accuracy is the comparison of modeled tide elevations and currents with measured or known values. A properly calibrated model can be expected to produce current velocity and tidal elevation results with 80% to 100% accuracy. Model calibrations are adjusted by the refinement of the model bathymetry, the accurate representation of bottom structure (i.e. vegetation, mud, sand) and the stipulation of model parameters that are artifacts of the numerical formulation and are functions of element size and empirical constants. Upon satisfactory completion of calibration, the model can be used to evaluate the impacts of physical changes to the system.

Model calibration is best achieved by means of a set of simultaneous measurements both along the model boundaries and throughout the estuarial system. Boundary conditions important to the present study include tidal elevation, flow velocity, freshwater discharge, suspended sediment concentration, and bottom change over time. For a given set of boundary conditions, the model should be calibrated to reproduce tidal elevations, tidal velocities, or sedimentation rates and patterns within the estuary. The sediment transport model is driven by results obtained from the hydrodynamic model; therefore, the latter is calibrated first.

5.2　HYDRODYNAMIC MODEL

The UCB-FEM model is controlled by boundary conditions as shown in Figure 5-1. Boundary condition values are either constant values or are variable time-dependent values. The major time-dependent boundary conditions are located on the southern boundary of the model in the vicinity of the Hooper Island Light, at the Conowingo Dam on the Susquehanna River and Chesapeake City on the C & D Canal on the northern boundaries. Additional time-dependent boundary conditions are stipulated at the Patuxent, Choptank and Chester Rivers. The values of the six time-dependent boundary conditions are shown in Figure 5-2. Constant flow values are used for boundary conditions for the Patapsco, Gunpowder, Bush and Elk Rivers. The values used at each of these boundaries are listed in Table 5-1.

MOFFATT & NICHOL ENGINEERS　　　　　　　　　　　　　　　　　　*5-1*

The type of boundary condition is based on the data available at each boundary. The Hooper Island Light boundary condition is comprised of tidal elevations while the C & D Canal, Patuxent River, Chester River and Choptank River boundary conditions consist of current velocities and directions and the Conowingo Dam boundary condition is described by volume flux (flow). Boundary conditions located at smaller tributaries are described as constant sources of flow into the bay based on historic average measured flow. Calibration was performed for a two-week period of predicted data from February 1-14, 2001, which is representative of an average tidal cycle and low freshwater inflow.

Table 5-1: Freshwater Inflow Boundaries	
Location	**Flowrate (cfs)**
Patapsco River	431
Gunpowder River	2888
Bush River	1149
Elk River	1874

Tide elevation and current velocity boundary conditions for the UCB-FEM model are based on NOS tidal predictions. NOS tidal predictions are based on historic harmonic constituents and represent idealized conditions which do not account for low frequency events including wind and storms. Figure 5-2 shows the water surface elevations and current velocities for the entire month of February 2001 at the boundary condition locations. The data used as boundary conditions in the UCB-FEM model calibration are for February 1 through February14.

Aside from the boundary conditions, the model is also influenced by bottom friction and eddy viscosity. Physically, bottom friction varies by bottom material and vegetation type and density and is best described by a map of Manning's roughness coefficient over the entire model domain. As is often the case, detailed information regarding bottom material is not available for the entire model domain. Standard practice is to then specify Manning's roughness relative to water depth resulting in a loose correlation with vegetation density. Eddy viscosity, or lateral mixing, also varies over the entire domain but is also dependent upon numerical element size and predicted current velocity in the model. Eddy viscosity is, therefore, specified based on a function

calculated at each element for each time step. The final set of eddy viscosity and Manning's roughness values which provided the best fit between measured and simulated water elevations and flow velocities at measurement stations within the estuarial system were implemented.

NOS predicted tides and currents were used to check the model calibration at the locations shown in Figures 5-3 and 5-4. Figures 5-5 and 5-6 show results for selected calibration locations, for water surface elevations and current velocities, respectively.

Comparisons of the NOS predicted and UCB-FEM modeled data show excellent correlation to both tidal phasing and amplitudes. Tables 5-2 and 5-3 show the statistical comparison of the model results to NOS predicted data at each station subdivided by geographical regions. Statistics are calculated for overall calibration correlation and peak condition amplitudes. Percent error is calculated by dividing the RMS (root mean square) error by the calculated mean range.

Table 5-2: Water Surface Elevation Calibration Statistics

	Time Series Statistics		
	Correlation	Peak RMS Error (ft)	Peak RMS Error %
Little Choptank River			
Taylor's Island	100%	0.07	5.5%
Hudson Creek	98%	0.07	4.9%
Choptank River			
Broad Neck Creek	98%	0.06	4.3%
Choptank River Light	95%	0.05	3.4%
Cambridge	96%	0.08	5.1%
Choptank	92%	0.06	3.3%
Eastern Bay			
Claiborne	96%	0.10	9.0%
Miles River	99%	0.10	7.8%
Chester River			
Love Point	98%	0.10	8.7%
Cliff's Point	98%	0.09	5.8%
Sassafras and Susquehanna River and C and D Canal			
Betterton	92%	0.26	15.1%

Courthouse Point	99%	0.17	7.1%
Havre de Grace	92%	0.27	14.4%
Port Deposit	96%	0.44	19.6%
Main Chesapeake Bay			
Sharps Island Light	92%	0.07	5.1%
Poplar Island	95%	0.06	5.1%
Bloody Point Light	94%	0.07	6.4%
Matapeake	97%	0.12	12.3%
Pooles Island	94%	0.18	14.0%
Western Chesapeake Bay			
Cedar Point	100%	0.08	6.6%
Cove Point	100%	0.08	5.7%
Long Beach	96%	0.08	7.6%
Chesapeake Beach	97%	0.08	8.1%
West River	98%	0.14	14.6%
Thomas Light	96%	0.14	15.3%
Sandy Point	96%	0.20	25.2%
Seven Foot Knoll Light	96%	0.15	16.0%
Patapsco, Middle, and Gunpowder Rivers			
Fort Carroll	97%	0.10	8.8%
Rocky Point	95%	0.12	9.9%
Bowley's Bar	95%	0.16	12.5%
Battery Point	95%	0.14	11.3%

The model calibration results shown in Table 5-2 show better than 90% correlation for all locations. Predicted tidal elevation percent error is typically less than 10% with the exception of some specific areas of the model domain which are under 20%. Under-prediction of the Coriolis force and over-simplification of the bottom friction in the bay result in higher percent errors for tides along the western shore of the Bay including the Middle and Gunpowder Rivers. Tides in the main Chesapeake Bay near James Island represent the project area and are well predicted. Correlation in the main Bay near James is about 92% at Sharps Island Light, 96% at Long Beach, and 100% at Cove Point, and the peak tide is under-predicted by 0.07 to 0.08 ft.

Table 5-3: Current Velocity Calibration Statistics

	Time Series Statistics		
	Correlation	RMS Error (ft/sec)	RMS Error %
Main Cedar Point			
Cedar Point 1.1 nmi ENE	93%	0.28	15.7%
Cedar Point 2.9 nmi ENE	96%	0.34	19.7%
Main Cove Point			
Cove Point 1.1 nmi E	97%	0.18	7.9%
Cove Point 2.7 nmi E	96%	0.17	12.3%
Cove Point 3.9 nmi E	97%	0.22	10.5%
Main James Island			
Kenwood Beach 1.5mi NE	94%	0.16	19.1%
James Island 3.4 mi W	97%	0.15	12.3%
James Island 2.5 mi WNW	87%	0.16	10.5%
Main Sharps Island			
Plum Pt 2.1 mi N	96%	0.11	9.1%
Sharps Is Lt. 3.4 mi W	95%	0.15	12.8%
Sharps Is Lt. 2.1 W	92%	0.11	9.1%
Main Poplar Island			
Holland Pt 2 mi E	95%	0.15	18.4%
Poplar Is 2.2 mi WSW	96%	0.20	10.2%
Poplar Island E of S end	90%	0.54	19.7%
Main Thomas Point Shoal			
Thomas Pt Shoal Lt 1.8 mi SW	92%	0.10	8.1%
Thomas Pt Shoal Lt 0.5 m SE	95%	0.19	10.3%
Thomas Pt Shoal Lt 2 mi E	97%	0.11	6.6%
Main Sandy Point			
Sandy Point 0.8 nmi ESE	97%	0.43	13.8%
Sandy Point 2.3 nmi E	98%	0.17	7.8%
Main Baltimore			
Brewerton Channel Eastern Ext, Buoy 7	97%	0.24	18.7%
Swan Point 1.6 mi NW	98%	0.42	17.7%
Main Pooles Island			
Gunpowder River Entrance	94%	0.48	38.1%
Robins Point 0.7 mi ESE	89%	0.59	17.6%
Pooles Island 1.6 nmi E	98%	0.23	7.6%

MOFFATT & NICHOL
E N G I N E E R S

Main Upper			
Howell Point 0.4 mi NNW	97%	0.49	15.8%
Turkey Point 1.2 nmi W	88%	0.33	19.4%
Patuxent River			
Hog Point 0.6 mi N	92%	0.09	6.9%
Choptank River			
Sharps ls Lt. 2.3 mi SE	97%	0.19	9.0%
Holland Pt 2 mi SSW	94%	0.09	12.9%
Chlora Pt 0.5 mi SSW	93%	0.16	11.8%
Cambridge Highway Bridge W of Swingspan	97%	0.28	22.6%
Poplar Pt S of	100%	0.08	3.1%
Eastern Bay			
Long Point 1 mi SE	88%	0.21	13.5%
Tilghman Point 1 mi N of	92%	0.12	10.9%
Parson's Island 0.7 NNE of	94%	0.08	15.1%
Kent Island Narrows Highway Bridge	95%	0.53	16.9%
Chester River			
Love Point 1.6 nmi E	95%	0.29	21.0%
Hail Point 0.7 nmi E	96%	0.17	11.0%
C & D Canal			
Arnold Point 0.4 mi W	87%	0.21	12.95%
C & D Canal, Chesapeake City Bridge	100%	0.01	0.13%

The above model calibration results show better than 90% correlation for most currents with the remaining better than 85%. Predicted current velocity percent error is typically less than 15% with the exception of some specific areas of the model which are closer to 20%. Near James Island, the correlation is between 87% to 97%. The factors affecting tidal elevation calibration, compounded with depth averaging in the model not reflecting the variation of currents with depth in the Bay, are the cause of the discrepancies between predicted and modeled currents.

5.3 SEDIMENTATION MODEL

Sedimentation model calibration typically requires historic sedimentation and erosion rates and detailed suspended sediment data. When these data are not available, the model can be used

empirically to determine patterns and relative rates of sedimentation and erosion.

5.3.1   Non-Cohesive Sediment (Sand)

Studies performed by E2CR show fine surface sand in the vicinity of James Island. The non-cohesive sediment model was run using 0.1mm (.004 inch) sediment under no-wind conditions. Analysis of results shows negligible sand transport due to tidal currents. The non-cohesive sediment model was then run for each of 16 wind directions (E, ENE, NE, NNE, N, NNW, NW, WNW, W, WSW, SW, SSW, S, SSE, SE, and ESE) for wind speeds of 4-, 13-, and 16-mph corresponding to wind speed ranges from the wind rose shown in Figure 2-4.

Modeled non-cohesive sediment transport for existing conditions is negligible for 4- and 13-mph winds for all directions. Sixteen-mph winds, when taken cumulatively with lower wind speeds, account for nearly 90% of the yearly wind occurrences and cause significant sediment transport for winds from the NNW, SSE and WNW directions with negligible to moderate sediment transport for winds from other directions.

Model results for 16-mph winds from the NNW, SSE and WNW directions are shown in Figures 5-7, 5-8 and 5-9, respectively. Results are shown using a normalized unitless scale due to the empirical use of the sedimentation model and the lack of available data to verify model calibration.

Figure 5-7 shows areas of both erosion (green to blue) and accretion (yellow to orange) due to NNW winds.   As shown in the figure, erosion generally occurs in the shallow waters around James Island, along the eastern shore of Taylors Island to the south, and within the Little Choptank River. Areas of accretion occur in the adjacent deeper areas west of James Island and Taylors Island, and within the Little Choptank River. To the north of James Island, erosion is observed in the shallows around Sharps Island Light, with accretion in the deeper waters east of the light.   Figure 5-8 shows increased erosion and accretion potential due to SSE winds, indicated by the more extensive blue areas and patches of red. Similar to the NNW winds, erosion occurs in the shallow waters with accretion in the adjacent deeper waters. Impacts to the bottom sediment are west of James Island, with no effects in the Little Choptank River. Figure 5-9 shows erosion and accretion patterns due to WNW winds. As shown in this figure, erosion is

not as pronounced, as the fetch distance from this direction is much shorter than the previous two directions. Erosion occurs mainly in the shallows close to James Island, along the Taylors Island shore, near Ragged Island in the Little Choptank River, and off Cook Point in Trippe Bay. Accretion again occurs in the deeper areas adjacent to the eroded shallow waters regions.

5.3.2 Cohesive Sediment (Clay and Silt)

Detailed cohesive sediment data, including suspended sediment concentrations, sedimentation and erosion rates, and spatial maps of specific surface sediment properties are not available for the project area. Since these data are unavailable, the sedimentation model was used empirically by assigning multiple thin layers of cohesive material with increasing cohesion and density over the entire domain. The layers erode and accrete in response to tidal current forcing and reach a dynamic equilibrium, meaning zero net sediment transport over a full lunar tidal cycle.

The UCB-FEM sedimentation model was initialized with nine cohesive layers of uniform thickness throughout the model domain. Layer calibration parameters include critical shear stresses of deposition (τ_{cd}) and erosion (τ_{ce}), erosion rate constant (E), bulk density (ρ), and settling velocity (w_s). The critical shear stress for deposition was set constant to 0.07 N/m^2 and settling velocity was set to 0.4 mm/second and increases as a function of concentration (Winterwerp, 1999). Other model layer parameters are shown in Table 5-4.

Sensitivity analyses show that sediment model boundary conditions are sufficiently far from the project area and have minimal impact on sediment transport in the project vicinity. Sediment model boundary conditions were set equal to the background values in the Bay. The resulting set of initial layer thicknesses shows the complete erosion of the upper layers in areas of high shear stress and deposition in quiescent areas.

Table 5-4: Sediment Model Initial Bed Layering

Layer Number	Thickness (inches)	Critical Shear Strength, τ_{ce} (N/m^2)	Erosion Rate Constant, E $(g/m^2/sec)$	Dry Density, ρ_{dry} (kg/m^2)
1	0.25	0.07	0.200	334
2	0.25	0.16	0.200	450
3	0.25	0.21	0.200	500
4	0.5	0.27	0.100	550
5	0.5	0.33	0.100	600
6	0.5	0.45	0.100	650
7	1.0	0.57	0.050	650
8	1.0	0.69	0.050	650
9	1.0	0.82	0.050	650

The cohesive sediment model was run for a 6-month simulation period at which point the model was operating in a dynamic equilibrium. Ensuing with-project simulations show negligible erosion and accretion due to tidal currents. The cohesive sediment model was then run for each of 16 wind directions for wind speeds of 4- and 13-mph corresponding to wind speed ranges from the wind rose shown in Figure 2-4.

Modeled cohesive sediment transport is negligible for 4-mph. Thirteen-mph winds cause significant sediment transport for winds from the NNW, SSE, and WNW as shown in Figures 5-10 through 5-12, respectively, with negligible to moderate sediment transport for winds from other directions. Results are shown using a normalized unitless scale due to the empirical use of the sedimentation model and the lack of available data to verify model calibration. In general, for cohesive sediments the areas of erosion and accretion are larger than for non-cohesive sediment, as properties of cohesive sediment (shape, plasticitiy, electric charge) cause the particles to remain in suspension for relatively long periods of time before they settle out.

Figure 5-10 shows erosion due to NNW winds in the shallow areas west of James Island and Taylors Island, in the shallow regions of the Little Choptank River and Trippe Bay, and at Sharps Island Light. Accretion occurs southeast of James Island due to its sheltering effect from the NNW. Accretion also occurs in the adjacent deeper waters, but extends over a greater distance across the Bay to the Western Shore, south past Cove Point and north to the Choptank River.

Figure 5-11 presents results from SSE winds, and shows a greater area of erosion west of James Island and south along Taylors Island extending to Barren Island and Hooper Island. Erosion is also greater around Sharps Island Light. Accretion is not as wide spread as with NNW winds, but has higher potential in the central deep waters of the Bay. Increased accretion potential exists in the Little Choptank River with winds from the SSE. Figure 5-12 shows model results for WNW winds. As shown in this figure, although erosion occurs along the entire shoreline that is exposed to this direction, the erosion potential is not as great as the previous two conditions. Accretion occurs in the deeper waters adjacent to the erosional areas within the Bay, the Little Choptank River, Trippe Bay, and the Choptank River.
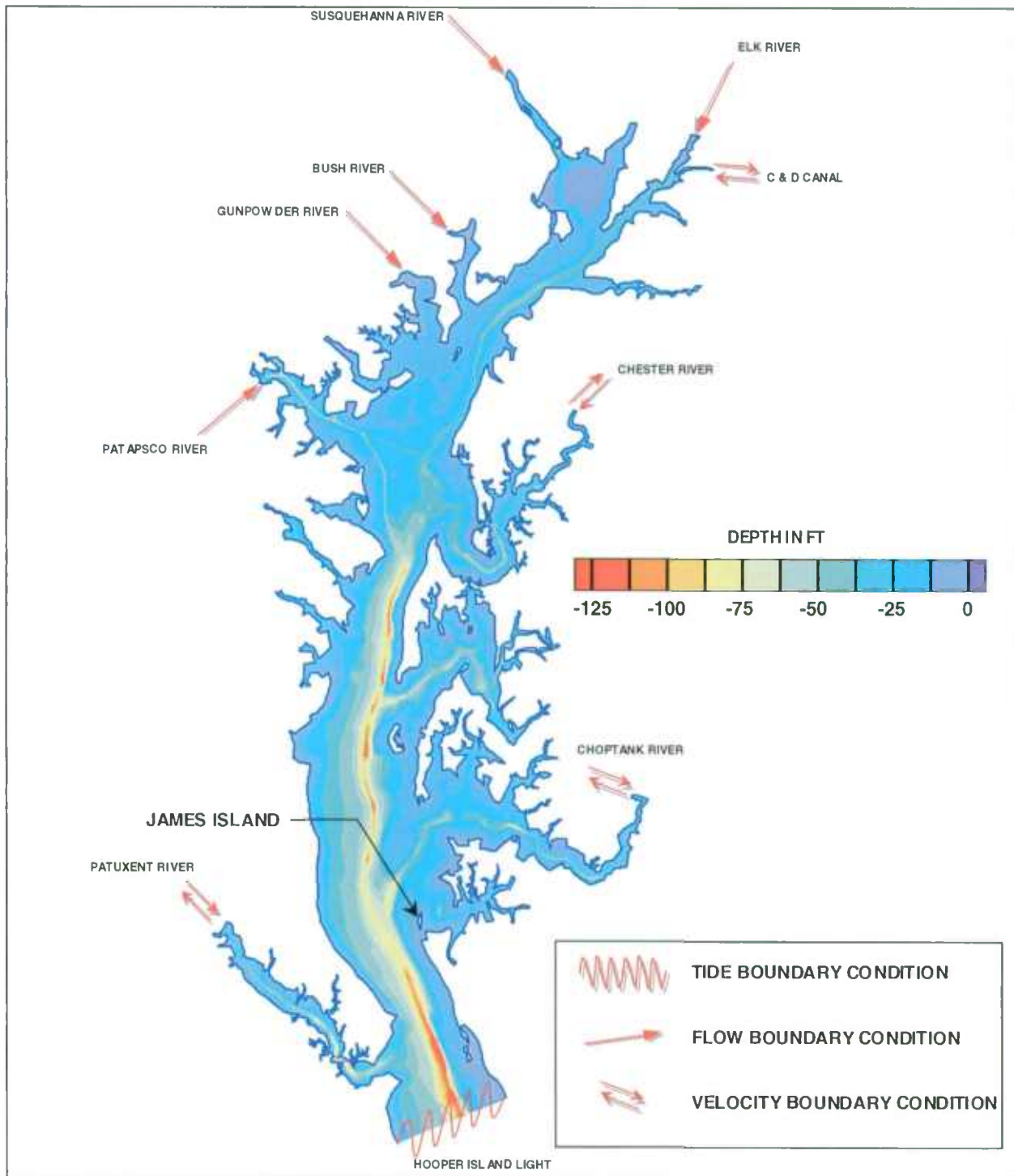
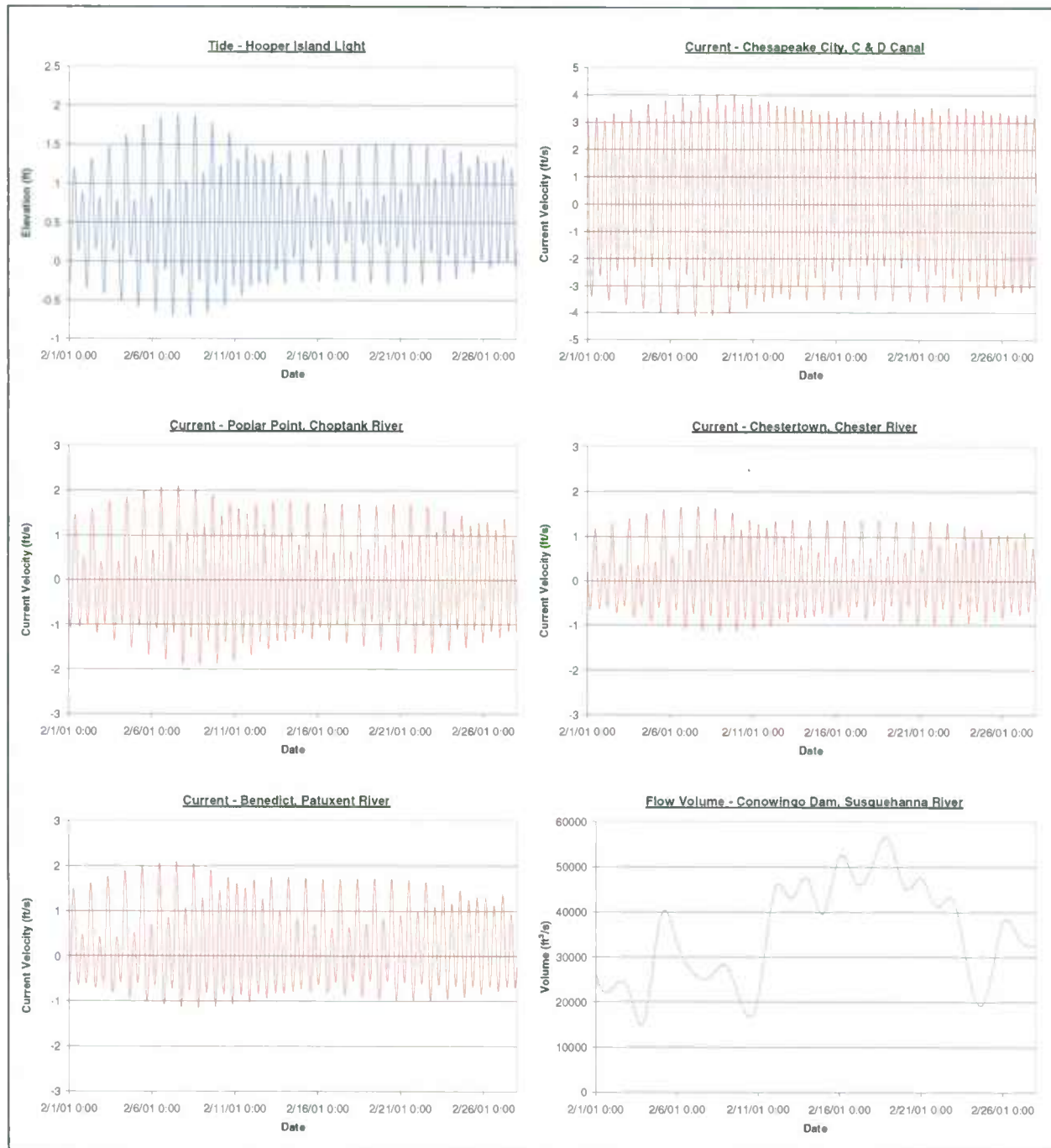**Figure 5-1:   UCB-FEM Boundary Condition Locations**
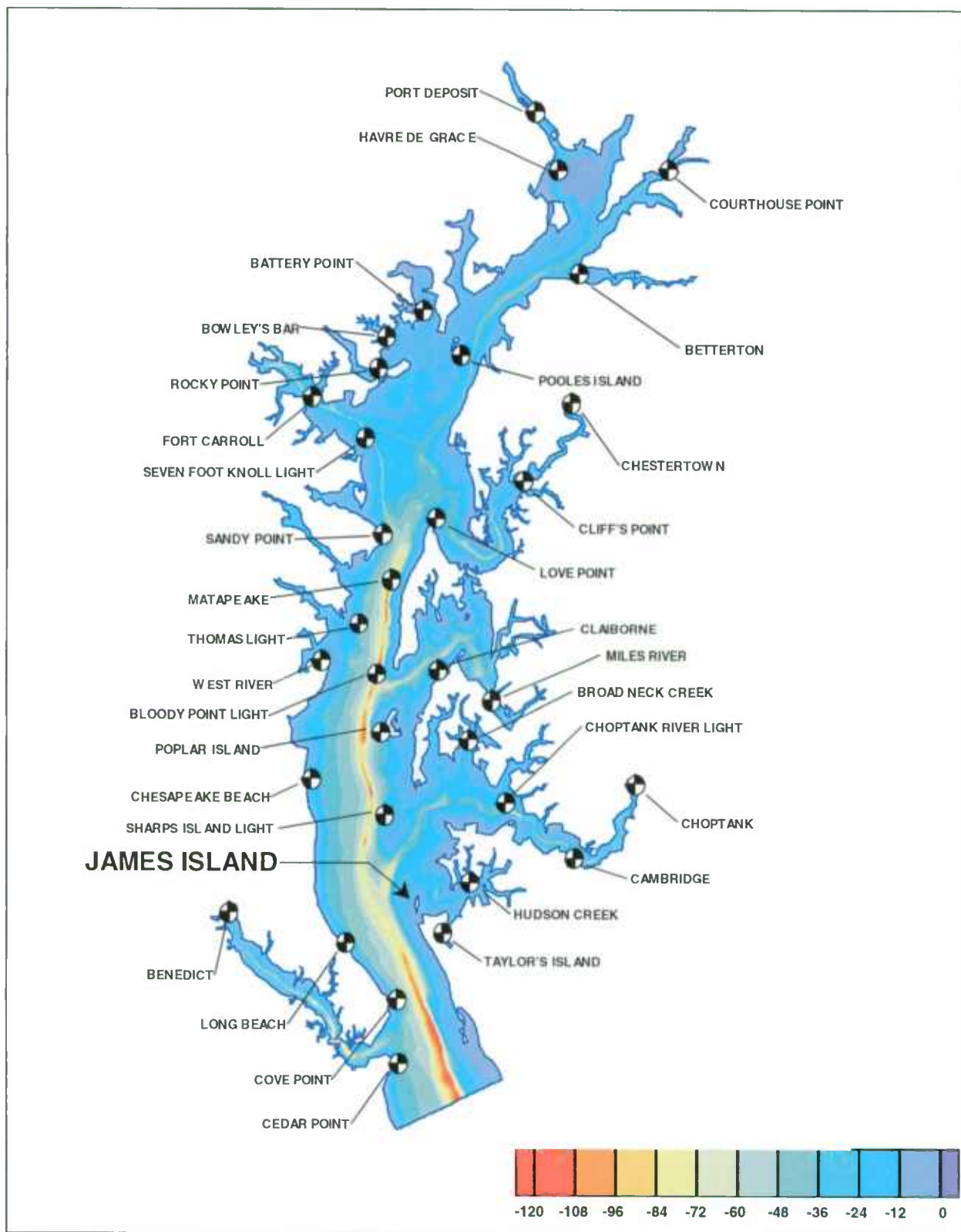
Figure 5-2:   UCB-FEM Boundary Conditions

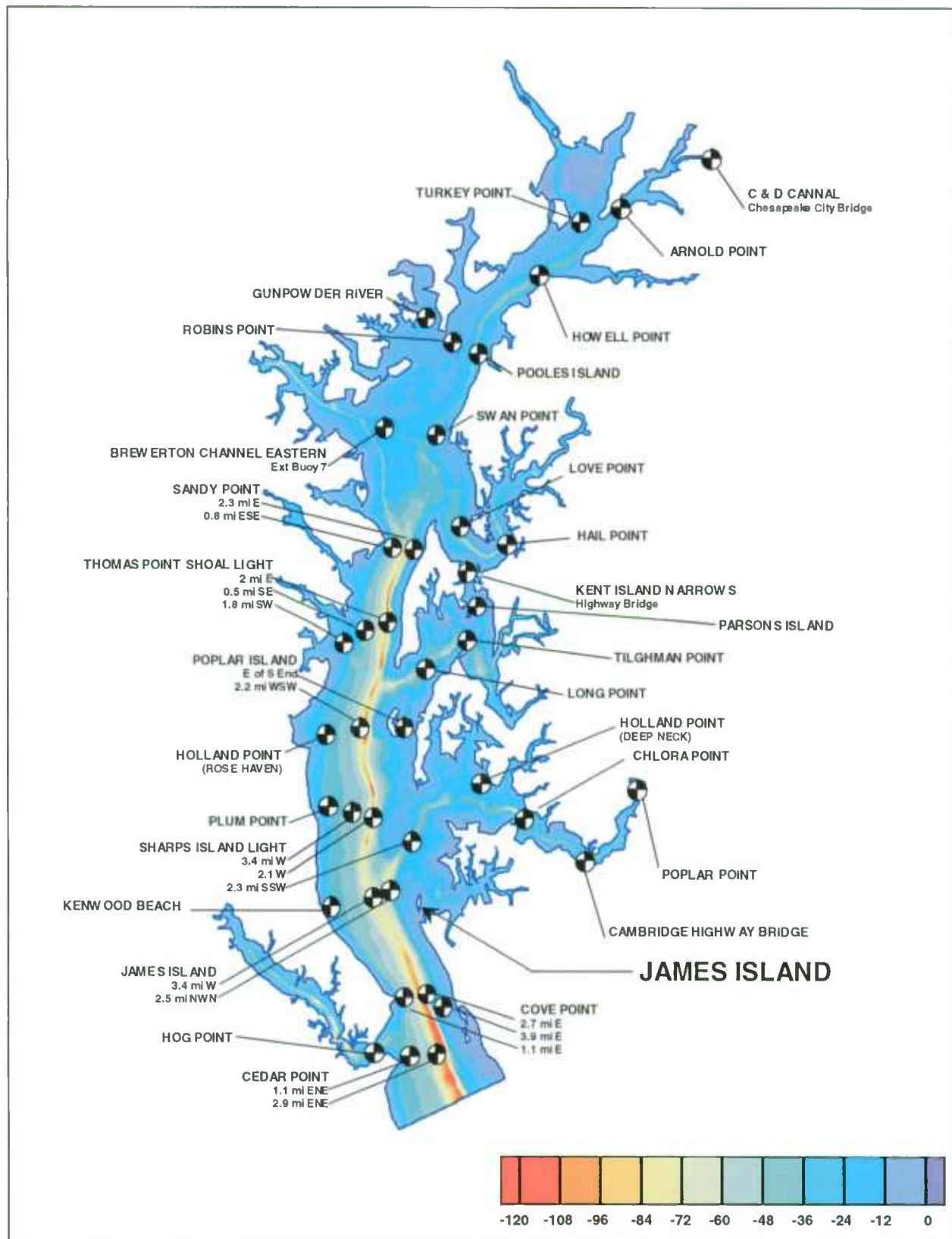**Figure 5-3:   UCB-FEM Tidal Elevation Calibration Points**

Figure 5-4:   UCB-FEM Current Velocity Calibration Points
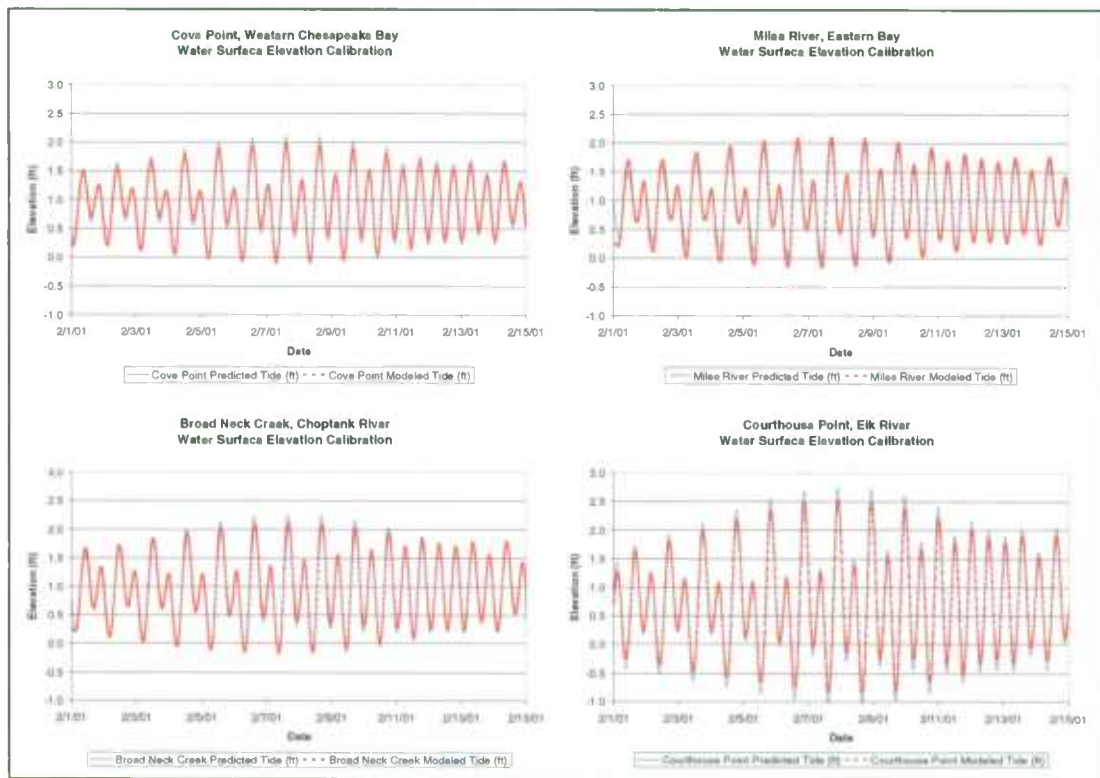
Figure 5-5:   Tidal Elevation Calibration Results
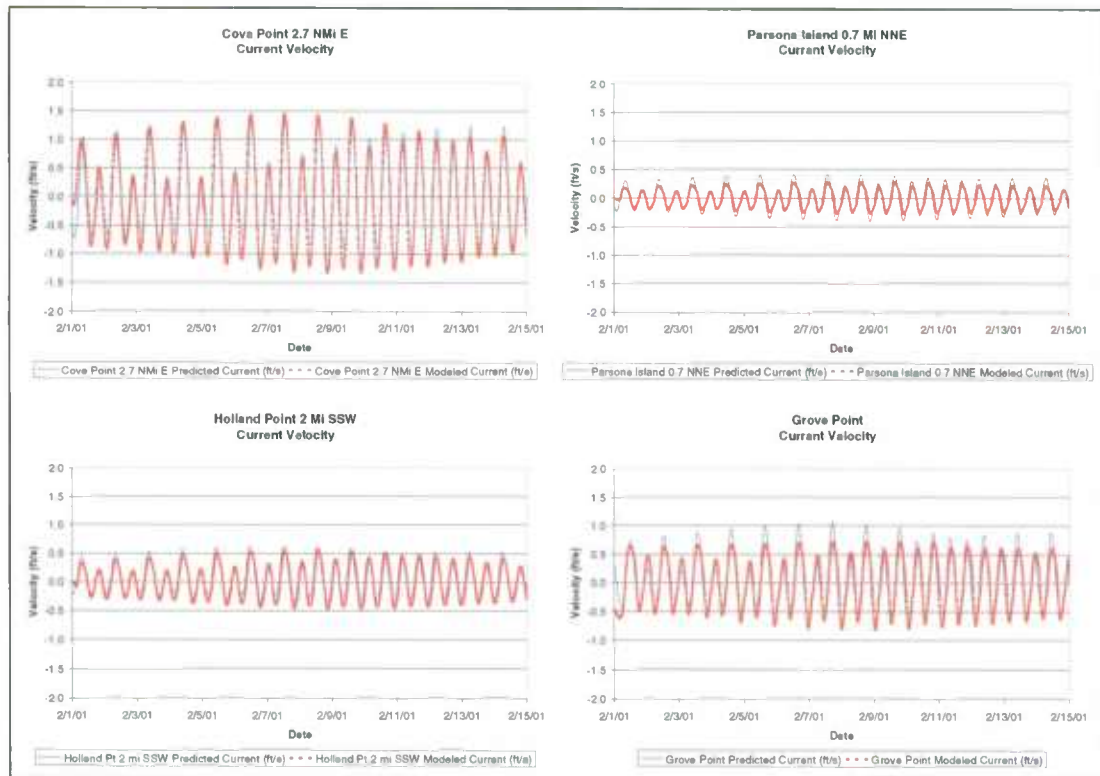
Figure 5-6:   Current Velocity Calibration Results

NORMALIZED SCALE (UNITLESS)

-1.0   -0.8   -0.6   -0.4   -0.2   0   0.2   0.4   0.6   0.8   1.0

EROSION   ACCRETION

Figure 5-7:   Non-Cohesive Sediment – NNW Wind 16 mph – Existing Conditions

Figure 5-8:   Non-Cohesive Sediment - SSE Wind 16 mph - Existing Conditions

NORMALIZED SCALE (UNITLESS)

| -1.0 | -0.8 | -0.6 | -0.4 | -0.2 | 0 | 0.2 | 0.4 | 0.6 | 0.8 | 1.0 |

EROSION   ACCRETION

Figure 5-9:   Non-Cohesive Sediment – WNW Wind 16 mph - Existing Conditions
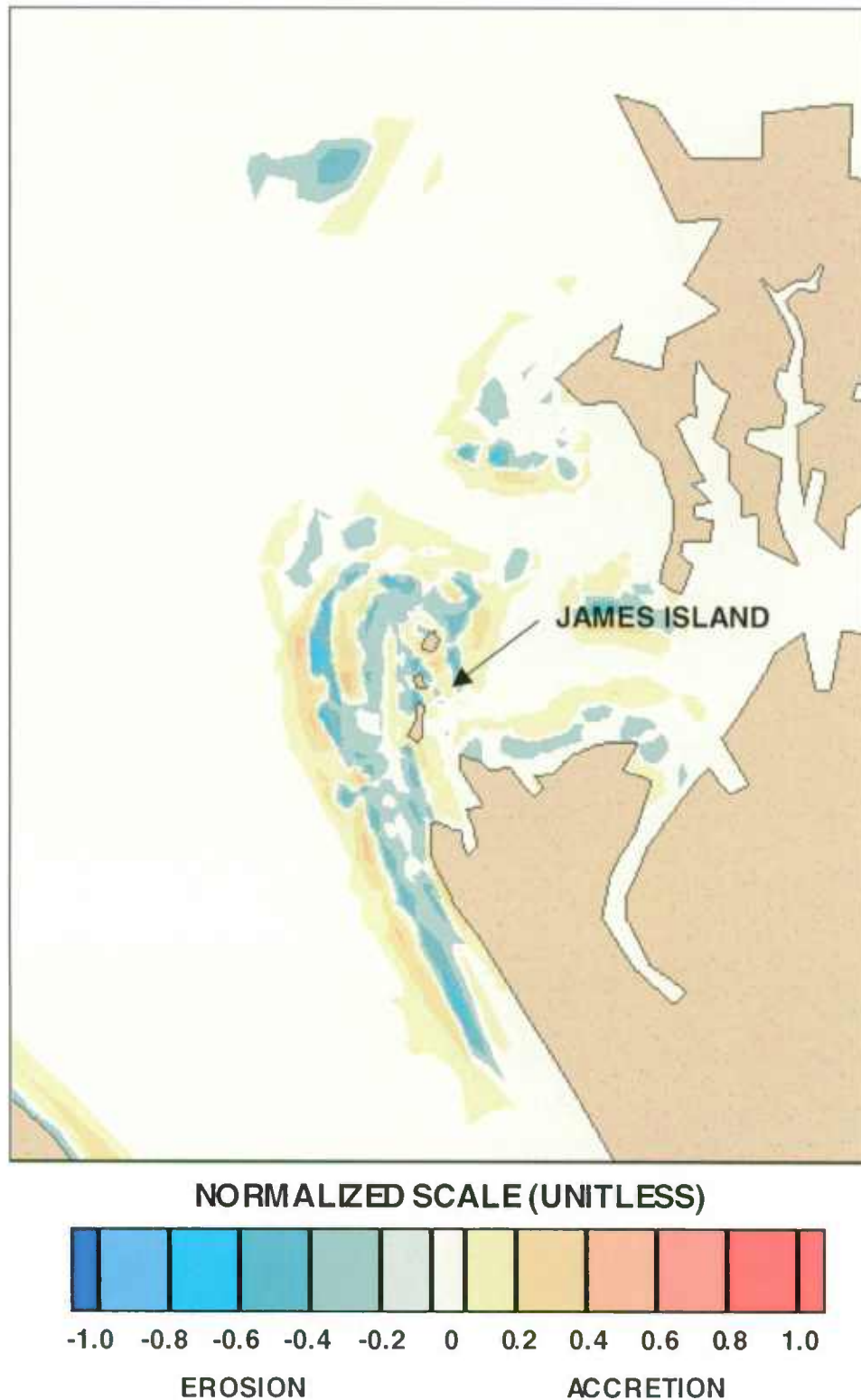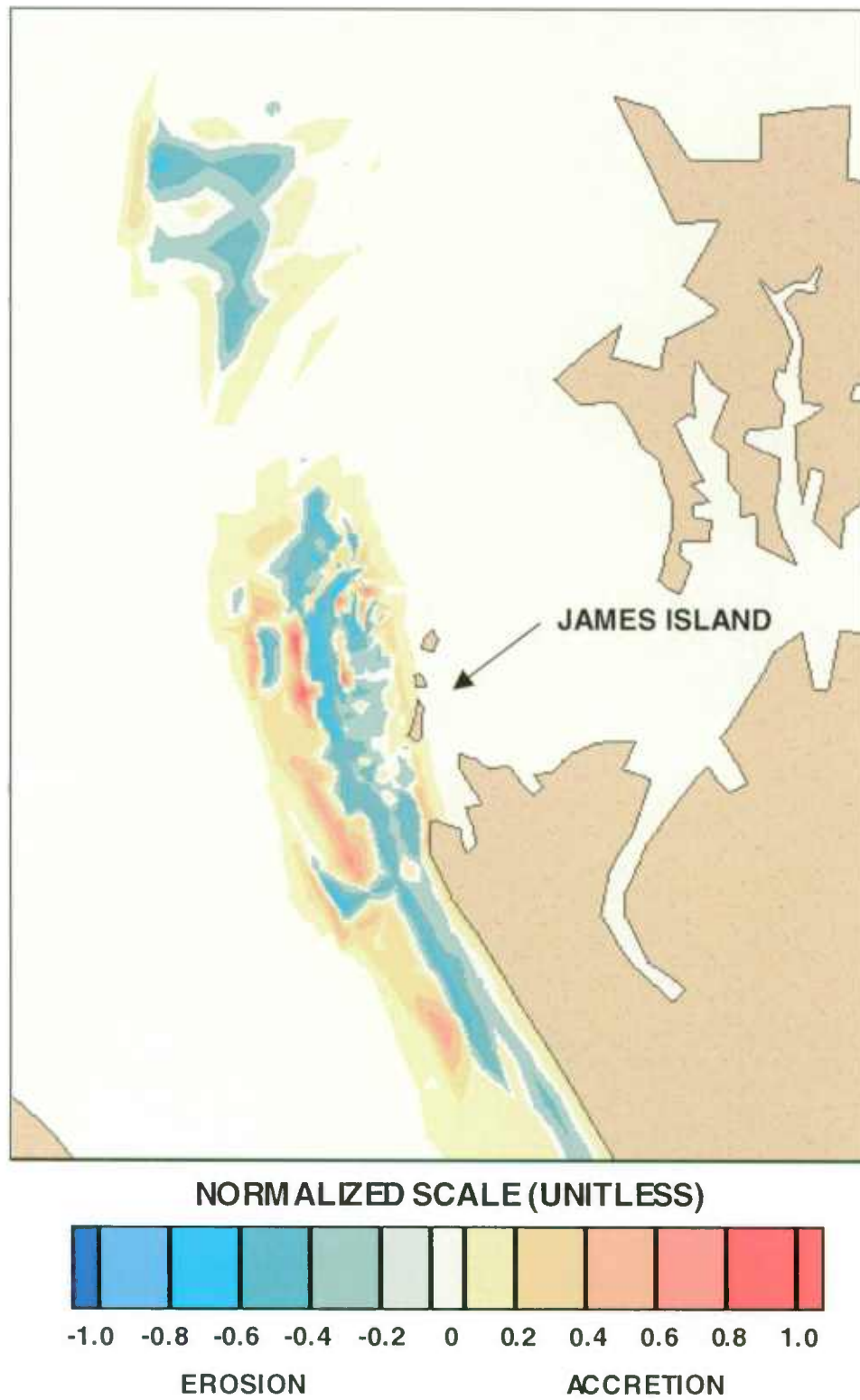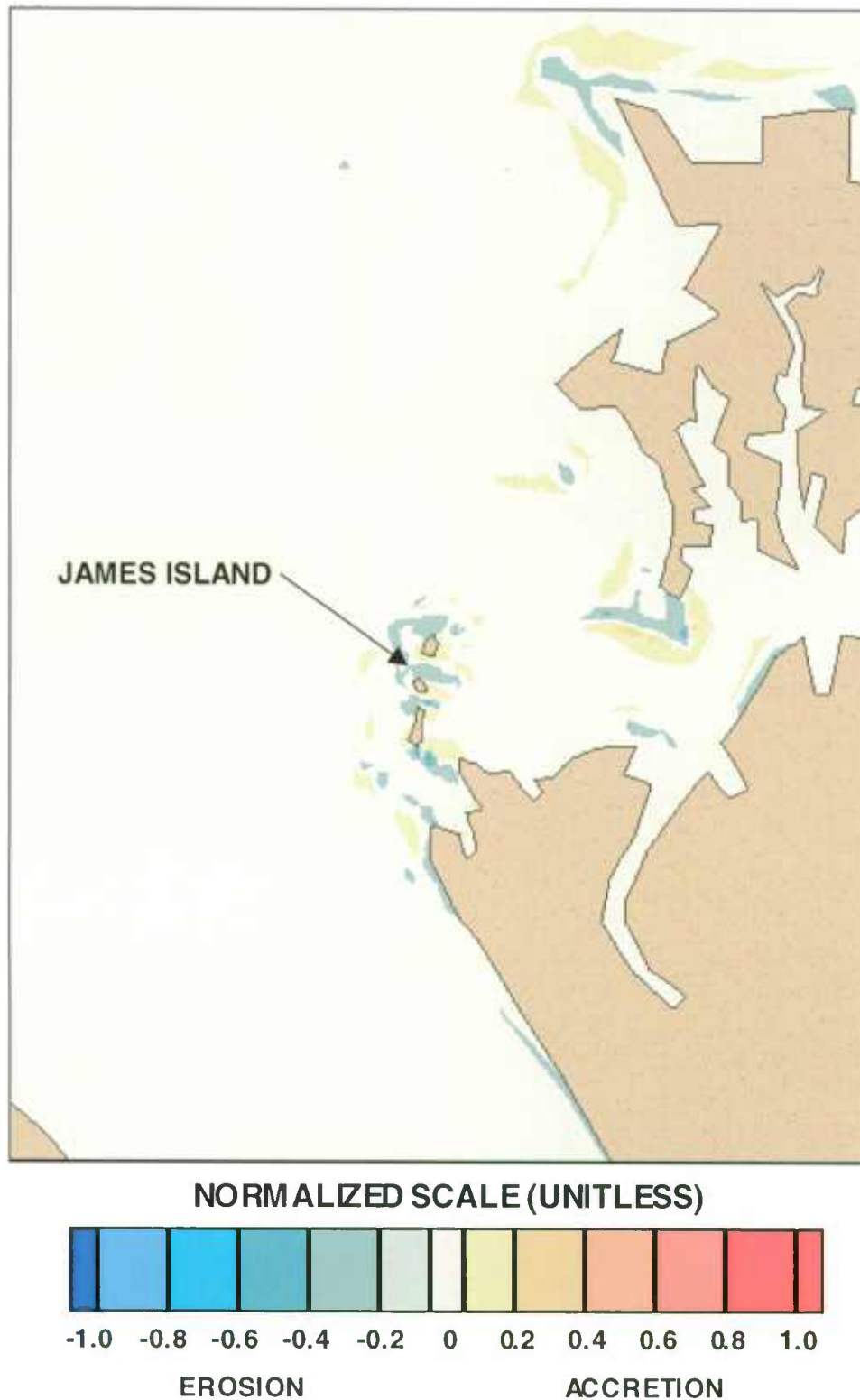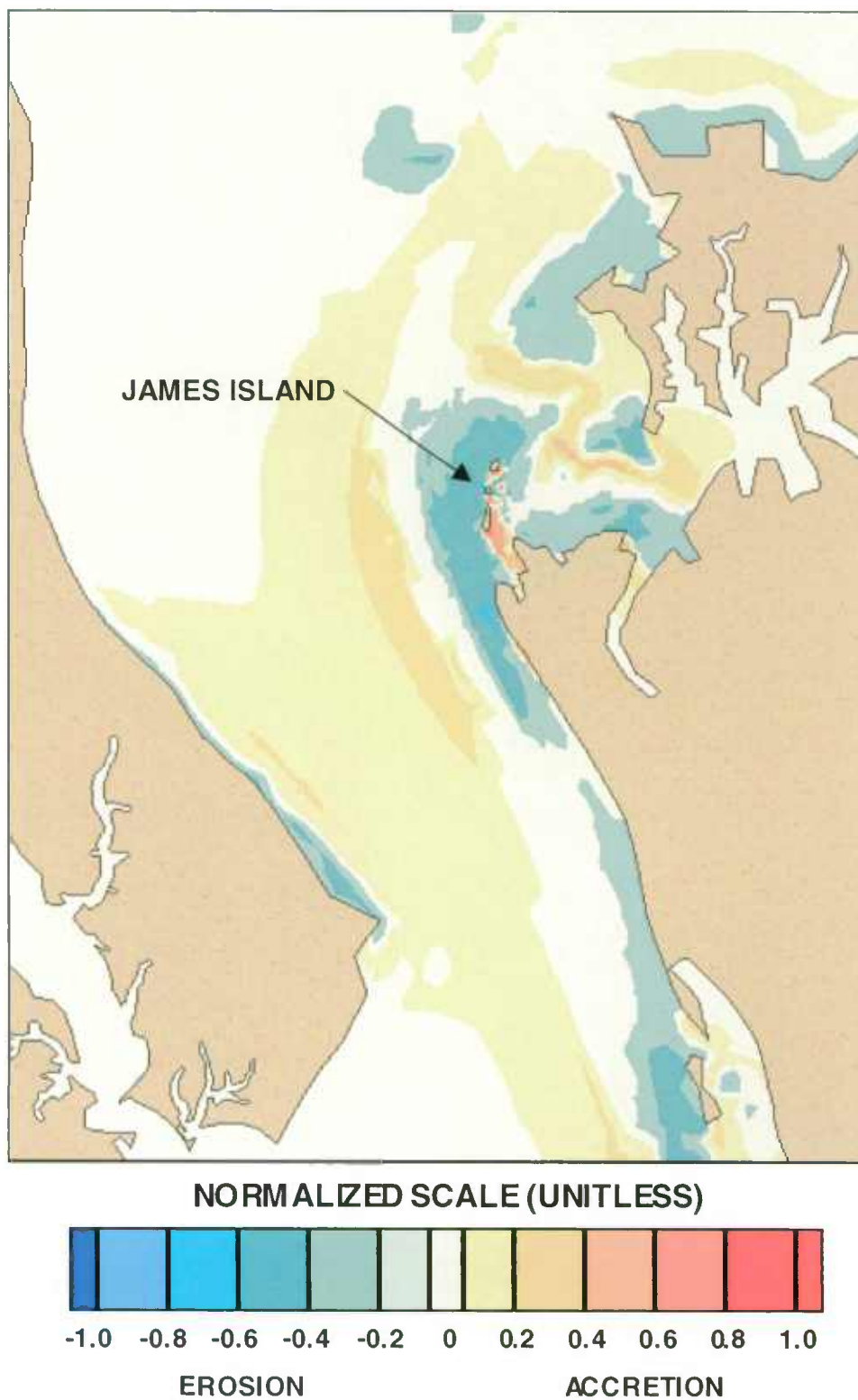
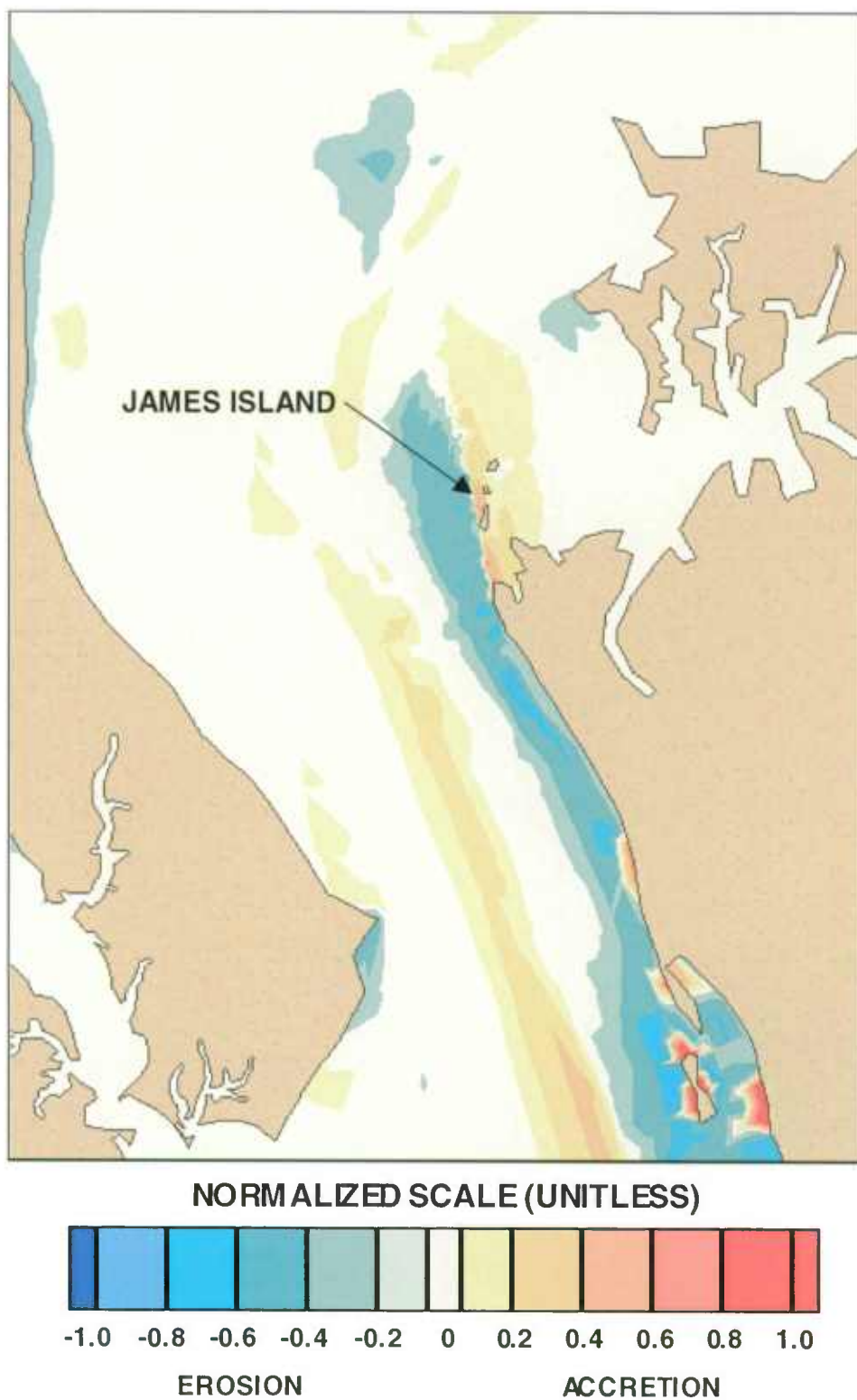Figure 5-10: Cohesive Sediment – NNW Wind 13 mph - Existing Conditions

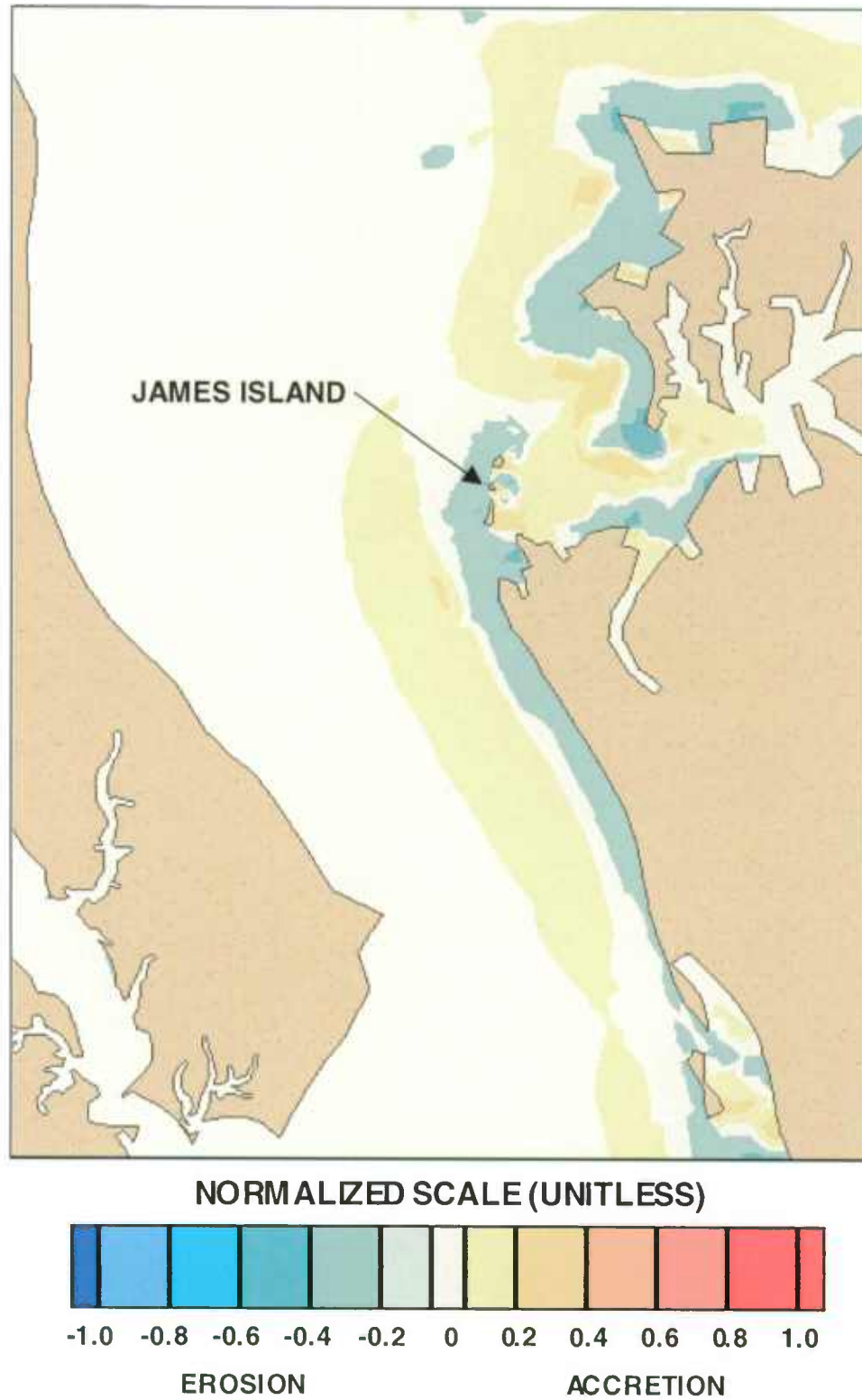Figure 5-11:   Cohesive Sediment – SSE Wind 13 mph - Existing Conditions

Figure 5-12:   Cohesive Sediment – WNW Wind 13 mph - Existing Conditions

6.   HYDRODYNAMIC MODELING RESULTS

6.1   GENERAL

Evaluation of the potential hydrodynamic impacts of the construction of the project at James Island has been conducted using the UCB-FEM model. The UCB-FEM model is used to assess potential impacts by applying identical hydrodynamic input boundary conditions to pre- and post- construction model bathymetry. Hydrodynamic results are then used as input into the sedimentation model which is also run using identical boundary conditions for pre- and post-construction conditions. The input conditions selected represent typical hydrodynamic conditions in the vicinity of James Island.

6.2   HABITAT ISLAND IMPACTS

Existing ebb and flood currents generally flow north and south in the main Bay west of James Island. In the gap between James Island and Taylors Island to the south, however, currents flow generally northeast on flood and southwest on ebb. The main flow into and out of the Little Choptank River generally follows the deeper natural channel around the north end of James Island. At peak flood tide, flow direction at this north end is towards the east, shifting southeast once past the mouth of the river. Ebb flow is reversed from flood; the magnitude of the flow velocities is about the same.

Results of the hydrodynamic simulations are compared numerically at locations north, east and south of the project site and visually for the entire project vicinity. The following sections describe the potential impacts of project construction on hydrodynamics.

6.2.1   Alignment 1

Figure 6-1 shows the location of three comparison stations in the vicinity of James Island and Alignment 1. Plots summarizing water surface elevation and current velocity results for Alignment 1 are presented in Figure 6-2 for these locations. Hydrodynamic model results indicate that projected water surface elevations would be unaffected by construction of the

project. The results are expected as the area of the project is small compared to the Bay. Relatively small impacts, however, do occur to current velocities. Figures 6-3 and 6-4 visually show the predicted differences in peak current velocity in the project area due to construction of the project. Peak ebb and flood currents in the main Bay are not predicted to change should Alignment 1 be constructed. Following construction, predicted flow would be displaced northward and southward, and current velocity would increase both north and south of the project. Predicted current velocity decreases primarily around the existing James Island to the east where flow is blocked by the project. To a lesser extent, velocity decreases are predicted west of the project. Maximum velocity increases are projected at the southeast dike, between the project and the existing southern James Island, and where flow is trained along the northwest dike of the project as it enters the Little Choptank River.

Comparisons of peak current velocity hydrodynamic modeling results between existing conditions and Alignment 1 for the three locations are shown in Figure 6-2 and Table 6-1. Maximum predicted change around existing James Island is about 0.44 ft/sec; a lesser change is predicted in the Little Choptank River.

Table 6-1: Hydrodynamic Modeling Results – Alignment 1				
	Existing Conditions		**Alignment 1**	
	Peak Flood Current (ft/sec)	*Peak Ebb Current (ft/sec)*	*Peak Flood Current (ft/sec)*	*Peak Ebb Current (ft/sec)*
North of Project	0.54	0.46	0.55	0.61
East of Project	0.50	**0.56**	**0.10**	**0.12**
South of Project	**0.32**	**0.32**	**0.74**	**0.72**

6.2.2 Alignment 2

Figure 6-5 shows the location of three comparison stations in the vicinity of James Island and Alignment 2. Plots summarizing predicted water surface elevation and current velocity results

for Alignment 2 are presented in Figure 6-6. As with Alignment 1, hydrodynamic model results predict that water surface elevations would be unaffected by construction of the project, with relatively small impacts to current velocities. Figures 6-7 and 6-8 show the predicted differences in peak current velocity in the project area due to construction of the project. Peak ebb and flood currents in the main Bay are not predicted to change should Alignment 2 be constructed. Following construction, predicted flow would be displaced northward and southward, and current velocity would increase both north and south of the project. Predicted current velocity decreases primarily around the existing James Island to the east where flow is blocked by the project, but the area where velocities are reduced is larger for this alignment than Alignment 1 as the larger project area affords more protection. Smaller velocity decreases are predicted west of the project. Similar to Alignment 1, maximum velocity increases are predicted at the southeast dike between the project and the existing southern James Island, and where flow is trained along the northwest dike of the project as it enters the Little Choptank River.

Comparisons of peak current velocity hydrodynamic modeling results between existing conditions and Alignment 2 for the three locations are shown in Figure 6-6 and Table 6-2. Maximum predicted change around existing James Island is about 0.46 ft/sec; a lesser change is predicted in the Little Choptank River.

Table 6-2: Hydrodynamic Modeling Results – Alignment 2				
	Existing Conditions		Alignment 2	
	Peak Flood Current (ft/sec)	*Peak Ebb Current (ft/sec)*	*Peak Flood Current (ft/sec)*	*Peak Ebb Current (ft/sec)*
North of Project	0.54	0.46	0.66	0.61
East of Project	0.50	**0.56**	**0.08**	**0.10**
South of Project	**0.49**	**0.47**	**0.74**	**0.75**

6.2.3 Alignment 3

Figure 6-9 shows the location of three comparison stations in the vicinity of James Island and Alignment 3, with plots summarizing predicted water surface elevations and current velocities presented in Figure 6-10. As before, results predict that water surface elevations would be unaffected by construction of the project and relatively small impacts occur to current velocities. Figures 6-11 and 6-12 visually show the predicted differences in peak current velocity in the project area due to construction of the project. Peak ebb and flood currents in the main Bay are not predicted to change should Alignment 3 be constructed. Following construction, flow is predicted to be displaced northward and southward, and current velocity is predicted to increase both north and south of the project. Current velocity decreases are predicted around the existing James Island to the east similarly to Alignment 2, and smaller velocity decreases are also predicted west of the project. Maximum velocity increases are predicted at the southeast dike between the project and the existing southern James Island, however, as this alignment extends further south, the increase in velocity is concentrated at the tip of the dike and extends to Taylors Island. Increase in velocity is also predicted where flow is trained along the northwest dike of the project as it enters the Little Choptank River.

Comparisons of peak current velocity hydrodynamic modeling results between existing conditions and Alignment 3 for the three locations are shown in Figure 6-10 and Table 6-3. Maximum predicted change around existing James Island is about 0.49 ft/sec; a lesser change is predicted in the Little Choptank River.

Table 6-3: Hydrodynamic Modeling Results – Alignment 3

	Existing Conditions		Alignment 3	
	Peak Flood Current (ft/sec)	*Peak Ebb Current (ft/sec)*	*Peak Flood Current (ft/sec)*	*Peak Ebb Current (ft/sec)*
North of Project	0.54	0.46	0.67	0.63
East of Project	0.50	**0.56**	**0.05**	**0.07**
South of Project	**0.53**	0.52	**0.81**	**0.82**

6.2.4   Alignment 4

Figure 6-13 shows the location of three comparison stations in the vicinity of James Island and Alignment 4, with plots summarizing predicted water surface elevation and current velocity results presented in Figure 6-14. As before, results predict that water surface elevations would be unaffected by construction of the project with relatively small impacts to current velocities. Figures 6-15 and 6-16 visually show the predicted differences in peak current velocity in the project area due to construction of the project. Peak ebb and flood currents in the main Bay are not predicted to change should Alignment 4 be constructed. Following construction, flow is predicted to be displaced northward and southward, and current velocity would increase both north and south of the project. Current velocity decreases are predicted primarily around the existing James Island to the east where flow is blocked by the project. This alignment provides the most protection to James Island and thus provides the greatest decrease in velocity. To a lesser extent, velocity decreases are predicted west of the project. This alignment also extends furthest south towards Taylors Island, and maximum velocity increases are predicted at the southeast dike between the project and Taylors Island. This predicted increase in velocity is greatest among all alignments. Velocity also is predicted to increase where flow is trained along the northwest dike of the project as it enters the Little Choptank River.

Comparisons of peak current velocity hydrodynamic modeling results between existing conditions and Alignment 4 for the three locations are shown in Figure 6-14 and Table 6-4. Maximum predicted change around existing James Island is about 0.50 ft/sec; a lesser change is predicted in the Little Choptank River.

Table 6-4: Hydrodynamic Modeling Results – Alignment 4				
	Existing Conditions		**Alignment 4**	
	Peak Flood Current (ft/sec)	*Peak Ebb Current (ft/sec)*	*Peak Flood Current (ft/sec)*	*Peak Ebb Current (ft/sec)*
North of Project	0.54	0.46	0.69	0.65
East of Project	0.50	**0.56**	**0.05**	**0.06**
South of Project	**0.54**	**0.59**	**0.92**	**1.00**

6.2.5   Alignment 5

Figure 6-17 shows the location of three comparison stations in the vicinity of James Island and Alignment 5, with plots summarizing predicted water surface elevation and current velocity results presented in Figure 6-18. As for all cases, results predict that water surface elevations would be unaffected by construction of the project and small impacts occur to current velocities. Figures 6-19 and 6-20 visually show the predicted differences in peak current velocity in the project area due to construction of the project. Peak ebb and flood currents in the main Bay are not predicted to change should Alignment 5 be constructed. Following construction, flow is predicted to be displaced northward and southward, and current velocity is predicted to increase both north and south of the project. Current velocity decreases are predicted primarily around the existing James Island to the east where flow is blocked by the project; the reduction in velocity is similar to Alignments 2 and 3. To a lesser extent, velocity decreases are predicted west of the project. Maximum velocity increases are predcited at the southeast dike between the project and the existing southern James Island, similar to Alignment 2 as these both have southern boundaries about the same location. Velocity increases are also predicted where flow is trained along the northwest dike of the project as it enters the Little Choptank River.

Comparisons of peak current velocity hydrodynamic modeling results between existing

conditions and Alignment 5 for the three locations are shown in Figure 6-18 and Table 6-5. Maximum predicted change around existing James Island is about 0.48 ft/sec; a lesser change is predicted in the Little Choptank River.

Table 6-5: Hydrodynamic Modeling Results – Alignment 5				
	Existing Conditions		**Alignment 5**	
	Peak Flood Current (ft/sec)	*Peak Ebb Current (ft/sec)*	*Peak Flood Current (ft/sec)*	*Peak Ebb Current (ft/sec)*
North of Project	0.54	0.46	0.66	0.62
East of Project	0.50	**0.56**	**0.06**	**0.08**
South of Project	**0.50**	0.52	0.84	0.92
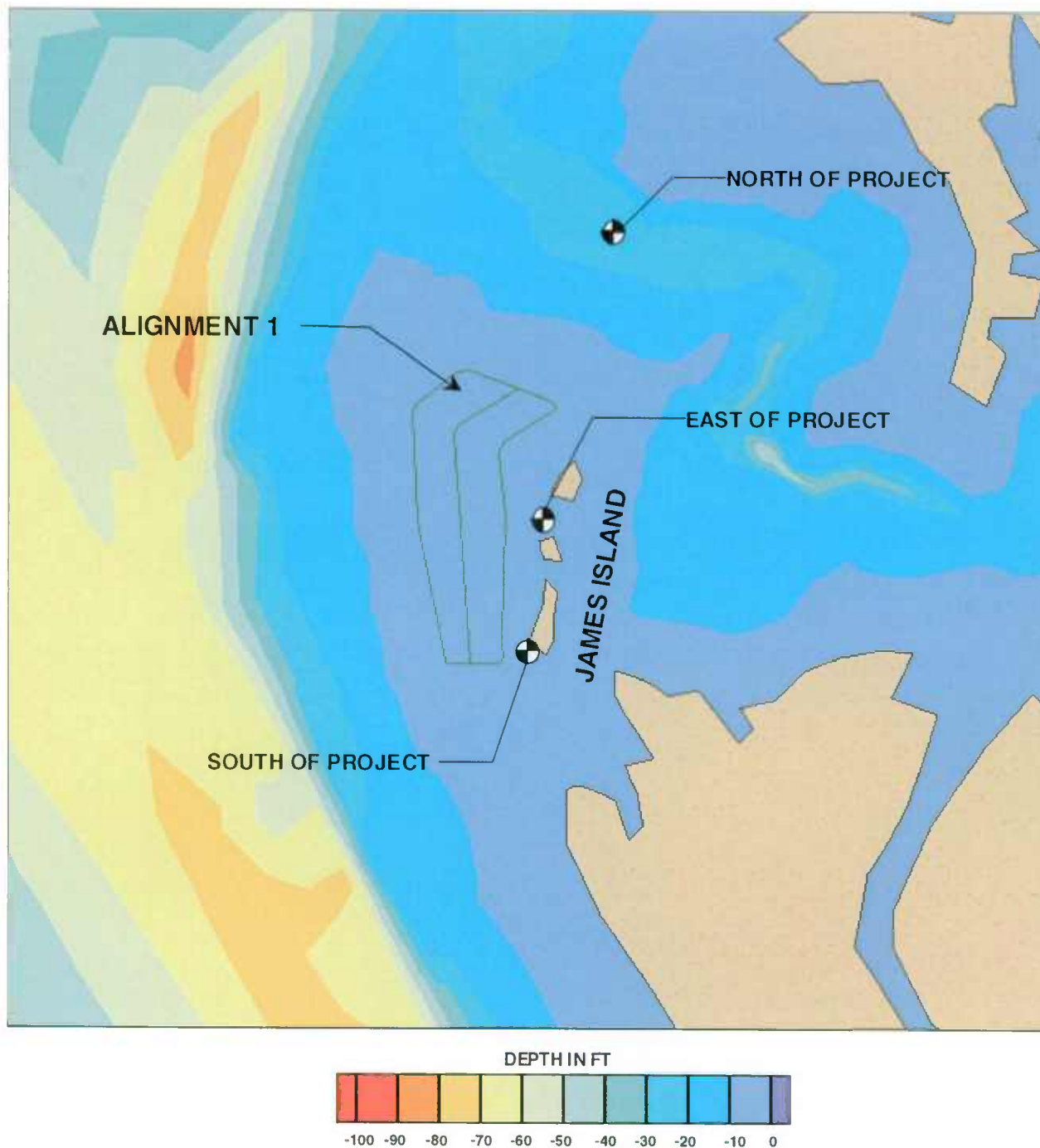
Figure 6-1:   Results Comparison Locations for Alignment 1
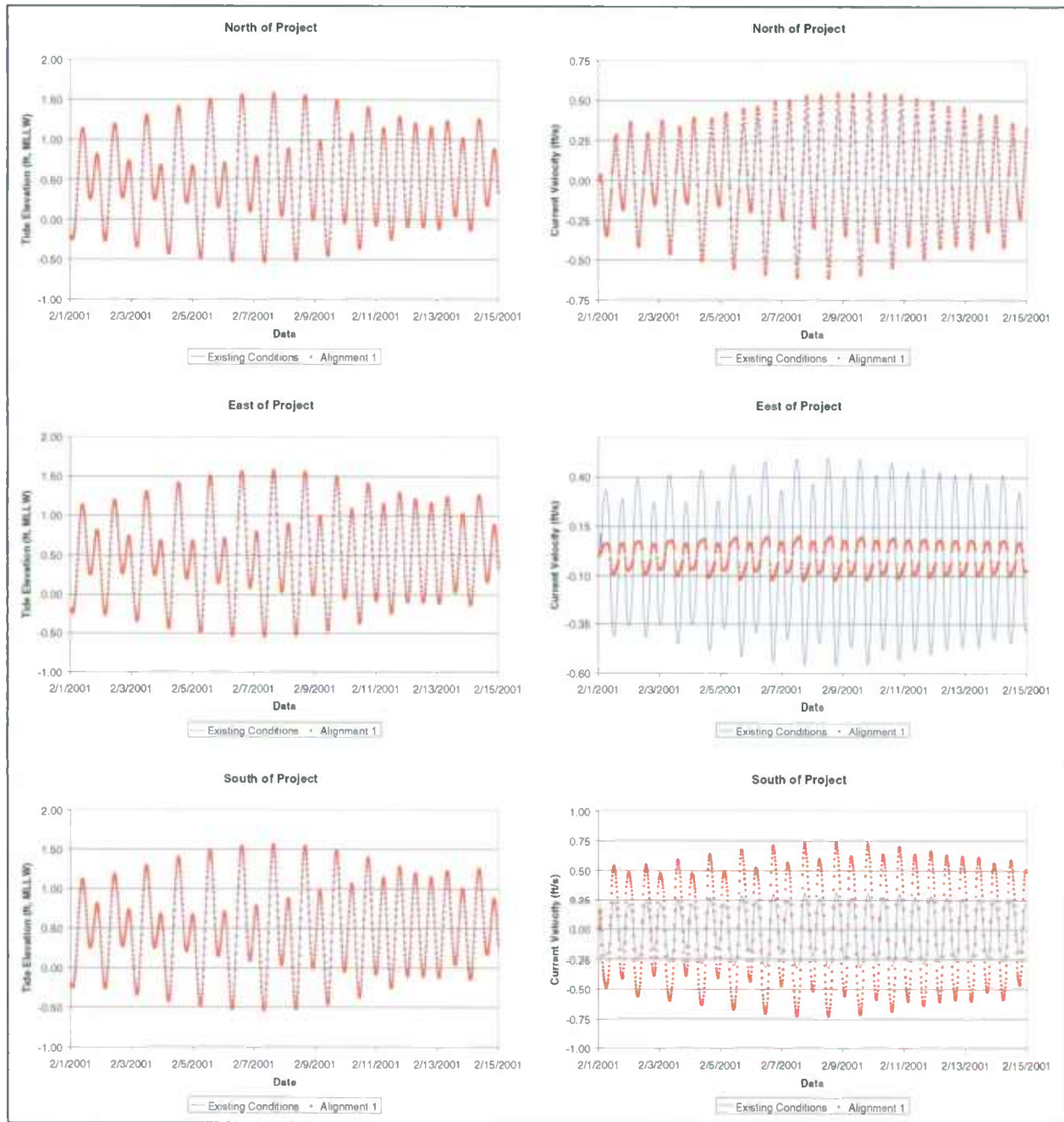
Figure 6-2:   James Island Tidal Results Comparison for Alignment 1

Figure 6-5:   Results Comparison Locations for Alignment 2

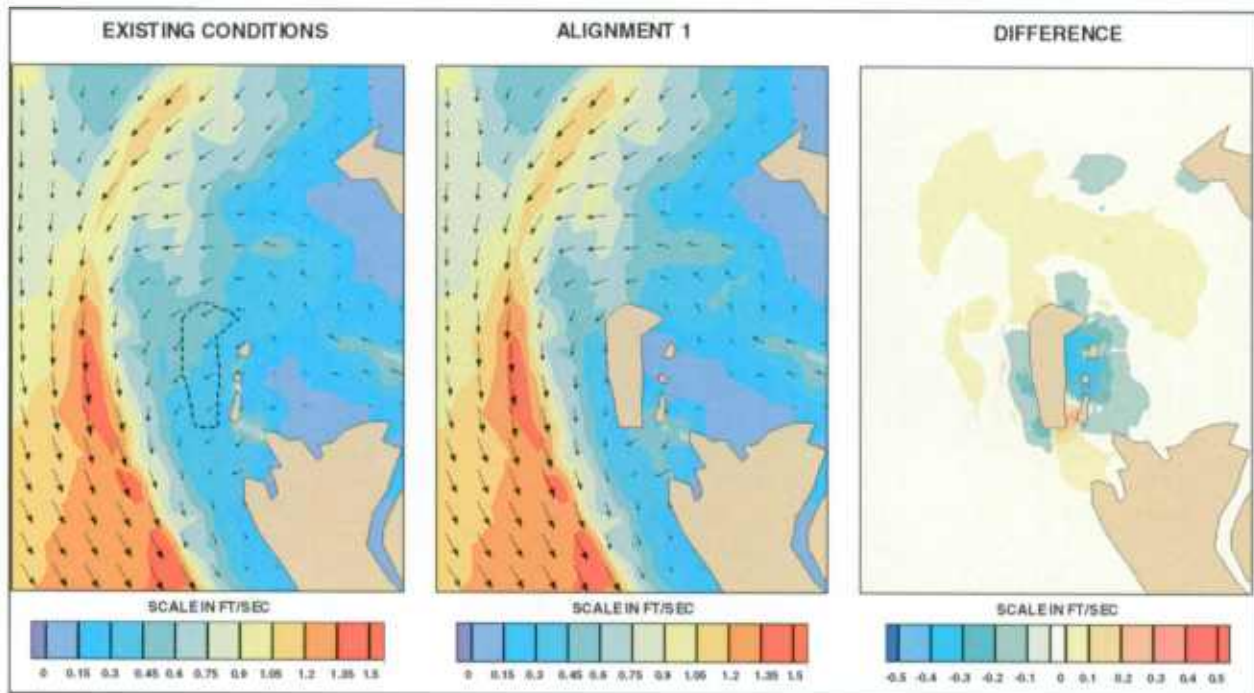**Figure 6-6:   James Island Tidal Results Comparison for Alignment 2**

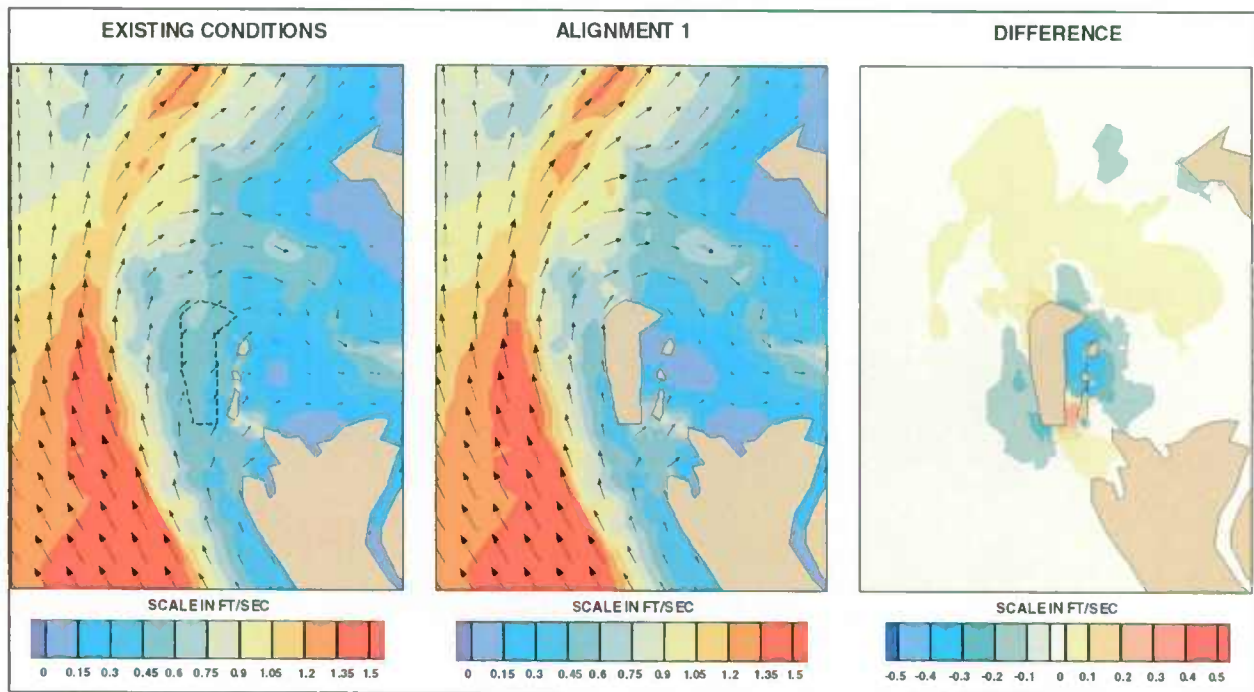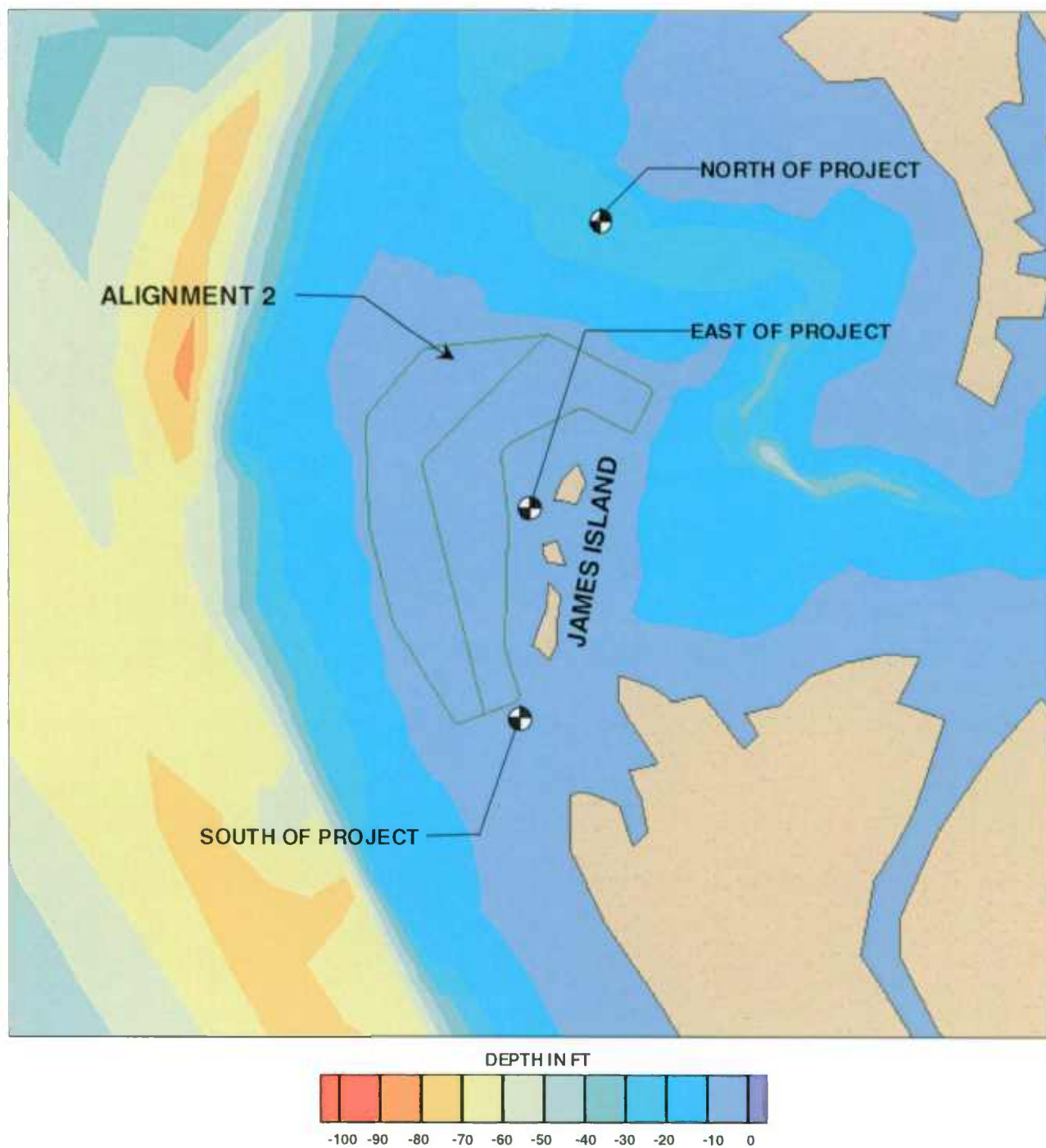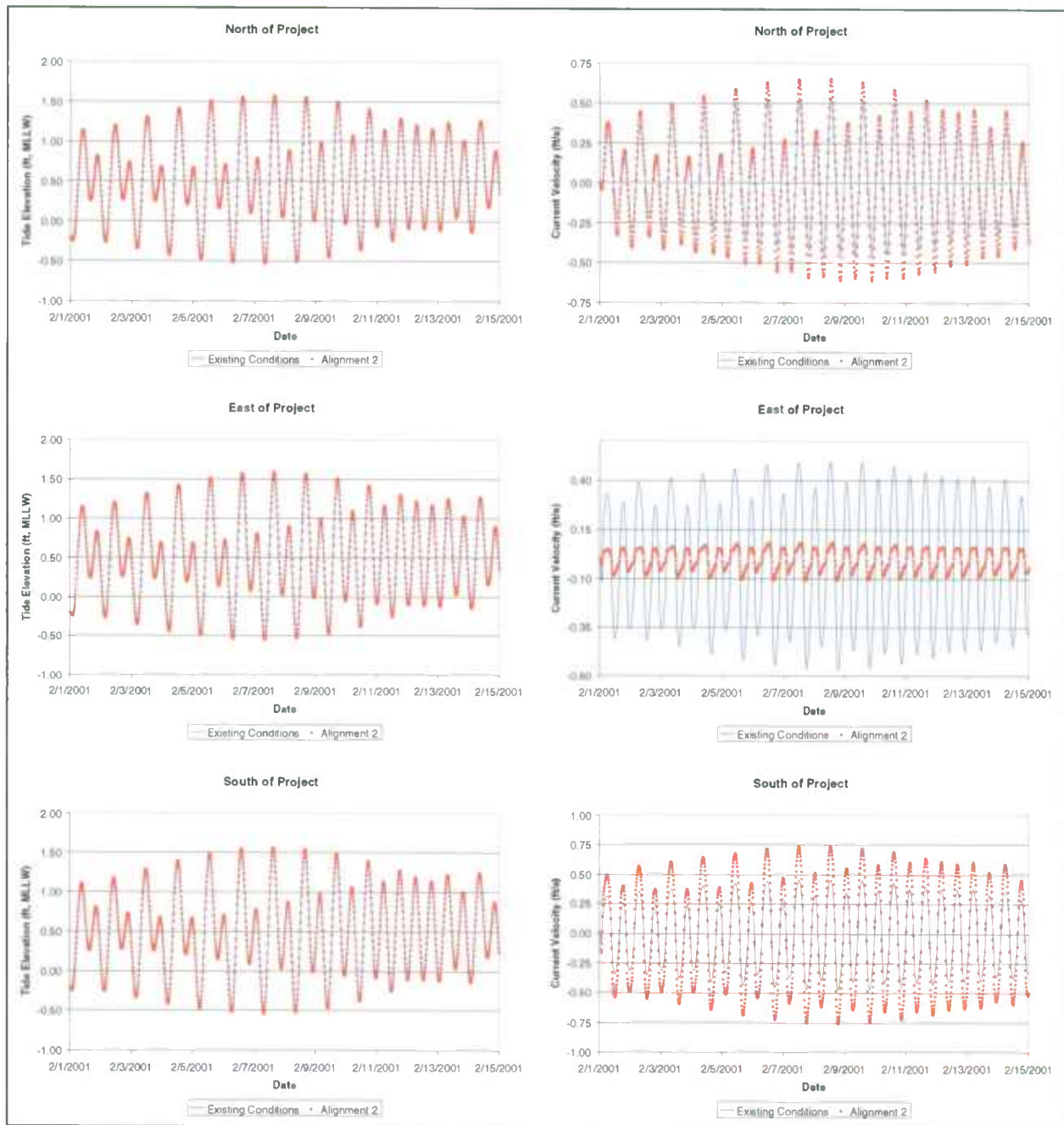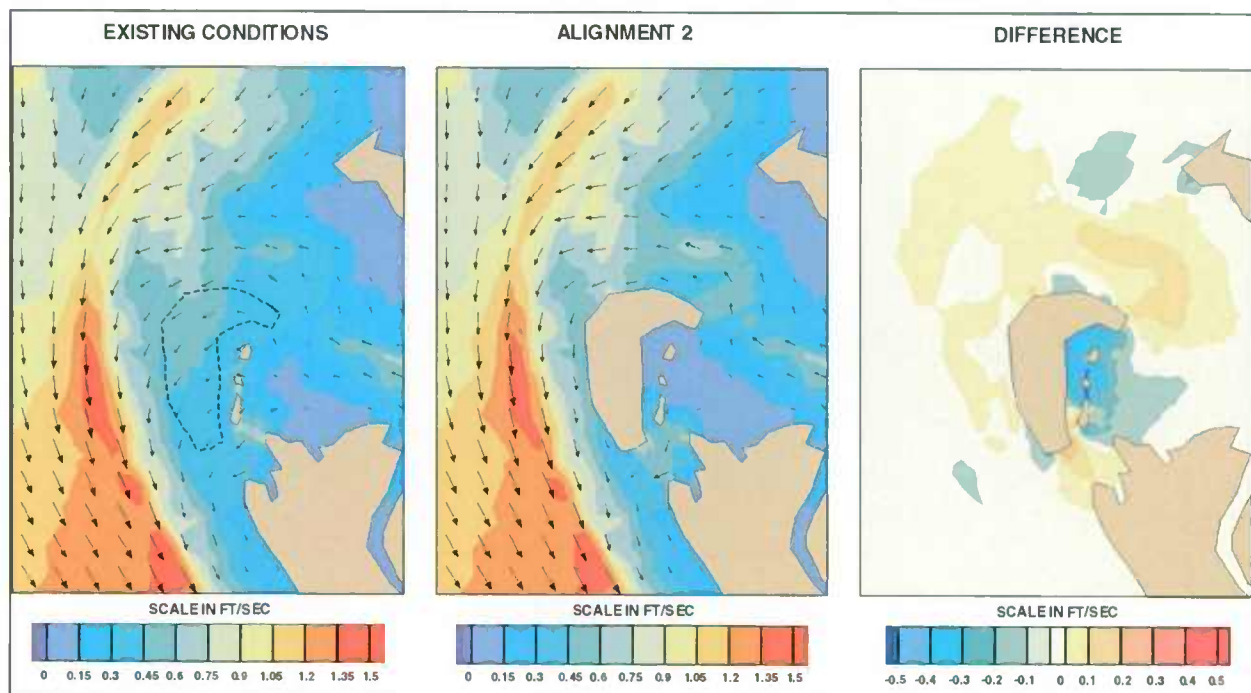**Figure 6-7:   Peak Ebb Current Velocity – Alignment 2 vs. Existing Conditions**
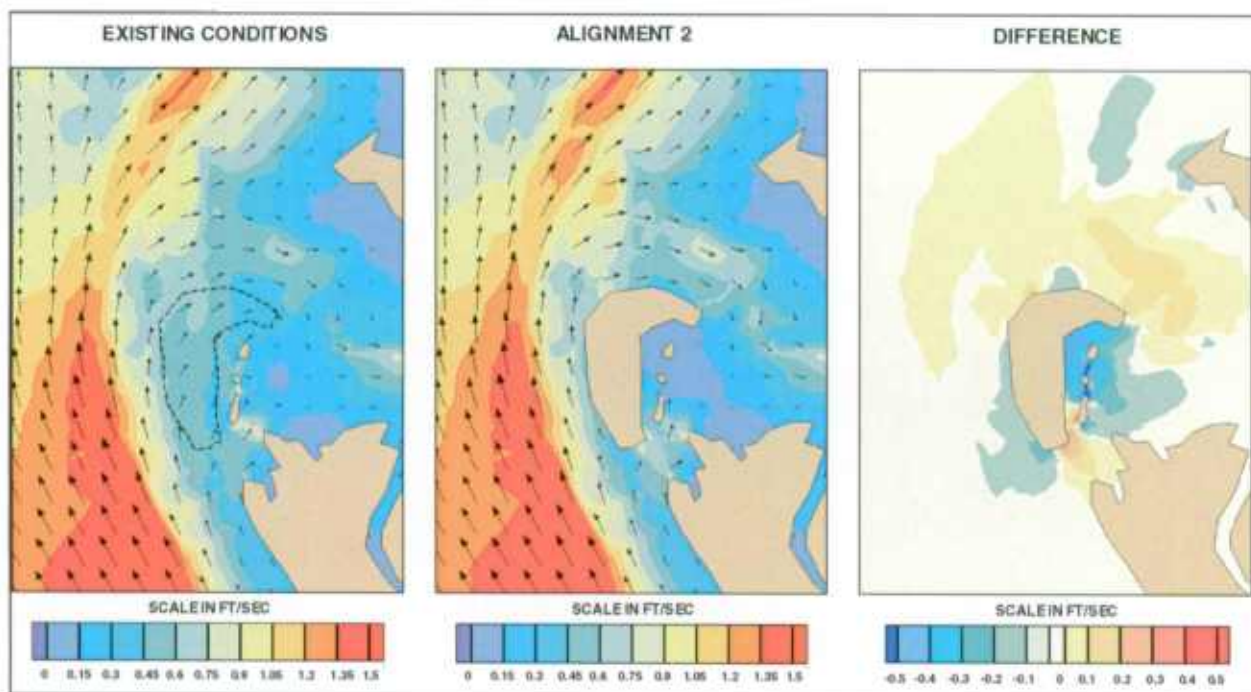
Figure 6-8:   Peak Flood Current Velocity – Alignment 2 vs. Existing Conditions

Figure 6-9:   Results Comparison Locations for Alignment 3

Figure 6-10: James Island Tidal Results Comparison for Alignment 3

Figure 6-11:   Peak Ebb Current Velocity – Alignment 3 vs. Existing Conditions

Figure 6-12:   Peak Flood Current Velocity – Alignment 3 vs. Existing Conditions
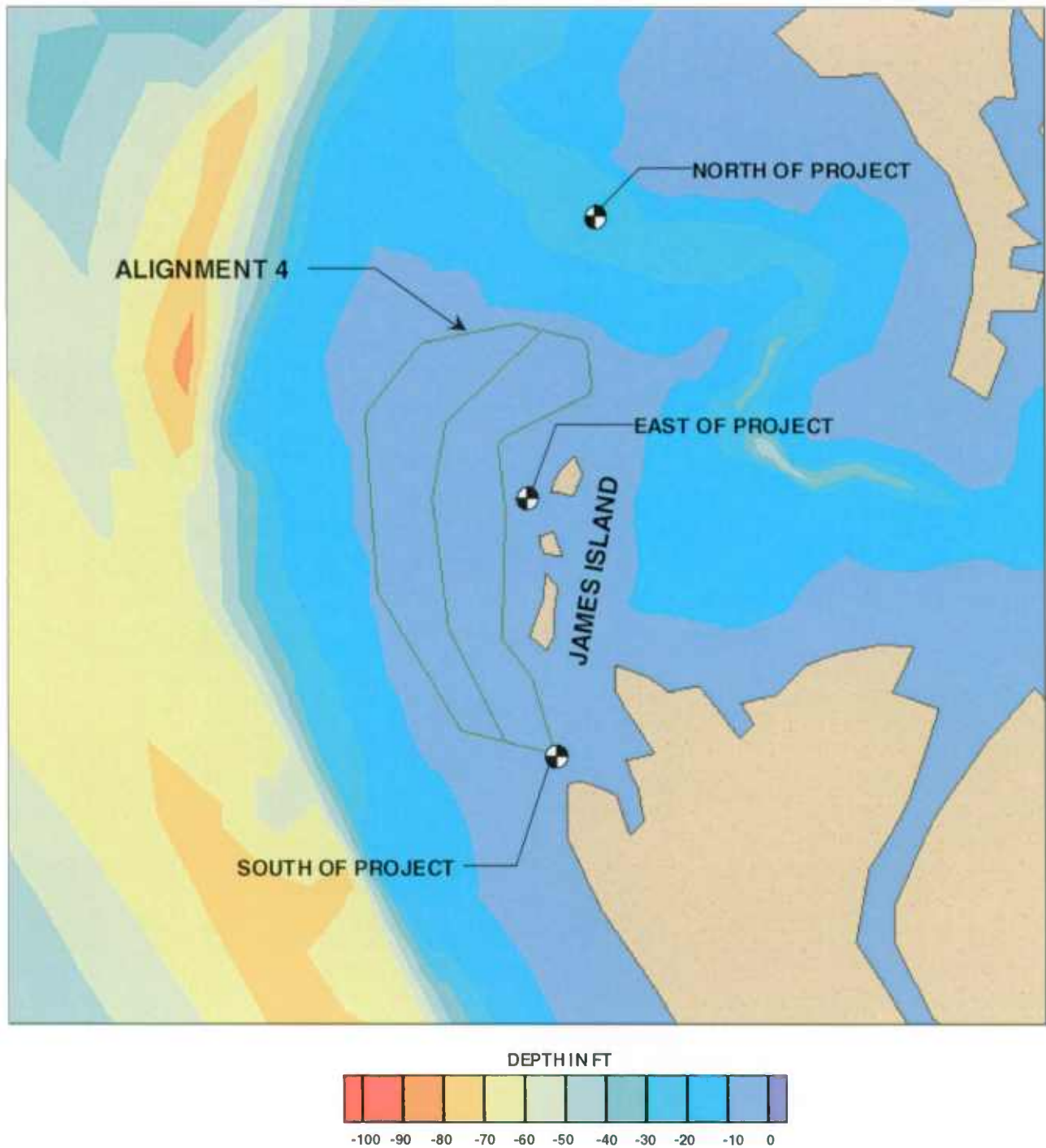
Figure 6-13:   Results Comparison Locations for Alignment 4

Figure 6-14:   James Island Tidal Results Comparison for Alignment 4

Figure 6-15:   Peak Ebb Current Velocity – Alignment 4 vs. Existing Conditions

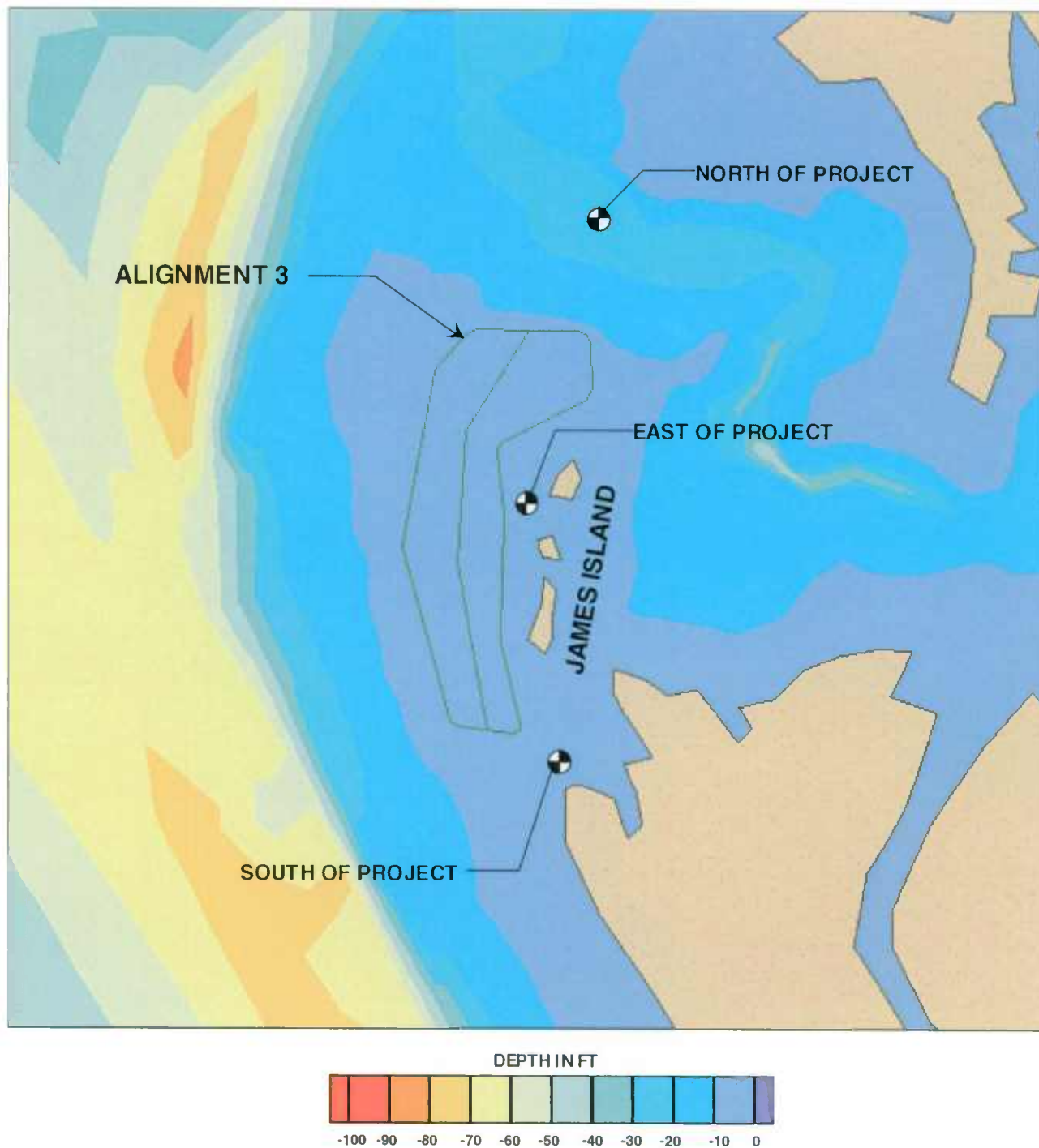**Figure 6-16:   Peak Flood Current Velocity – Alignment 4 vs. Existing Conditions**

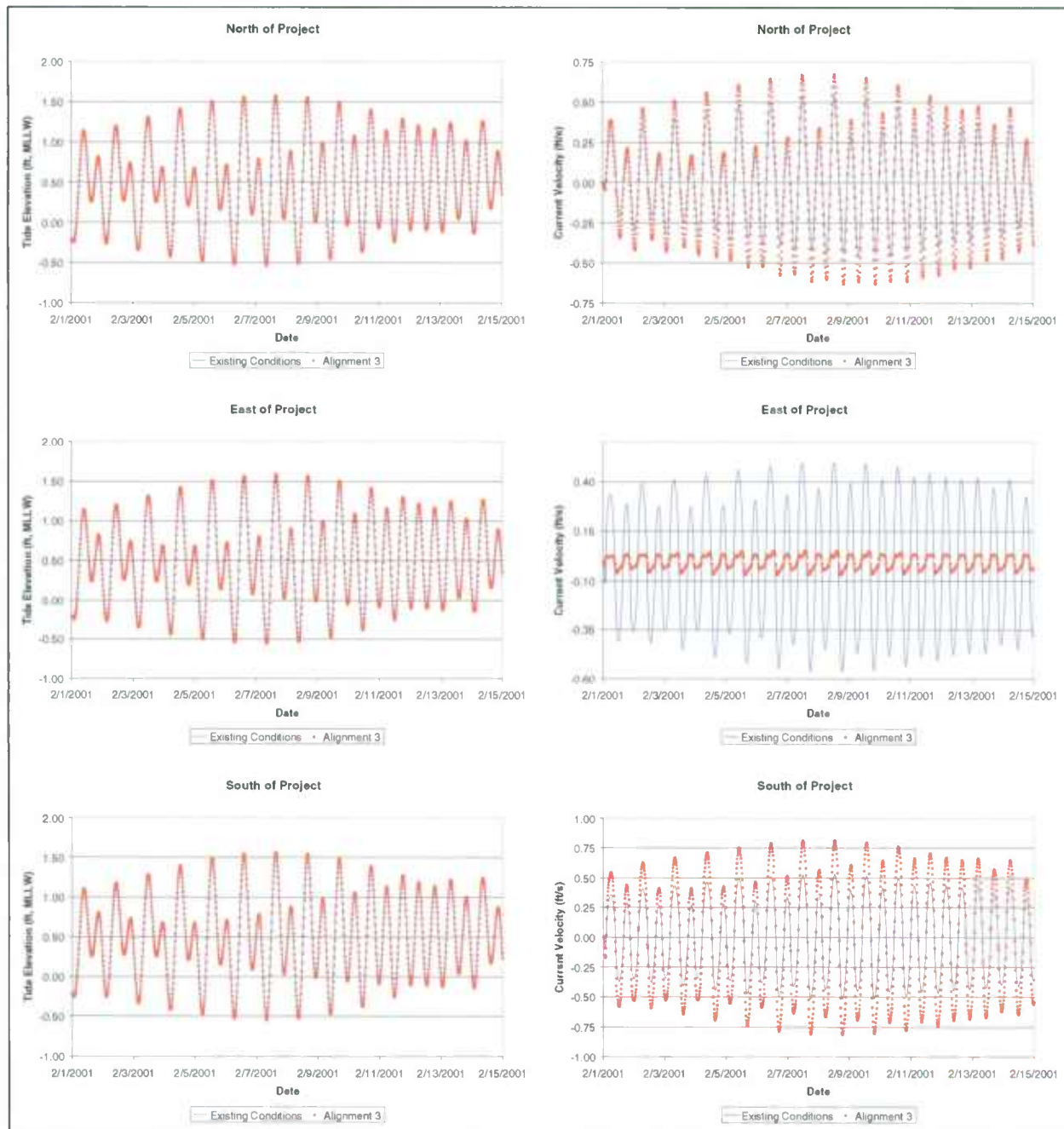**Figure 6-17: Results Comparison Locations for Alignment 5**

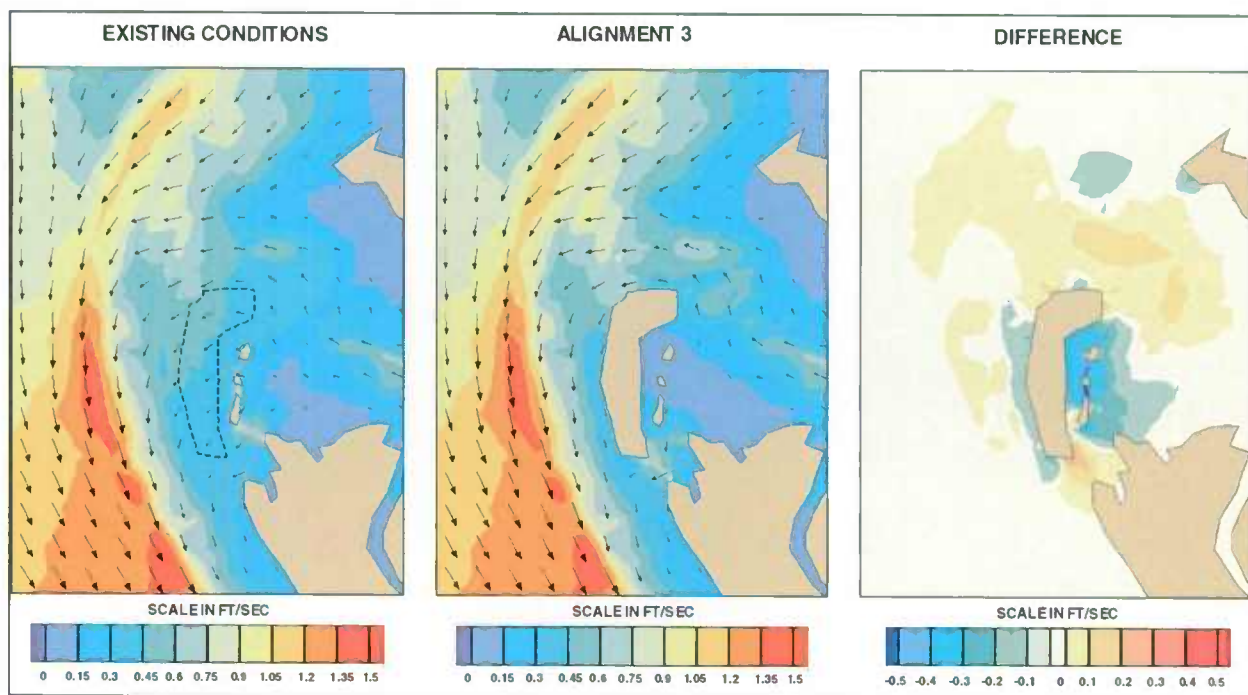**Figure 6-18: James Island Tidal Results Comparison for Alignment 5**

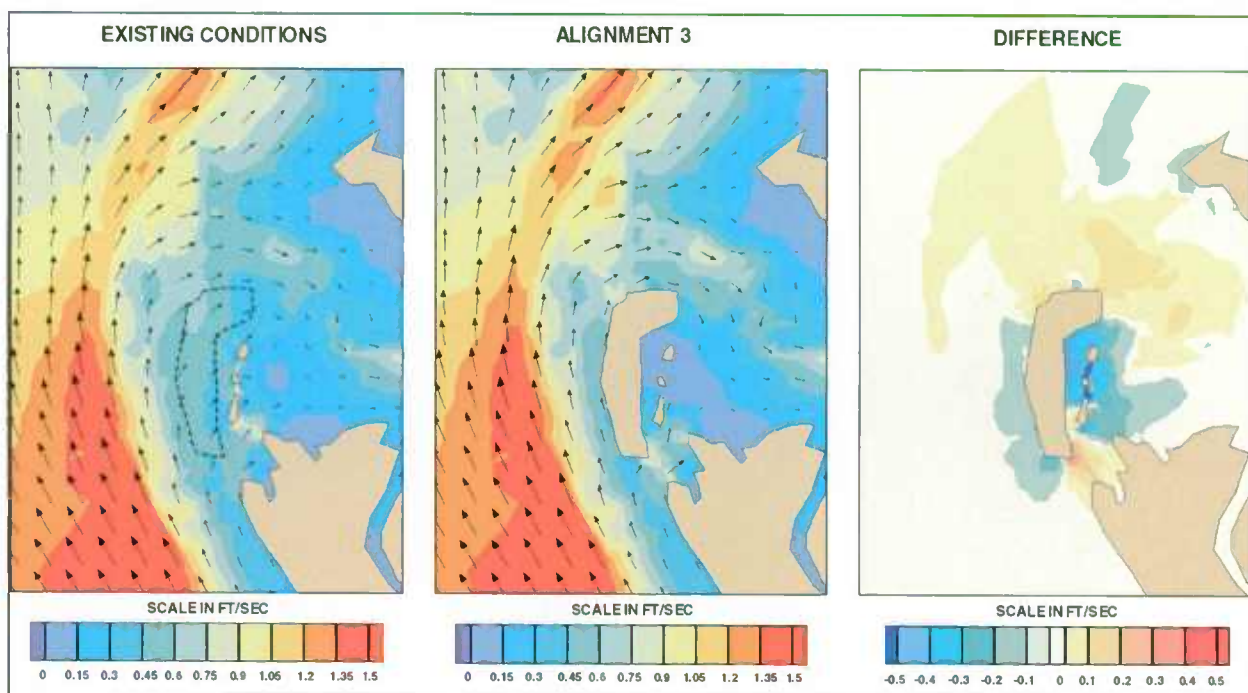**Figure 6-19:   Peak Ebb Current Velocity – Alignment 5 vs. Existing Conditions**

Figure 6-20:   Peak Flood Current Velocity – Alignment 5 vs. Existing Conditions
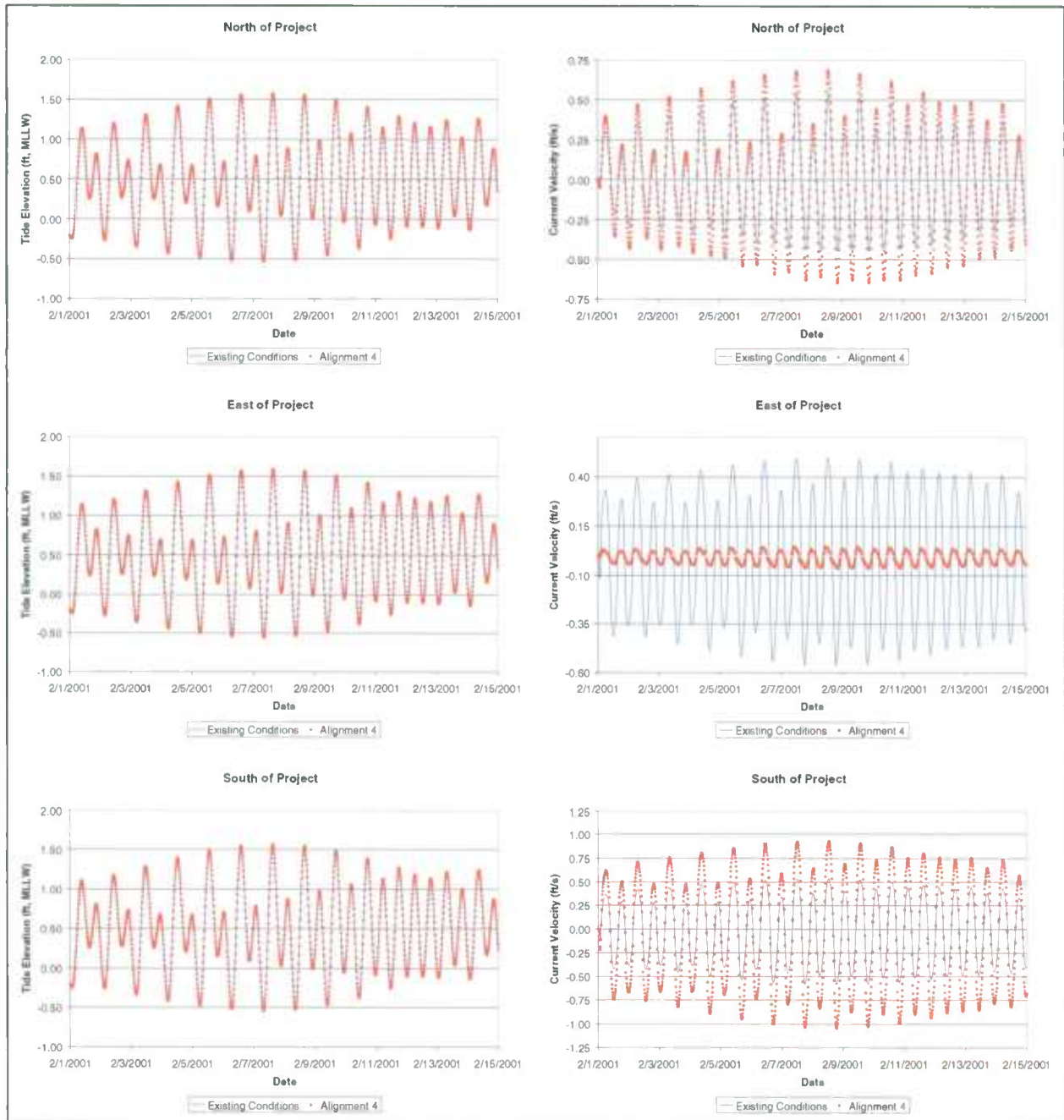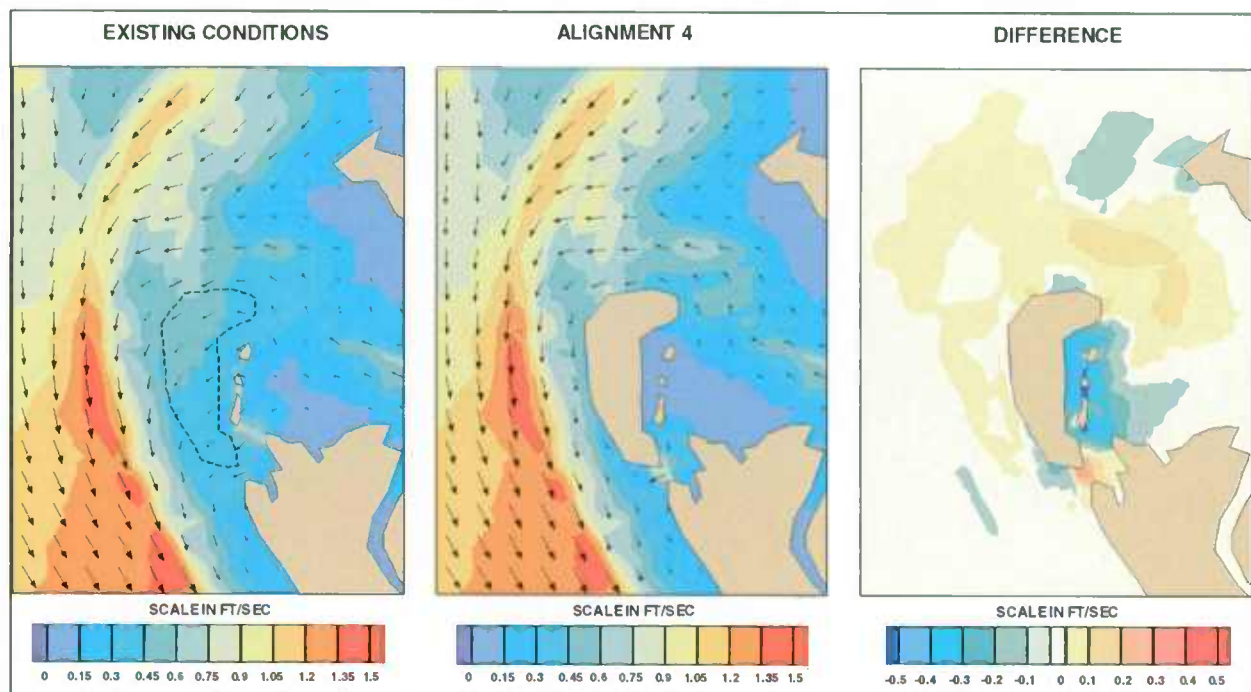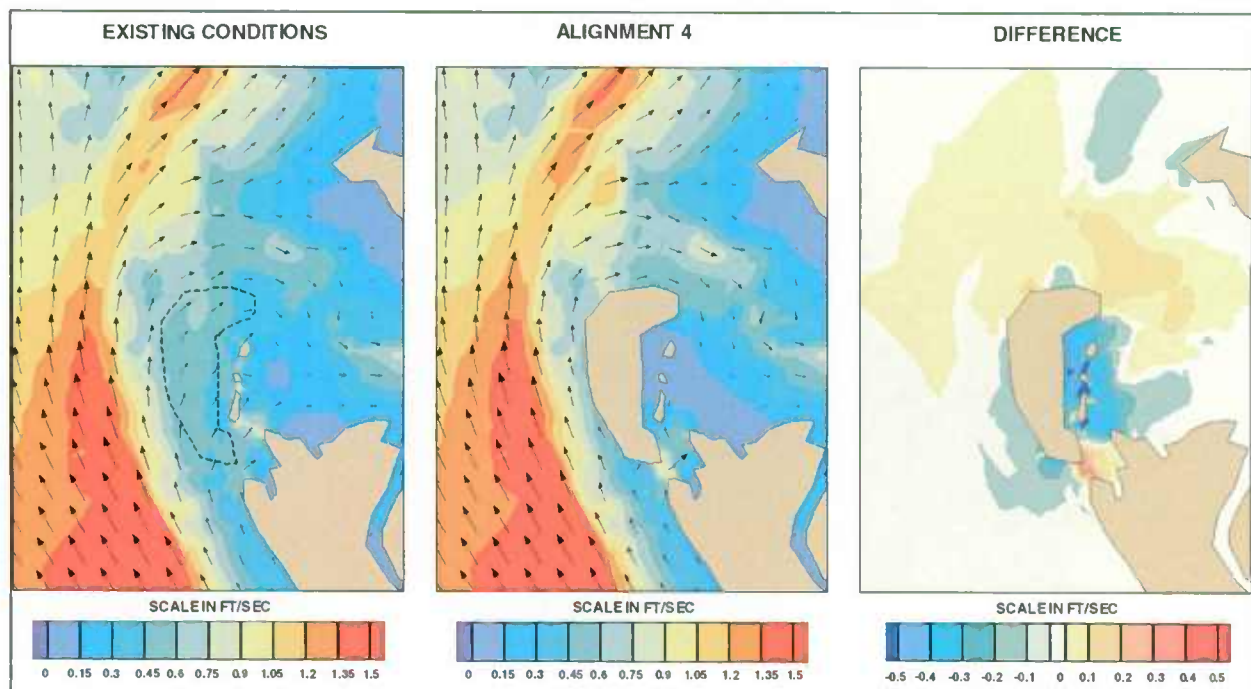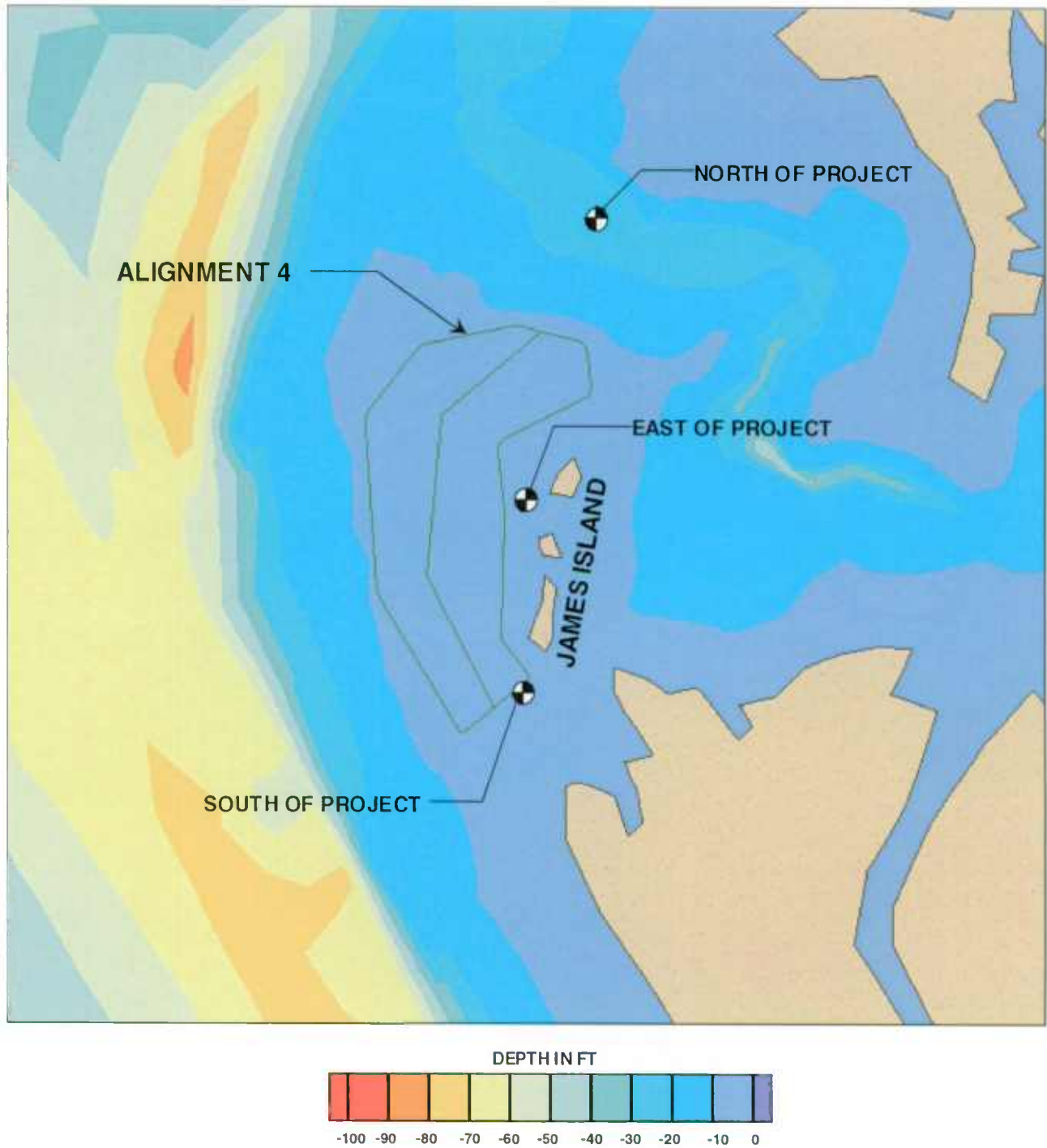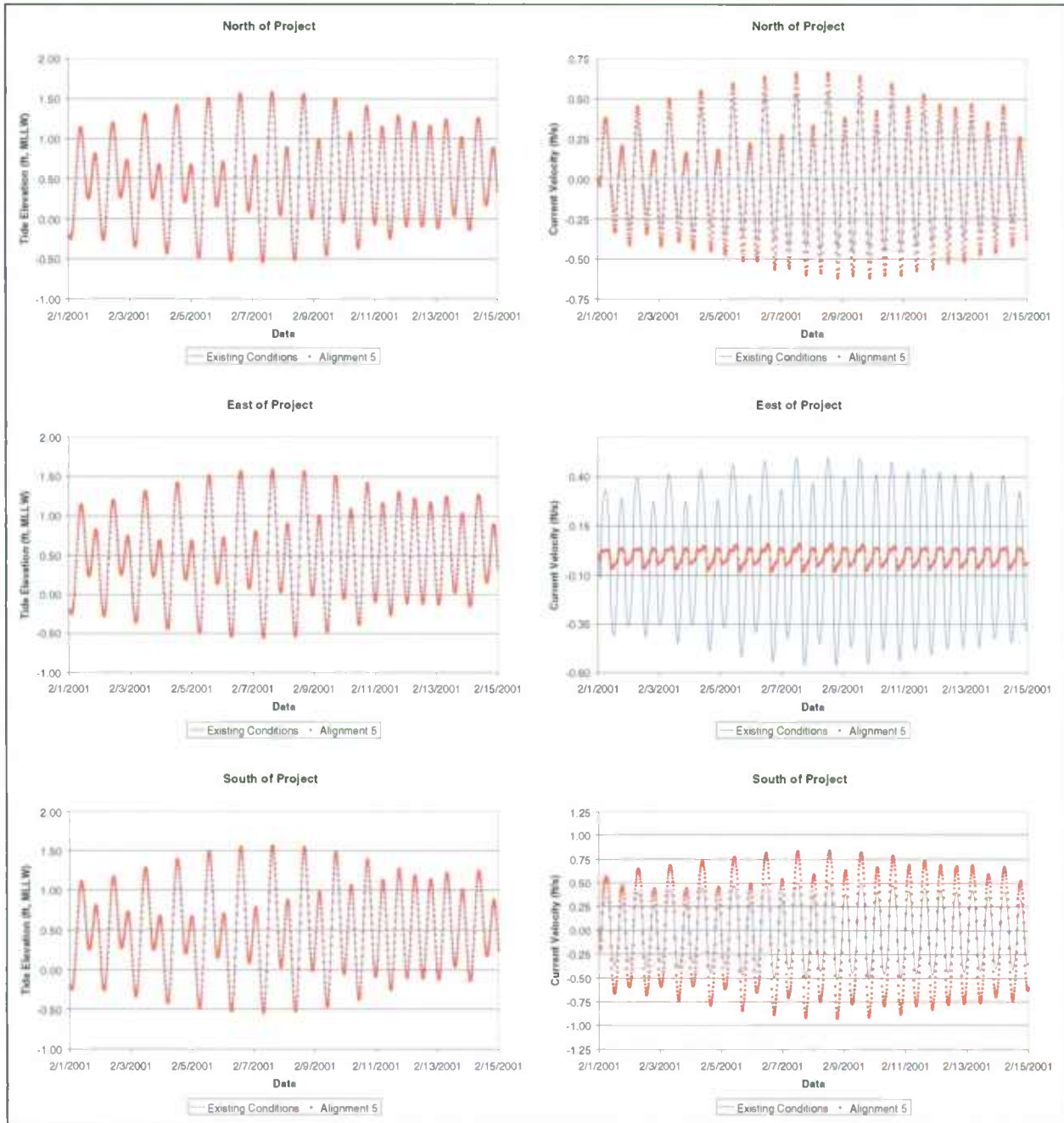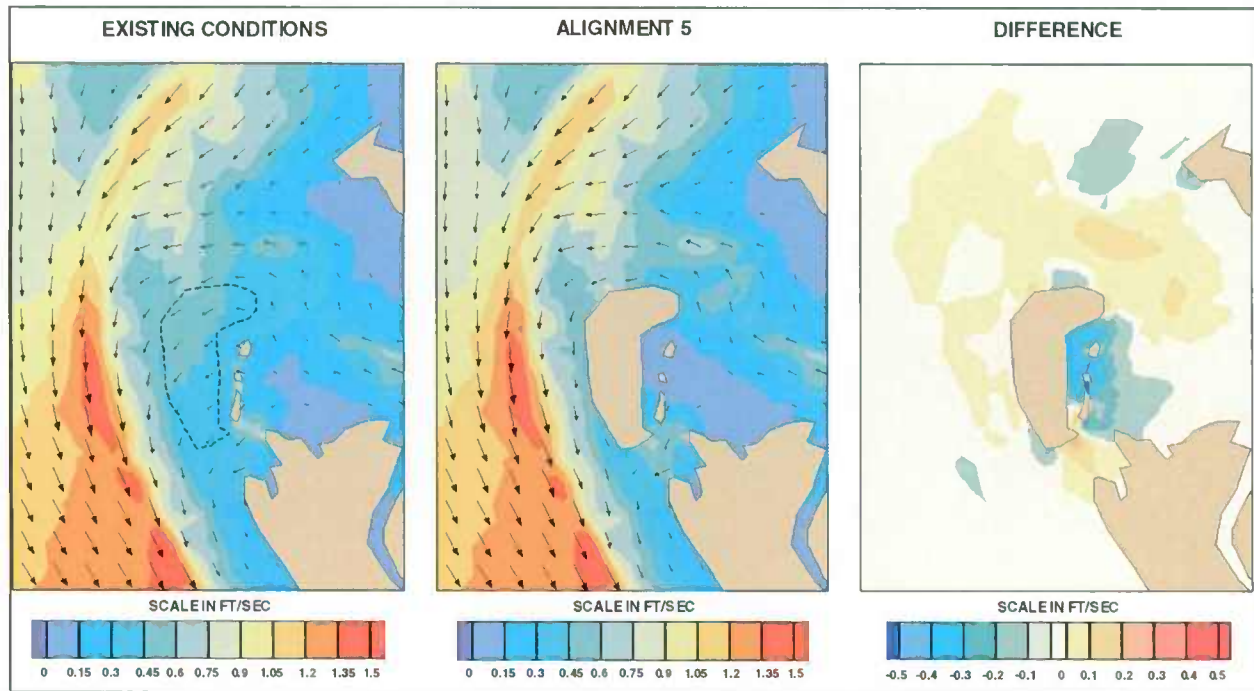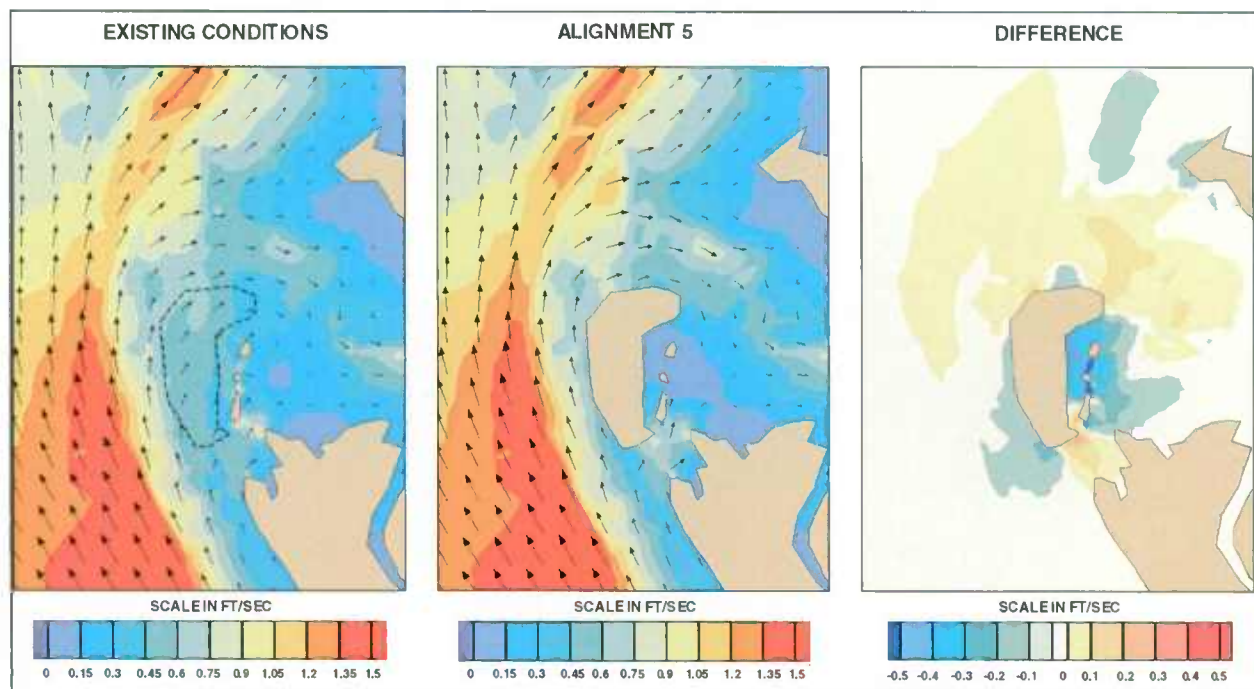
7. SEDIMENTATION MODELING RESULTS

7.1 GENERAL

The UCB-FEM sedimentation model was used to examine transport of non-cohesive and cohesive materials (i.e. sand and clay) which characterize sediment in the vicinity of the project site. Detailed sediment data for the vicinity of James Island were not available so the model was used empirically by running the model to dynamic equilibrium as discussed in Section 5.3 and interpreting the results with a normalized unit scale. Examination of model results for both non-cohesive and cohesive sediments indicates that normal tidal currents are insufficient to directly cause sediment suspension and transport. Wind generated waves increase bottom shear stresses significantly and can cause sediment suspension. Various wind speeds were modeled and 16-mph winds were determined to be the minimum necessary to cause sediment suspension and transport for non-cohesive sediments. Thirteen-mph winds were the minimum necessary to cause substantial sediment suspension and transport for cohesive sediments.

Numerical modeling analyses indicate that sedimentation in the vicinity of James Island would be affected by the construction of the project. Results of the UCB-FEM sedimentation model simulations are compared visually for the entire project vicinity.

The UCB-FEM sedimentation model was run for each alignment as well as existing conditions starting each simulation with the same initial conditions. The following sections describe the impacts of each habitat construction alignment on sedimentation. Results have been normalized to a unitless scale due to the empirical use of the sedimentation model as a result of insufficient local calibration data. Cohesive sediments have properties (shape, plasticity, electric charge) that cause the particles to remain in suspension for relatively long periods of time before they settle out, resulting in a larger area affected by sedimentation and erosion than for non-cohesive sediments.

7.2 ALIGNMENT 1 IMPACTS

Non-cohesive and cohesive sediment model results for Alignment 1 are presented in Figures 7-1

through 7-6.

7.2.1   Non-Cohesive Sediment

Figures 7-1 through 7-3 show sedimentation modeling results for 0.004 inch non-cohesive sediments for 16-mph NNW, SSE and WNW winds, respectively. Comparison of sedimentation patterns with bathymetry shows that the areas of erosion correspond to shallow water depths while deposition occurs in adjacent deep water areas.

Construction of Alignment 1 would interrupt the long NNW wind fetch from across the Bay, thereby reducing erosion in the project area as shown in Figure 7-1. Figure 7-1 shows a large area south of the project extending to and along the shoreline of Taylors Island where erosion of the shallow water is reduced. The difference plot of Figure 7-1 shows a yellow to orange area (labeled more sediment on the scale) that represents areas that are eroding under existing conditions would have reduced or no erosion for the with-project conditions.

For winds from the SSE, construction of Alignment 1 would also interrupt a large portion of the long wind fetch, reducing the rates of erosion and accretion at James Island as shown in the difference plot of Figure 7-2. The orange to red region along the west dike labeled as more sediment represents an area that is currently eroding would become an accretion area. The difference plot also shows areas labeled less sediment (green) where accretion is reduced that is due to the reduced erosion of the shallow areas, and subsequently less sediment in the water column.

Figure 7-3 shows results from construction of Alignment 1 for winds from the WNW. This figure shows that less erosion occurs for these winds, as the fetch length is much less. The with-project plot and difference plot in Figure 7-3 shows reduced erosion of areas around James Island and near the northern tip of Taylors Island.

7.2.2   Cohesive Sediment

Figures 7-4 through 7-6 show sedimentation modeling results for cohesive sediments for 13-mph NNW, SSE, and WNW winds, respectively. Figure 7-4 shows a significant reduction in erosion in the project area following construction, plus significantly more sediment accretion in the lee

of the project, extending south to Taylors Island. Of interest to note in the difference plot is a bluish area labeled less sediment southeast of James Island, which is actually a reduction in accretion. Figure 7-5 shows modeling results for 13-mph SSE winds. The difference plot in this figure shows that north of the project some areas have less erosion and some areas have accretion. Figure 7-6 shows modeling results for 13-mph WNW winds. This figure shows that current erosion around James Island would essentially be eliminated.

7.3   ALIGNMENT 2 IMPACTS

Non-cohesive and cohesive sediment model results for Alignment 2 are presented in Figures 7-7 through 7-12.

7.3.1   Non-Cohesive Sediment

Figures 7-7 through 7-9 show sedimentation modeling results for 0.004 inch non-cohesive sediments for 16-mph NNW, SSE and WNW winds, respectively. Comparison of sedimentation patterns with bathymetry shows that the areas of erosion correspond to shallow water depths while deposition occurs in adjacent deep water areas.

Construction of Alignment 2 provides the most protection to James Island from the long NNW wind fetch from across the Bay, preventing erosion in the lee of the project as shown in Figure 7-7. Figure 7-7 shows that the large area south of the project extending to and along the shoreline of Taylors Island where erosion would be reduced upon construction of Alignment 1 is completely eliminated upon construction of Alignment 2. This is because Alignment 2 extends further to the west. The difference plot of Figure 7-7 shows that areas that are accreting under existing conditions would either erode or accrete less along the dikes exposed to the N, NW and W.

For winds from the SSE, construction of Alignment 2 would also interrupt a large portion of the long wind fetch, reducing the rates of erosion in the shallows around James Island. This results in reduced accretion, as indicated by the less sediment area as shown in the difference plot of Figure 7-8. Figure 7-9 shows results from construction of Alignment 2 for winds from the WNW. As for Alignment 1, this figure shows that less erosion occurs for these winds, as the

fetch length is much less. The with-project plot and difference plot in Figure 7-9 shows reduced erosion of areas around James Island and near the northern tip of Taylors Island.

7.3.2 Cohesive Sediment

Figures 7-10 through 7-12 show sedimentation modeling results for cohesive sediments for 13-mph NNW, SSE, and WNW winds, respectively. Figure 7-10 shows a significant reduction in erosion in the project area following construction, plus significantly more sediment accretion in the lee of the project, extending south to Taylors Island. This area is greater than expected for Alignment 1 as shown by the difference plot. Similarly to Alignment 1, in the difference plot is a bluish area labeled less sediment southeast James Island, which is actually a reduction in accretion. Figure 7-11 shows modeling results for 13-mph SSE winds. The difference plot in this figure shows less erosion in addition to accretion north of the project, plus reduced accretion east of the project. Once again, the area of impact is greater than for Alignment 1, although not to the same extent as for NNW winds. Figure 7-12 shows modeling results for 13-mph WNW winds. This figure shows that current erosion around James Island would essentially be eliminated.

7.4   ALIGNMENT 3 IMPACTS

Non-cohesive and cohesive sediment model results for Alignment 3 are presented in Figures 7-13 through 7-18.

7.4.1   Non-Cohesive Sediment

Figures 7-13 through 7-15 show sedimentation modeling results for 0.004 inch non-cohesive sediments for 16-mph NNW, SSE and WNW winds, respectively. Comparison of sedimentation patterns with bathymetry shows that the areas of erosion correspond to shallow water depths while deposition occurs in adjacent deep water areas.

Construction of Alignment 3 would interrupt the long NNW wind fetch from across the Bay, thereby reducing erosion in the project area as shown in Figure 7-13. Figure 7-13 shows a large area south of the project extending to and along the shoreline of Taylors Island where erosion of

the shallow water is reduced. Erosion would still occur along the west dikes of the project.

For winds from the SSE, construction of Alignment 3 would also interrupt a large portion of the long wind fetch, reducing the rates of erosion and accretion around James Island as shown in the difference plot of Figure 7-14. The orange to red region along the west dike labeled as more sediment represents an area that is currently eroding would become an accretion area. The difference plot also shows areas labeled less sediment (green) where accretion is reduced that is due to the reduced erosion of the shallow areas, and subsequently less sediment in the water column.

Figure 7-15 shows results from construction of Alignment 3 for winds from the WNW. This figure shows that less erosion occurs for these winds, as the fetch length is much less. Similar to the other two alignments, the with-project plot and difference plot in Figure 7-15 shows reduced erosion of areas around James Island and near the northern tip of Taylors Island.

7.4.2   Cohesive Sediment

Figures 7-16 through 7-18 show sedimentation modeling results for cohesive sediments for 13-mph NNW, SSE, and WNW winds, respectively. Figure 7-16 shows a significant reduction in erosion in the project area following construction, plus significantly more sediment accretion in the lee of the project, extending south to Taylors Island. This is similar to Alignment 1, where in the difference plot the bluish area labeled less sediment southeast James Island, which is actually a reduction in accretion. Figure 7-17 shows modeling results for 13-mph SSE winds. The difference plot in this figure shows less erosion in addition to accretion north of the project, plus reduced accretion east of the project. Figure 7-18 shows modeling results for 13-mph WNW winds. As for the other two alignments, erosion around James Island due to WNW winds would essentially be eliminated.

7.5   ALIGNMENT 4 IMPACTS

Non-cohesive and cohesive sediment model results for Alignment 4 are presented in Figures 7-19 through 7-24.

7.5.1   Non-Cohesive Sediment

Figures 7-19 through 7-21 show sedimentation modeling results for 0.004 inch non-cohesive sediments for 16-mph NNW, SSE and WNW winds, respectively. Comparison of sedimentation patterns with bathymetry shows that the areas of erosion correspond to shallow water depths while deposition occurs in adjacent deep water areas. Sedimentation changes due to construction of this alignment are similar to that for Alignment 2 and 5.

Construction of Alignment 4 would interrupt the long NNW wind fetch from across the Bay, thereby reducing erosion in the project area as shown in Figure 7-19. Figure 7-19 shows a large area south of the project extending to and along the shoreline of Taylors Island where erosion of the shallow water is reduced. The difference plot of Figure 7-19 shows a yellow to orange area (labeled more sediment on the scale) that represents areas that are eroding under existing conditions would have reduced or no erosion for the with-project conditions.

For winds from the SSE, construction of Alignment 4 would also interrupt a large portion of the long wind fetch, reducing the rates of erosion and accretion James Island as shown in the difference plot of Figure 7-20. The orange to red region along the west dike labeled as more sediment represents an area that is currently eroding would become an accretion area. The difference plot also shows areas labeled less sediment (green) where accretion is reduced that is due to the reduced erosion of the shallow areas, and subsequently less sediment in the water column.

Figure 7-21 shows results from construction of Alignment 4 for winds from the WNW. This figure shows that less erosion occurs for these winds, as the fetch length is much less. Similar to the other alignments, the with-project plot and difference plot in Figure 7-15 shows reduced erosion of areas around James Island and near the north tip of Taylors Island.

7.5.2   Cohesive Sediment

Figures 7-22 through 7-24 show sedimentation modeling results for cohesive sediments for 13-mph NNW, SSE, and WNW winds, respectively. Figure 7-22 shows a significant reduction in erosion in the project area following construction, plus significantly more sediment accretion in

the lee of the project, extending south to Taylors Island. Results are similar to Alignment 2, but over less area. The same bluish area southeast of James Island labeled less sediment is a reduction in accretion. Figure 7-23 shows modeling results for 13-mph SSE winds. The difference plot in this figure shows less erosion in addition to accretion north of the project, plus reduced accretion east of the project. Figure 7-24 shows modeling results for 13-mph WNW winds, which also show that current erosion around James Island would essentially be eliminated.

7.6   ALIGNMENT 5 IMPACTS

Non-cohesive and cohesive sediment model results for Alignment 5 are presented in Figures 7-25 through 7-30.

7.6.1   Non-Cohesive Sediment

Figures 7-25 through 7-27 show sedimentation modeling results for 0.004 inch non-cohesive sediments for 16-mph NNW, SSE and WNW winds, respectively. Comparison of sedimentation patterns with bathymetry shows that the areas of erosion correspond to shallow water depths while deposition occurs in adjacent deep water areas. Sedimentation changes are similar to Alignment 2 and 4.

Construction of Alignment 5 would interrupt the long NNW wind fetch from across the Bay, thereby reducing erosion in the project area as shown in Figure 7-25. Figure 7-25 shows a large area south of the project extending to and along the shoreline of Taylors Island where erosion of the shallow water is reduced. The difference plot of Figure 7-25 shows a yellow to orange area (labeled more sediment on the scale) that represents areas that are eroding under existing conditions would have no erosion for the with-project conditions.

For winds from the SSE, construction of Alignment 5 would also interrupt a large portion of the long wind fetch, reducing the rates of erosion and accretion James Island as shown in the difference plot of Figure 7-26. The orange to red region along the west dike labeled as more sediment represents an area that is currently eroding would become an accretion area. The difference plot also shows areas labeled less sediment (green and blue) where accretion is

reduced that is due to the reduced erosion of the shallow areas, and subsequently less sediment in the water column.

Figure 7-27 shows results from construction of Alignment 5 for winds from the WNW. Results are similar to the previous alignments and show reduced erosion of areas around James Island and near the northern tip of Taylors Island.

7.6.2   Cohesive Sediment

Figures 7-28 through 7-30 show sedimentation modeling results for cohesive sediments for 13-mph NNW, SSE, and WNW winds, respectively. Figure 7-28 shows a significant reduction in erosion in the project area following construction, plus significantly more sediment accretion in the lee of the project, extending south to Taylors Island. Similar to all alignments, the difference plot shows a bluish area labeled less sediment southeast James Island that is a reduction in accretion. Figure 7-29 shows modeling results for 13-mph SSE winds. The difference plot in this figure shows less erosion in addition to accretion north of the project, plus reduced accretion east of the project. Figure 7-30 shows modeling results for 13-mph WNW winds that indicate erosion around James Island would essentially be eliminated.
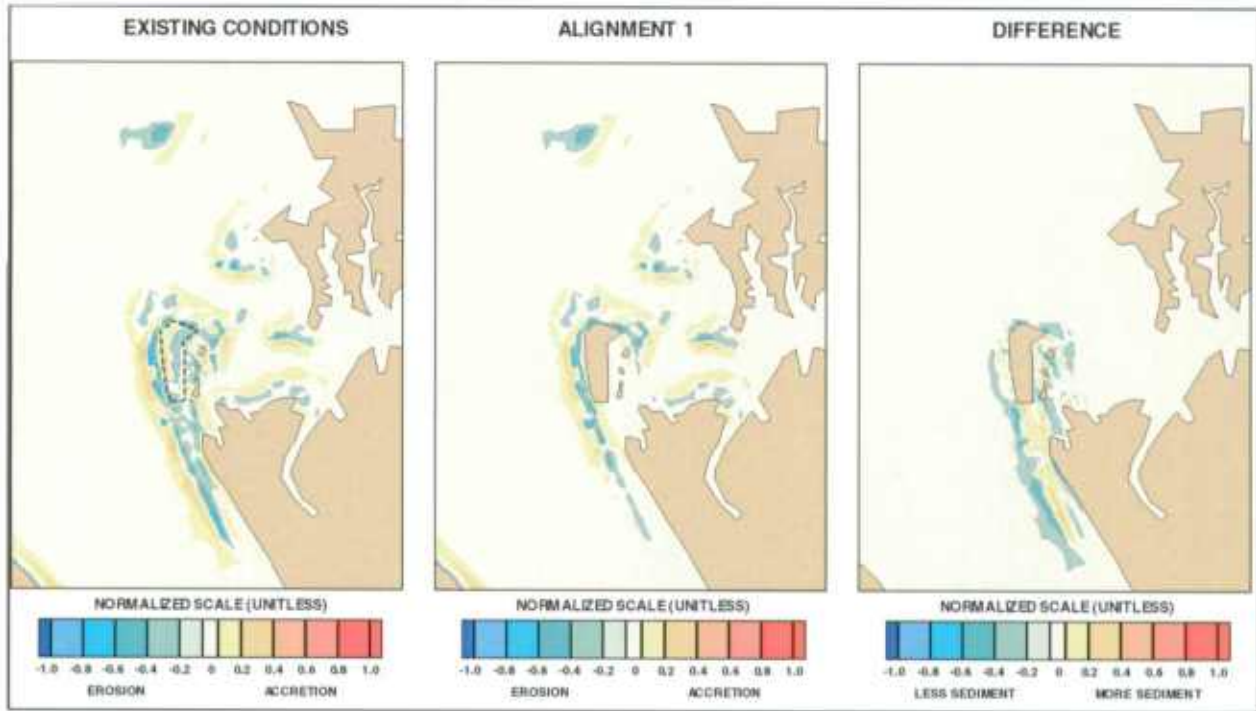
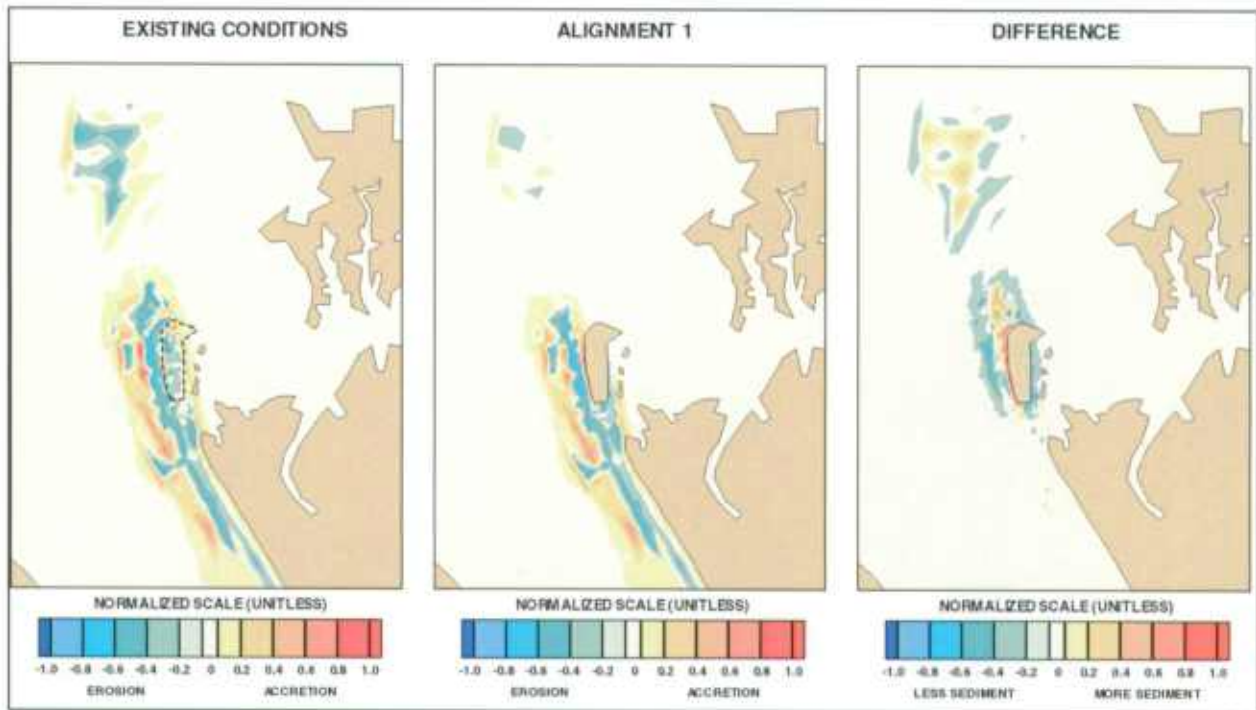**Figure 7-1:** Non-Cohesive Sediment – North-Northwest Wind 16 mph – Alignment 1 vs. Existing Conditions

Figure 7-2: Non-Cohesive Sediment – South-Southeast Wind 16 mph – Alignment 1 vs. Existing Conditions

Figure 7-3:   **Non-Cohesive Sediment – West -Northwest Wind 16 mph – Alignment 1 vs. Existing Conditions**

Figure 7-4:   **Cohesive Sediment – North-Northwest Wind 13 mph Alignment 1 vs. Existing Conditions**

Figure 7-5: Cohesive Sediment – South-Southeast Wind 13 mph – Alignment 1 vs. Existing Conditions
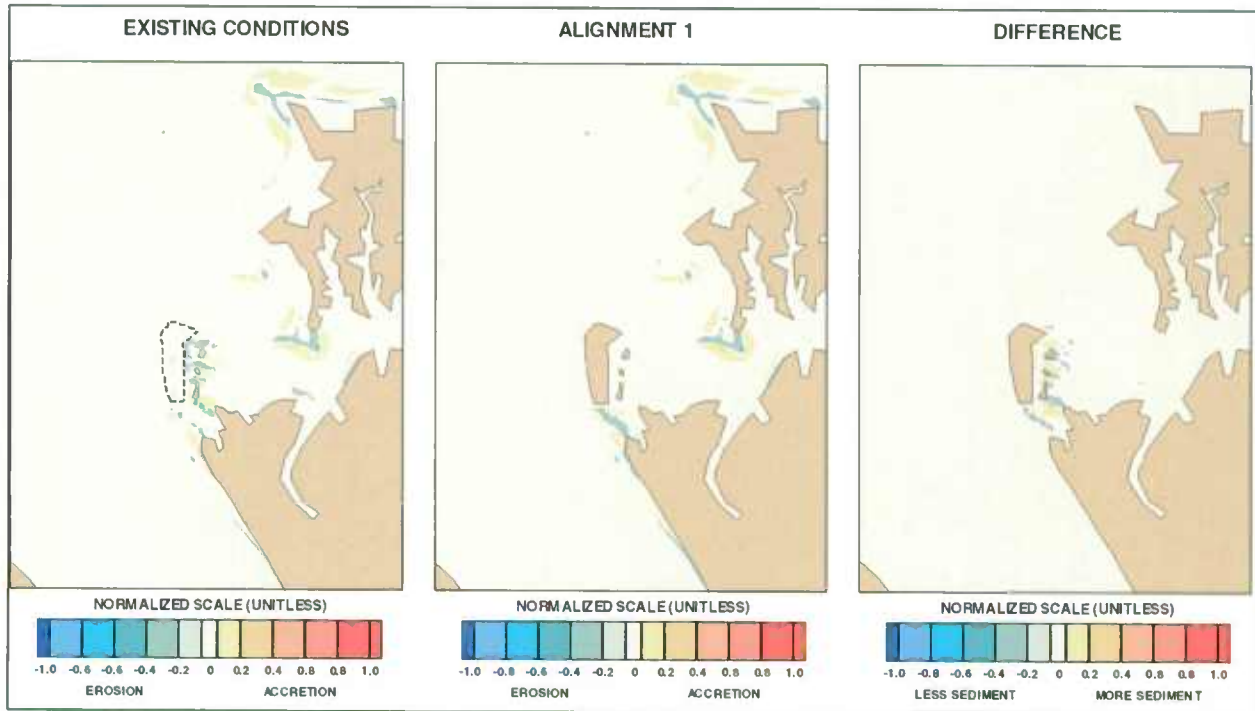

Figure 7-6: Cohesive Sediment – West-Northwest Wind 13 mph – Alignment 1 vs. Existing Conditions

Figure 7-7:   Non-Cohesive Sediment – North-Northwest Wind 16 mph – Alignment 2 vs. Existing Conditions

Figure 7-8:   Non-Cohesive Sediment – South-Southeast Wind 16 mph – Alignment 2 vs. Existing Conditions

Figure 7-9: Non-Cohesive Sediment – West -Northwest Wind 16 mph – Alignment 2 vs.
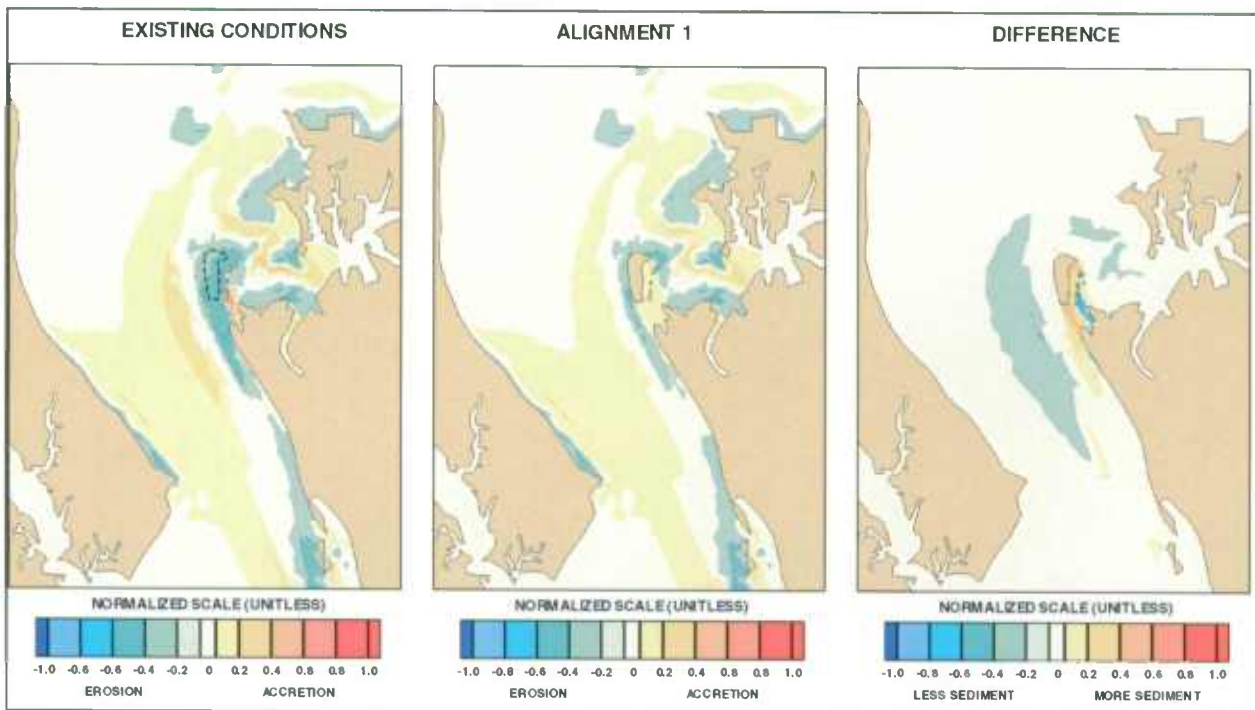
Existing Conditions

Figure 7-10: Cohesive Sediment – North-Northwest Wind 13 mph Alignment 2 vs.
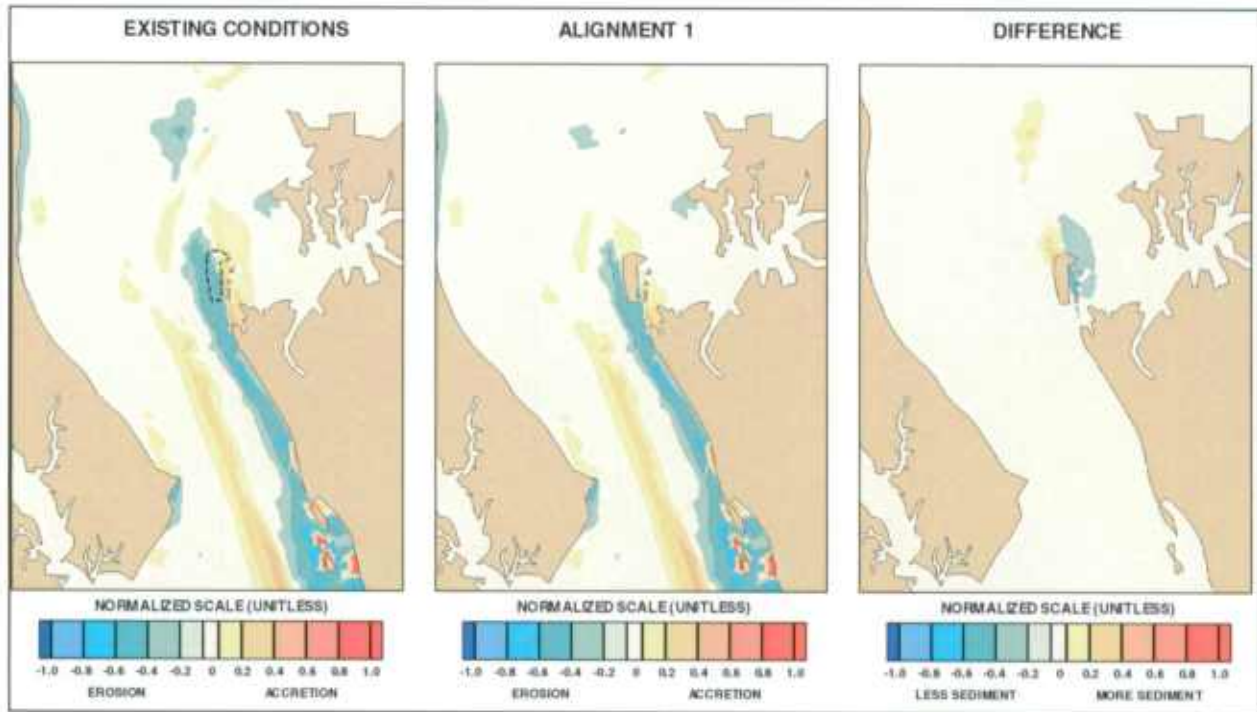
Existing Conditions

Figure 7-11:   Cohesive Sediment – South-Southeast Wind 13 mph – Alignment 2 vs.
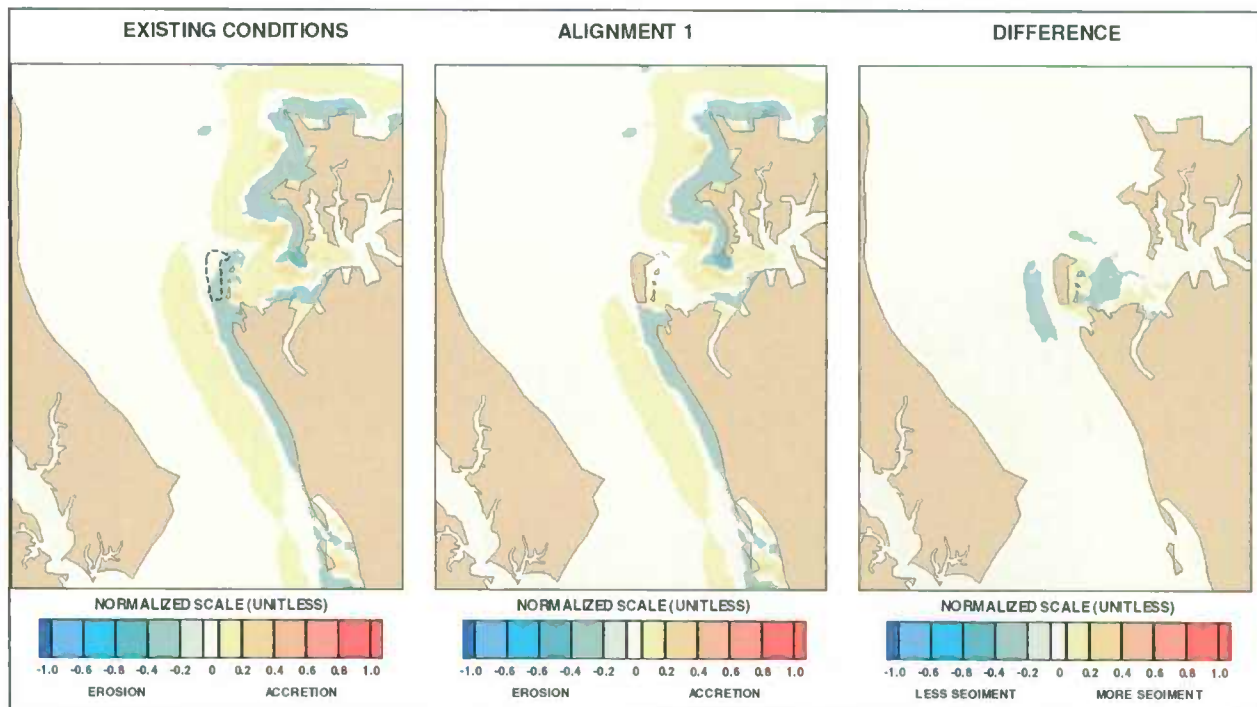Existing Conditions

Figure 7-12:   Cohesive Sediment – West-Northwest Wind 13 mph – Alignment 2 vs.
Existing Conditions
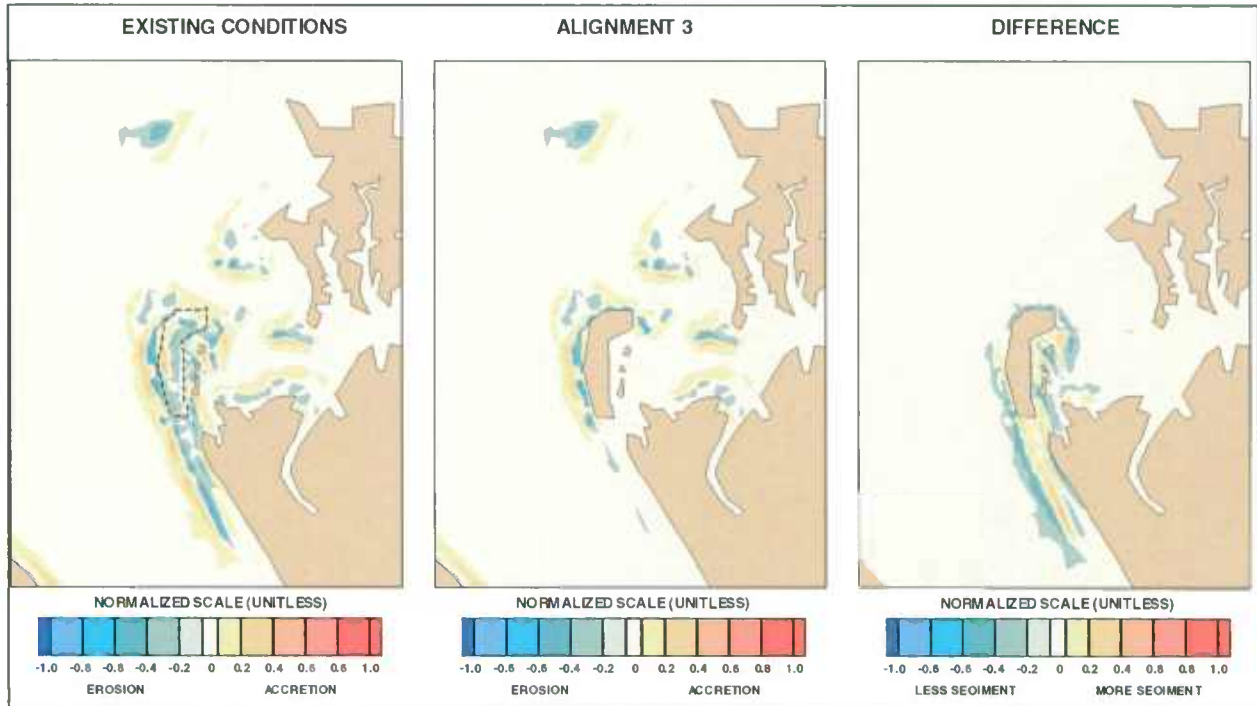
Figure 7-13:   Non-Cohesive Sediment – North-Northwest Wind 16 mph – Alignment 3 vs. Existing Conditions
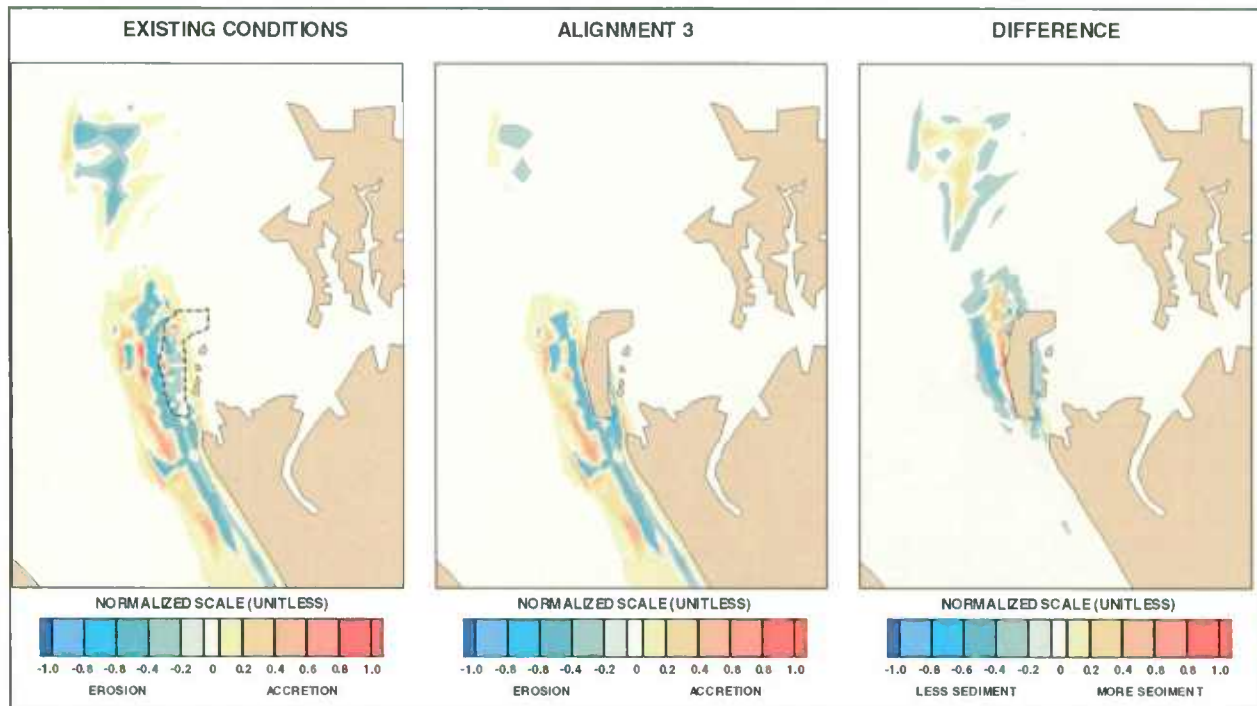
Figure 7-14:   Non-Cohesive Sediment – South-Southeast Wind 16 mph – Alignment 3 vs. Existing Conditions
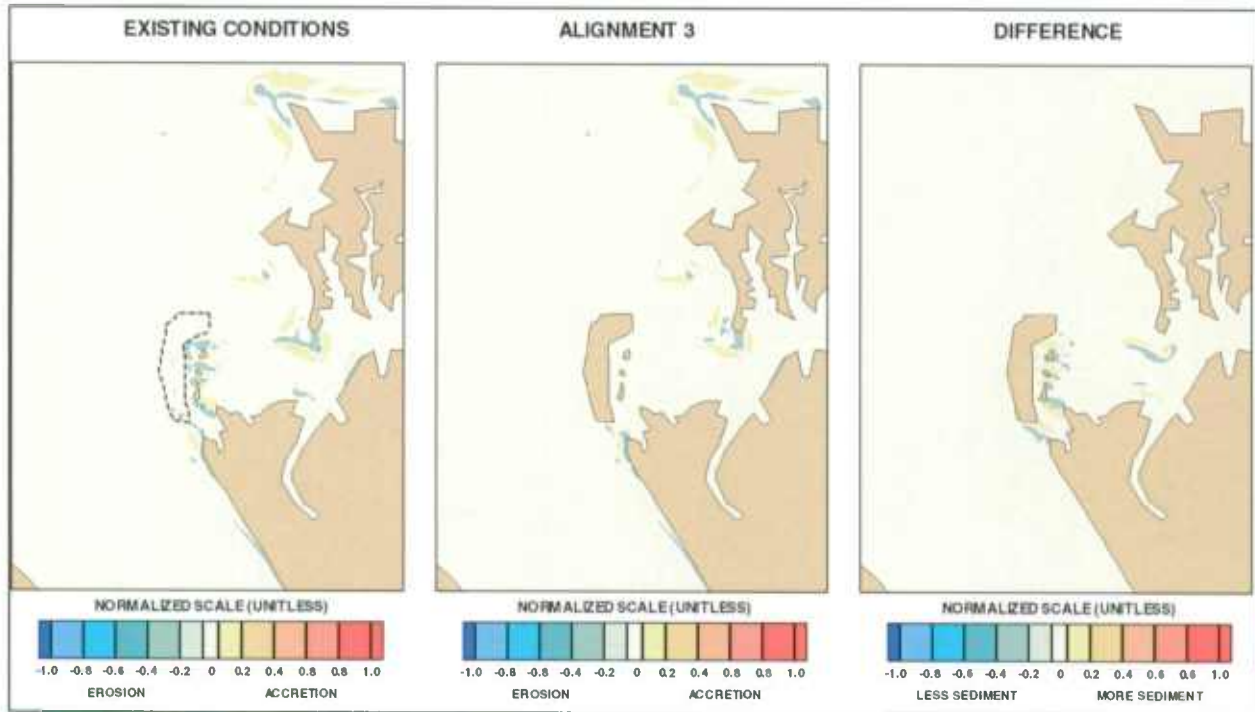
Figure 7-15: Non-Cohesive Sediment – West -Northwest Wind 16 mph – Alignment 3 vs. Existing Conditions
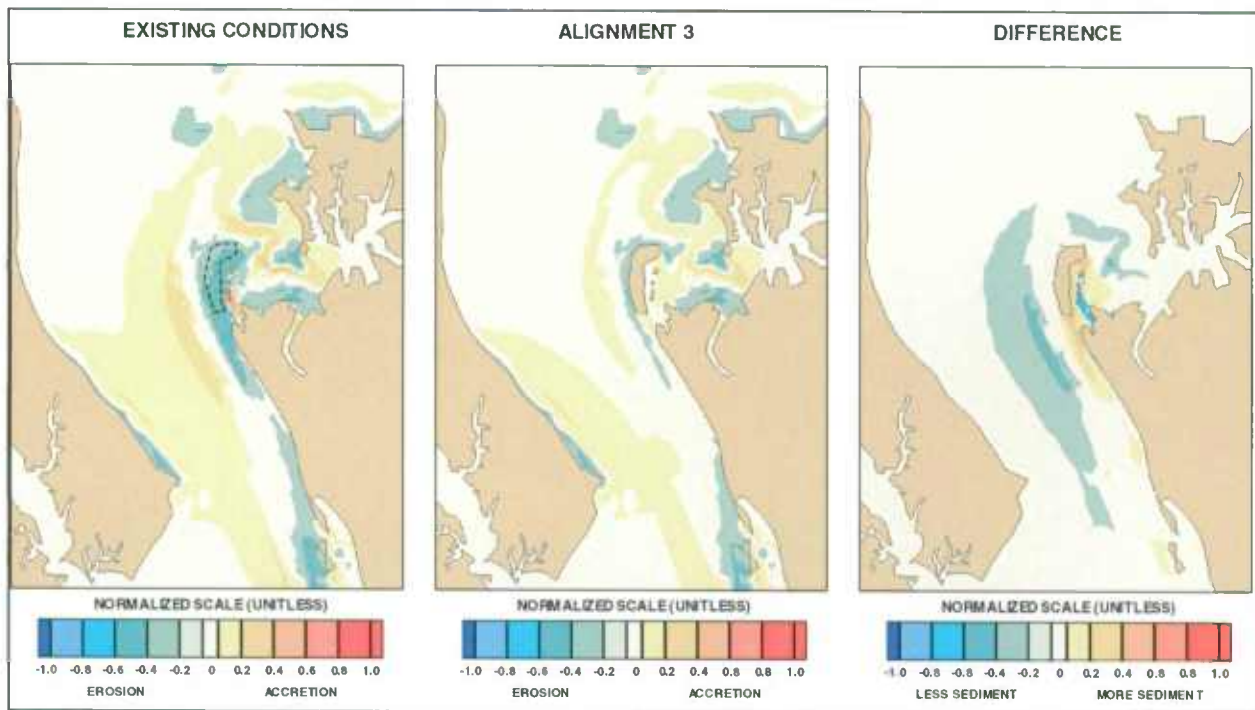
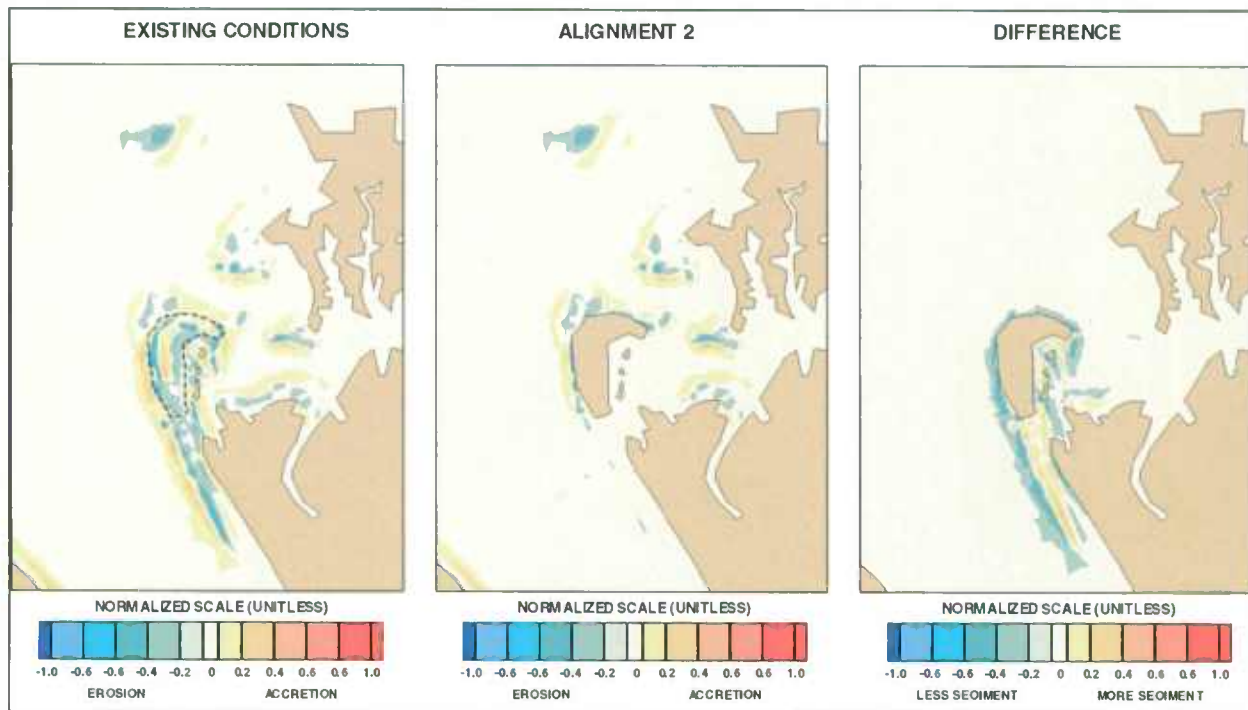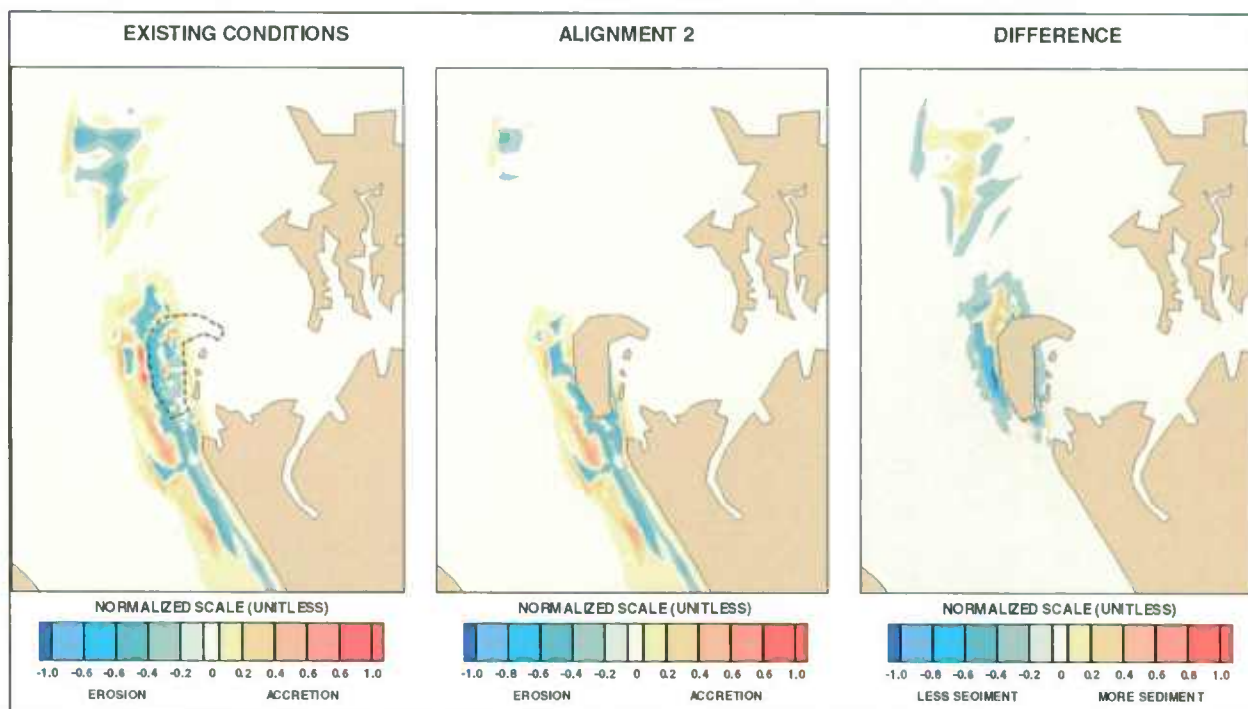Figure 7-16: Cohesive Sediment – North-Northwest Wind 13 mph Alignment 3 vs. Existing Conditions
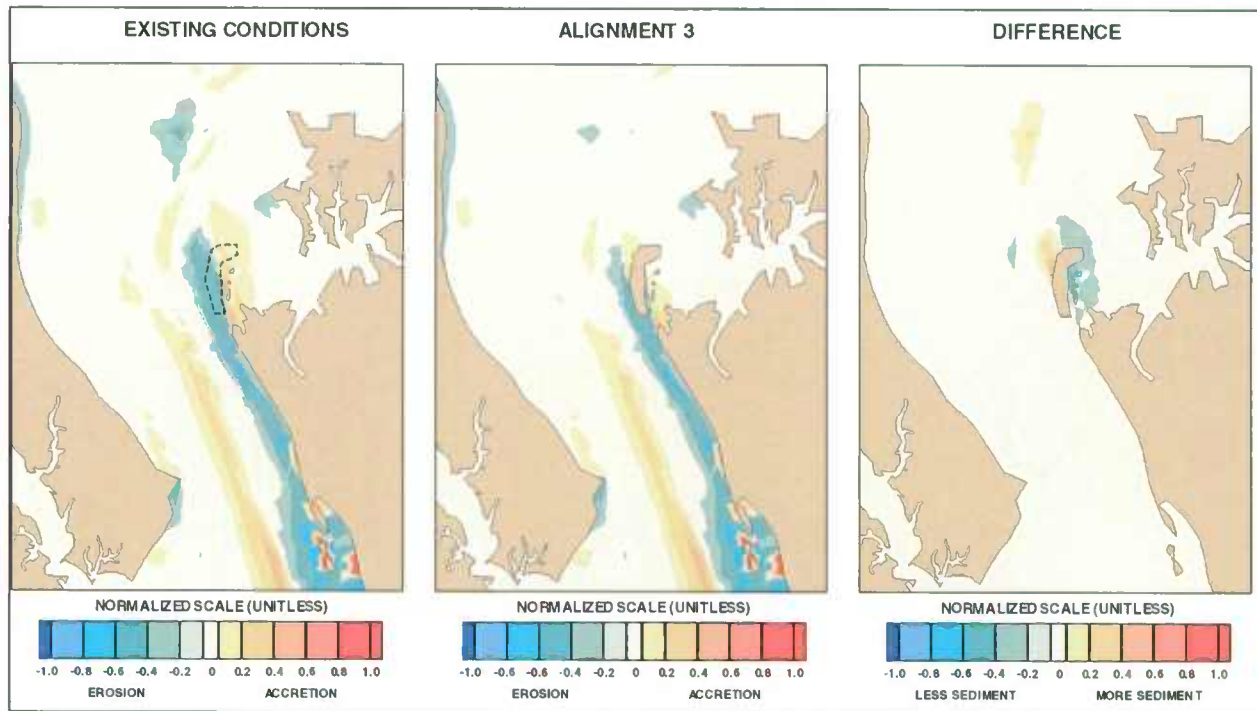
Figure 7-17:   Cohesive Sediment – South-Southeast Wind 13 mph – Alignment 3 vs. Existing Conditions
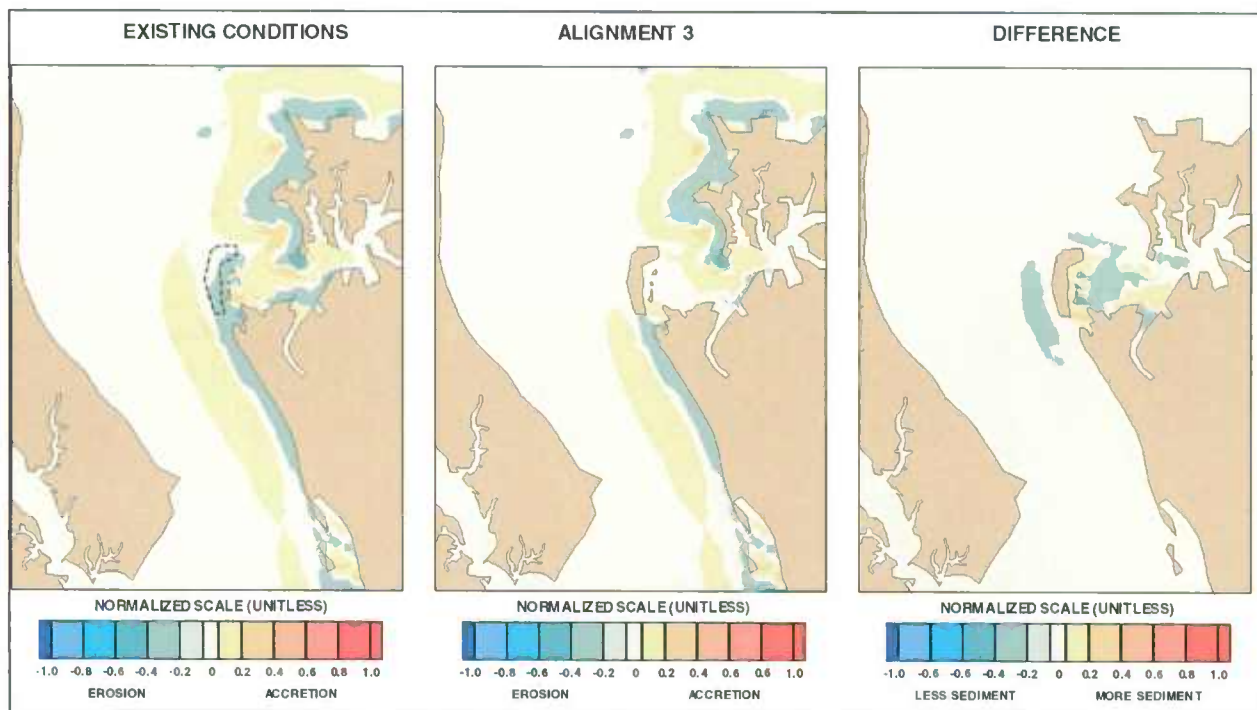
Figure 7-18:   Cohesive Sediment – West-Northwest Wind 13 mph – Alignment 3 vs. Existing Conditions
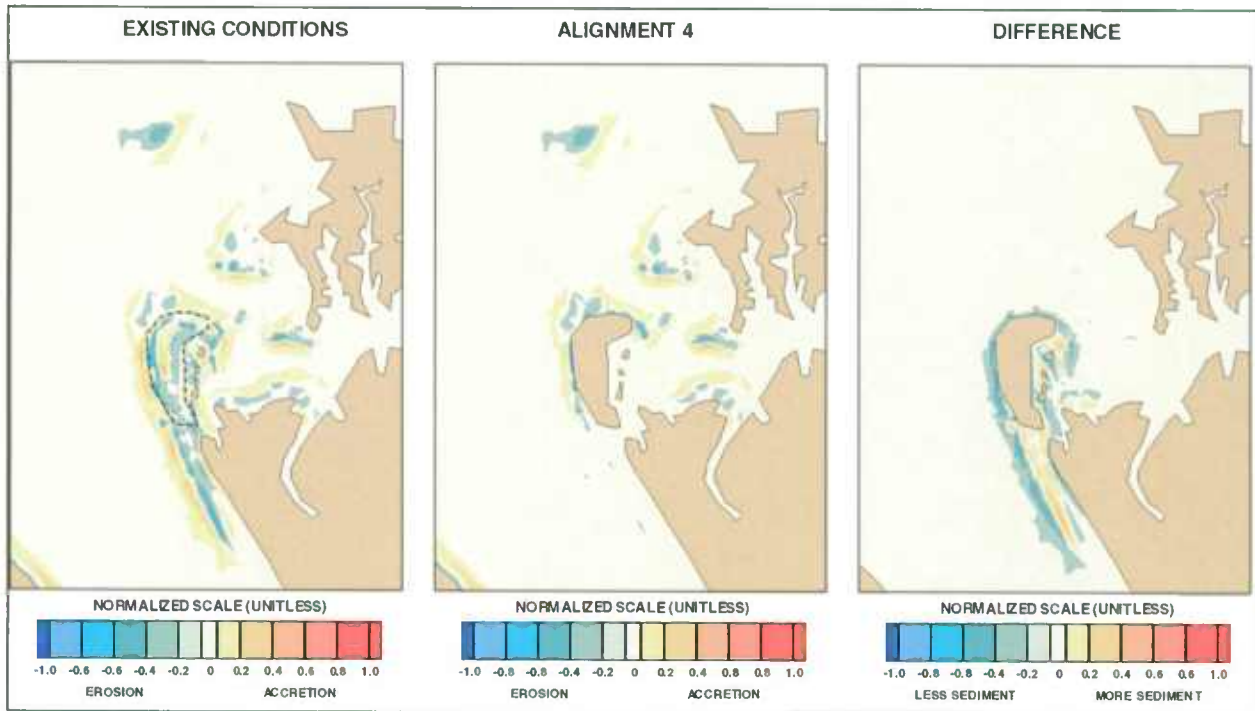
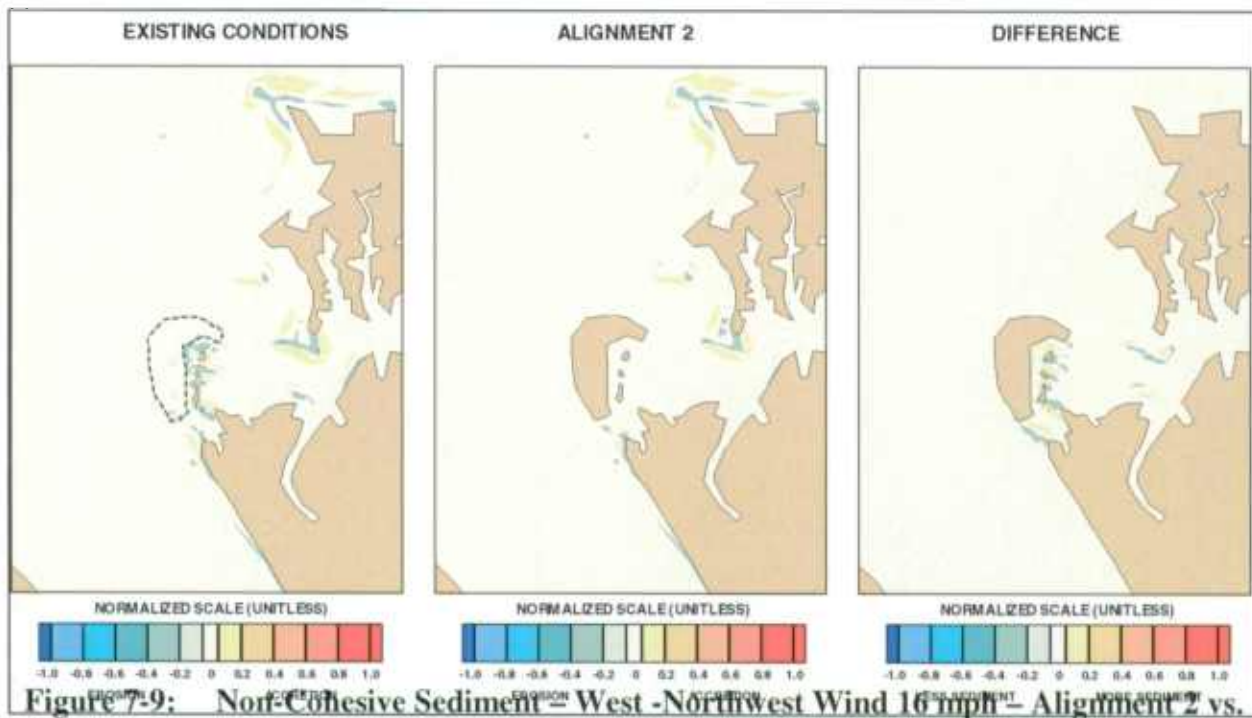Figure 7-19:   Non-Cohesive Sediment – North-Northwest Wind 16 mph – Alignment 4 vs. Existing Conditions
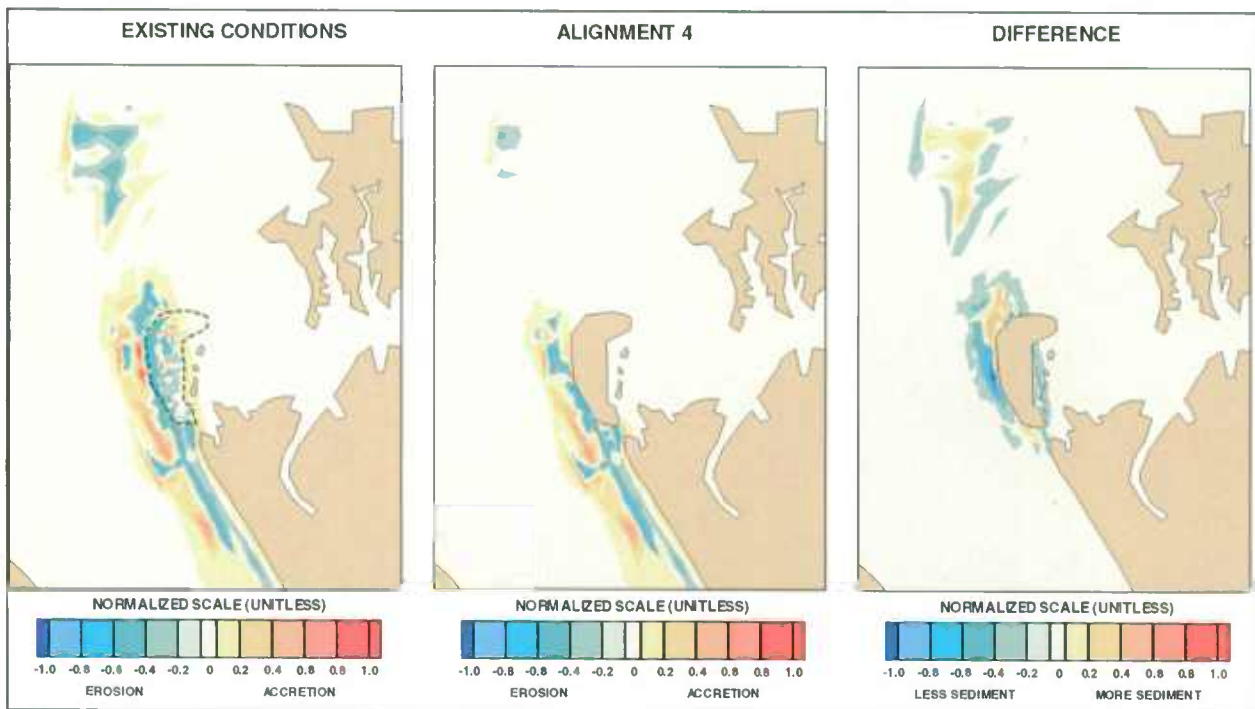
Figure 7-20:   Non-Cohesive Sediment – South-Southeast Wind 16 mph – Alignment 4 vs. Existing Conditions
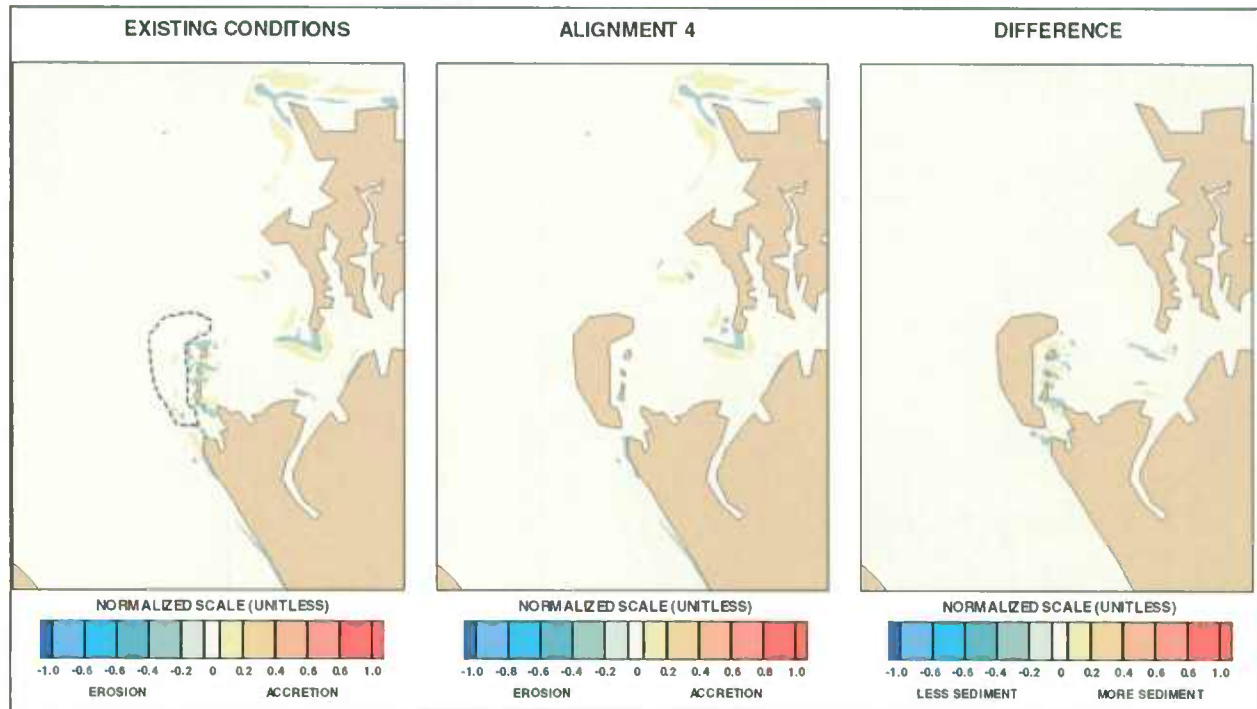
Figure 7-21:   Non-Cohesive Sediment – West -Northwest Wind 16 mph – Alignment 4 vs. Existing Conditions
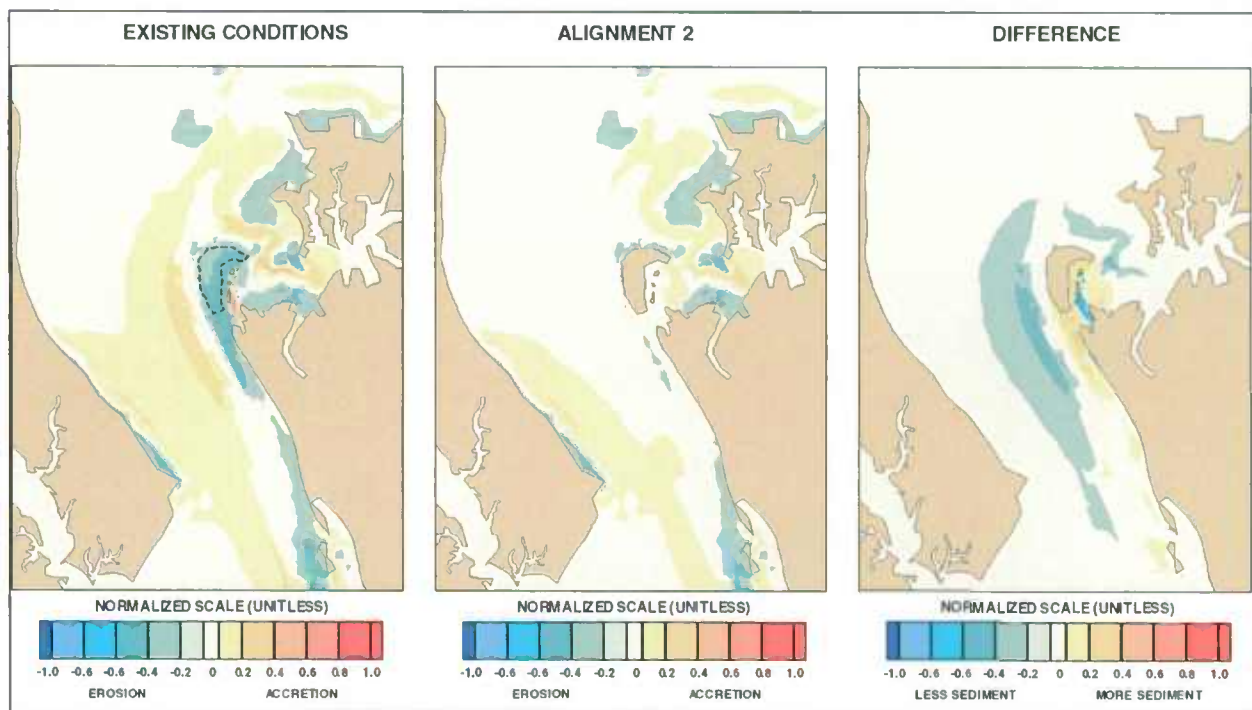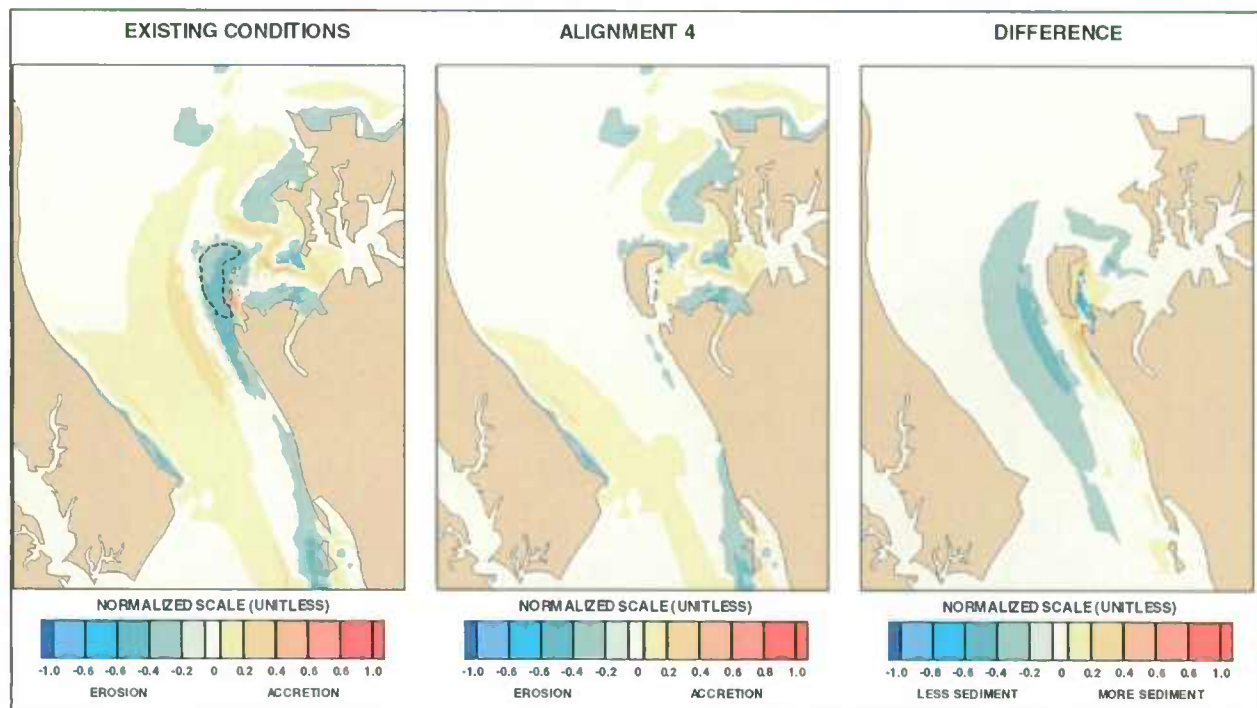

Figure 7-22:   Cohesive Sediment – North-Northwest Wind 13 mph Alignment 4 vs. Existing Conditions
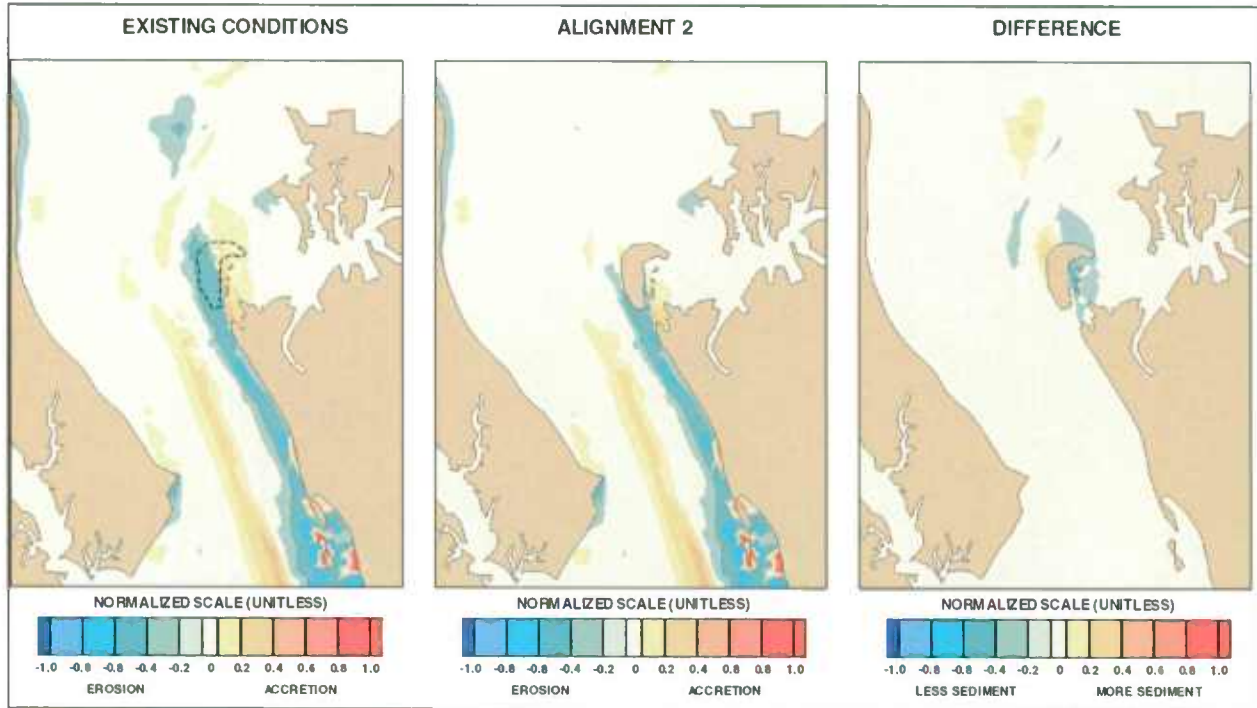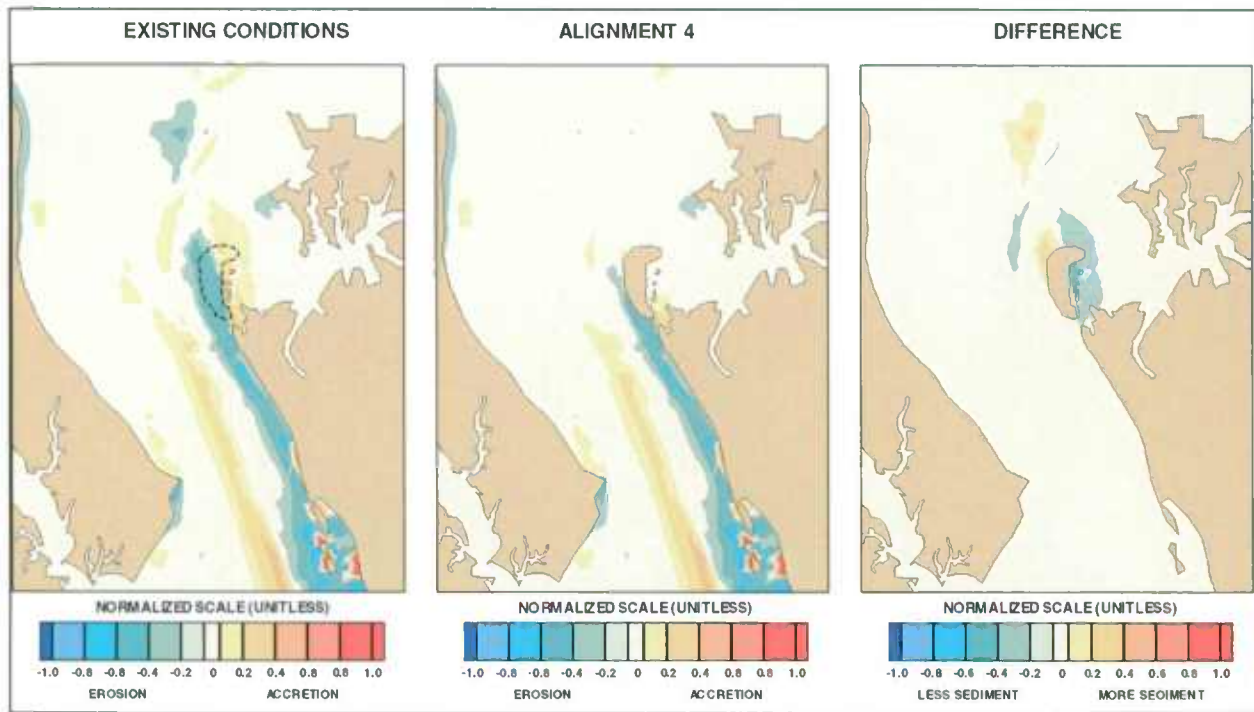
Figure 7-23: Cohesive Sediment – South-Southeast Wind 13 mph – Alignment 4 vs. Existing Conditions
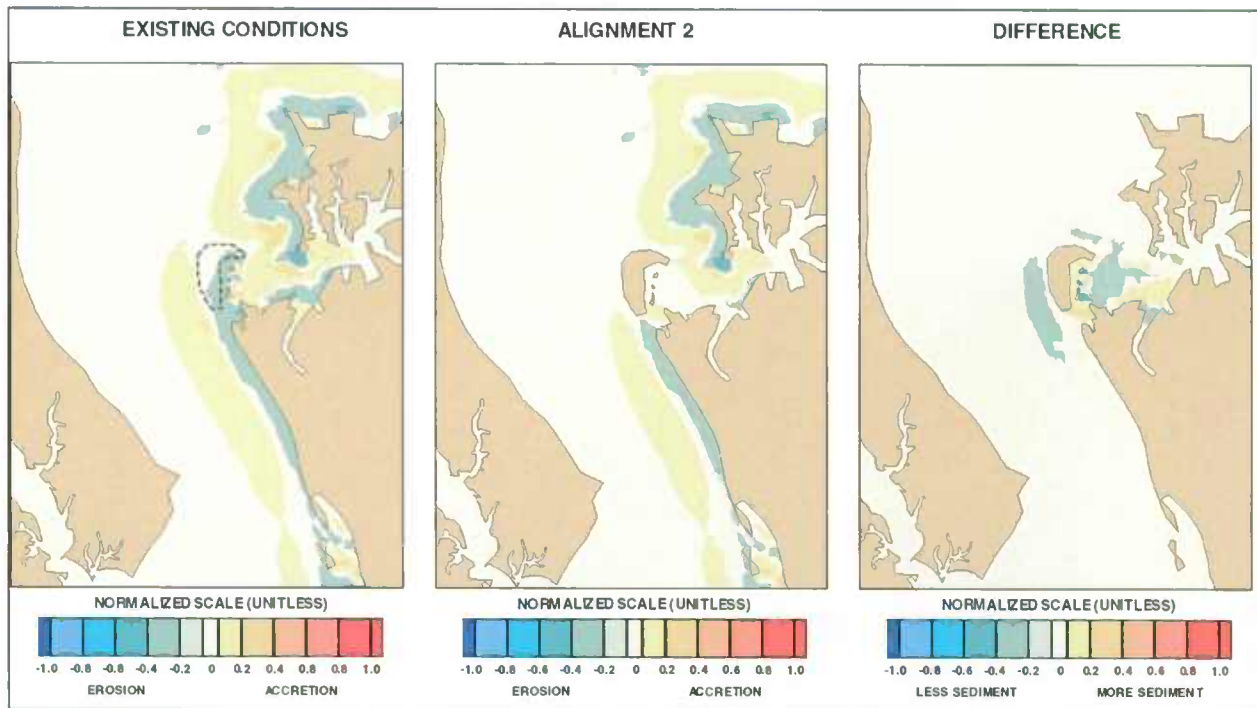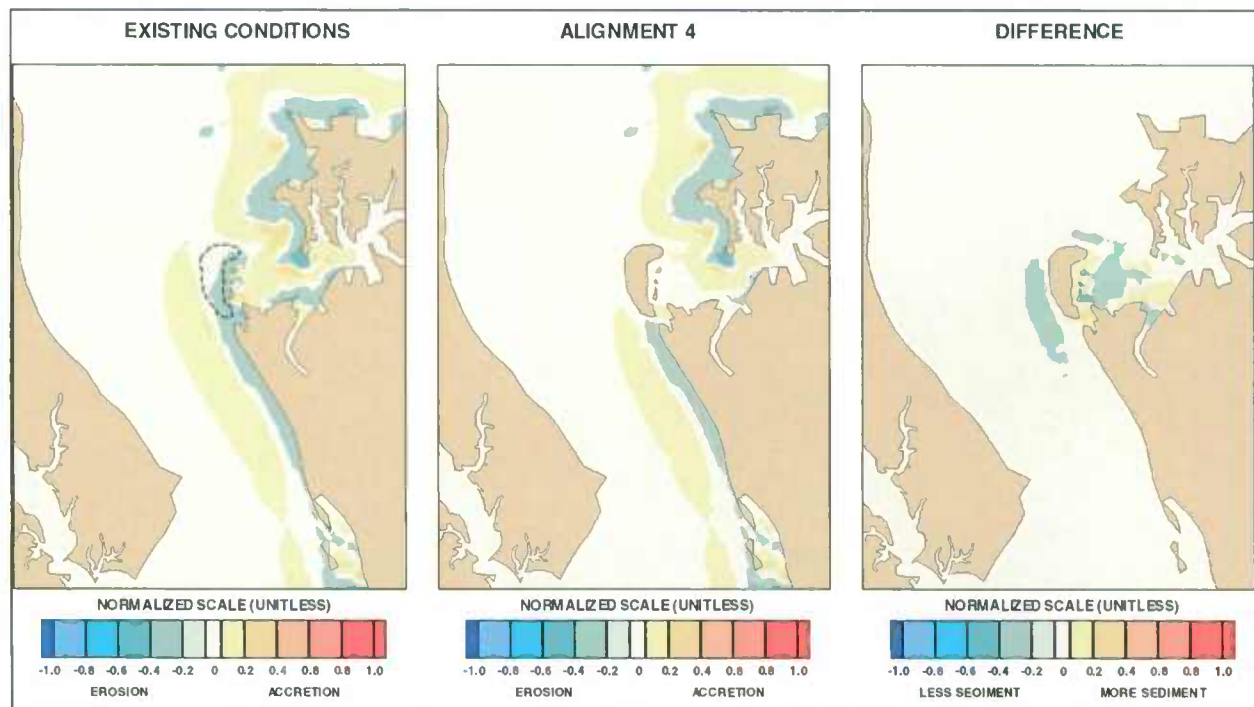

Figure 7-24: Cohesive Sediment – West-Northwest Wind 13 mph – Alignment 4 vs. Existing Conditions
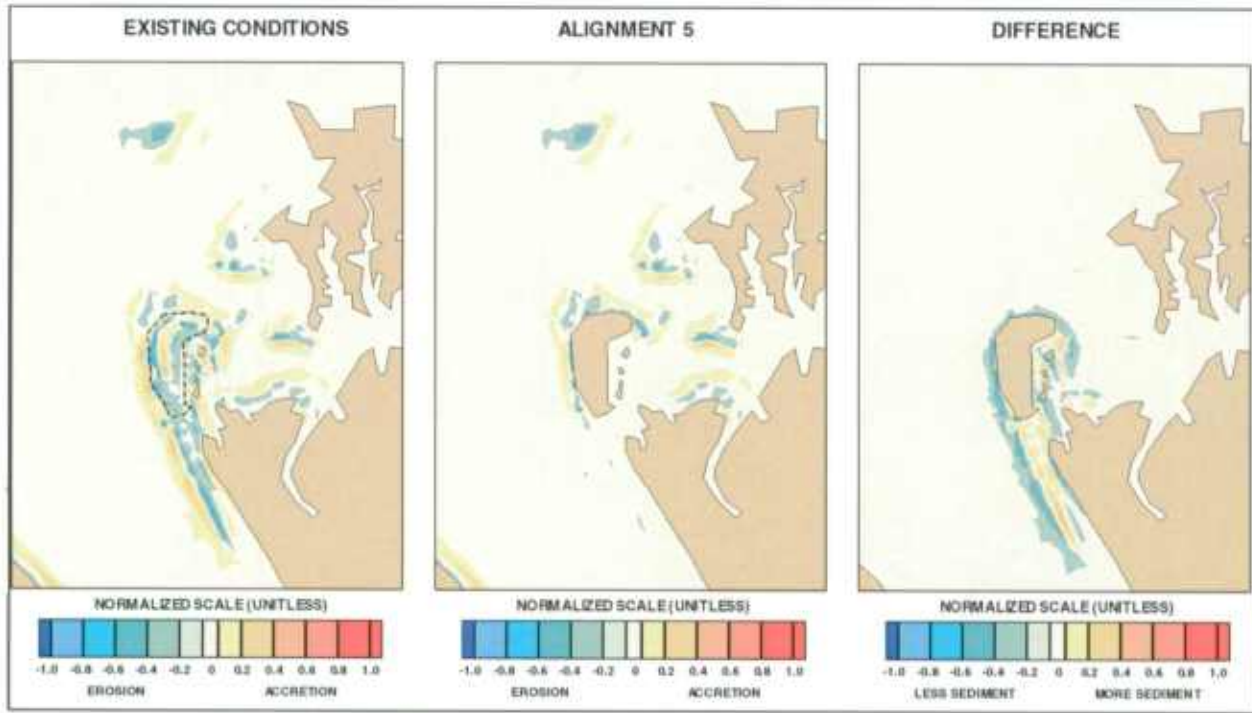
Figure 7-25: Non-Cohesive Sediment – North-Northwest Wind 16 mph – Alignment 5 vs. Existing Conditions
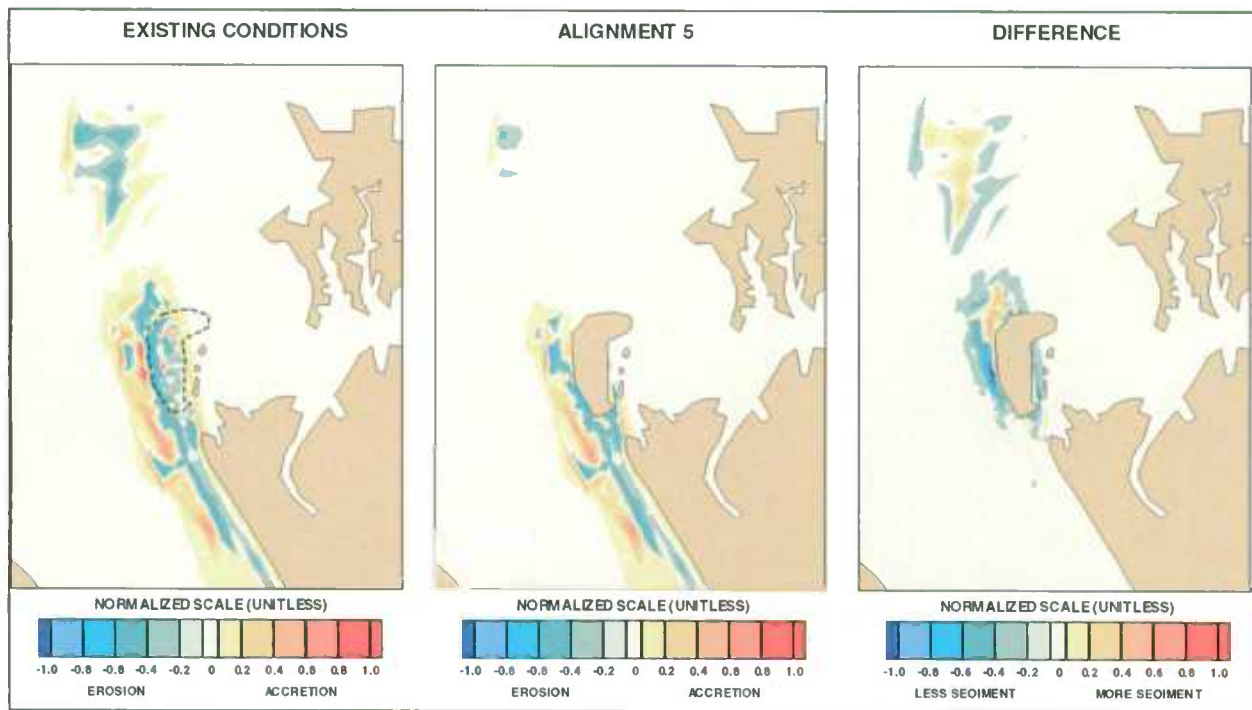
Figure 7-26: Non-Cohesive Sediment – South-Southeast Wind 16 mph – Alignment 5 vs. Existing Conditions
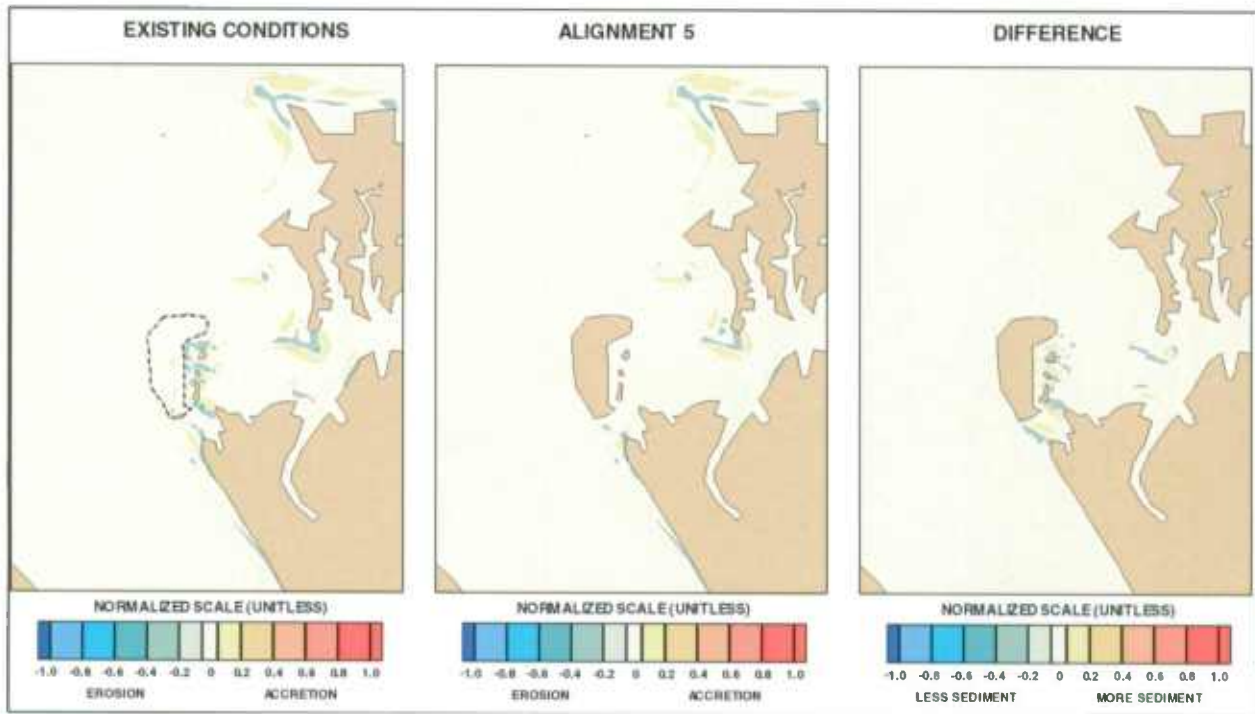
Figure 7-27: Non-Cohesive Sediment – West -Northwest Wind 16 mph – Alignment 5 vs. Existing Conditions
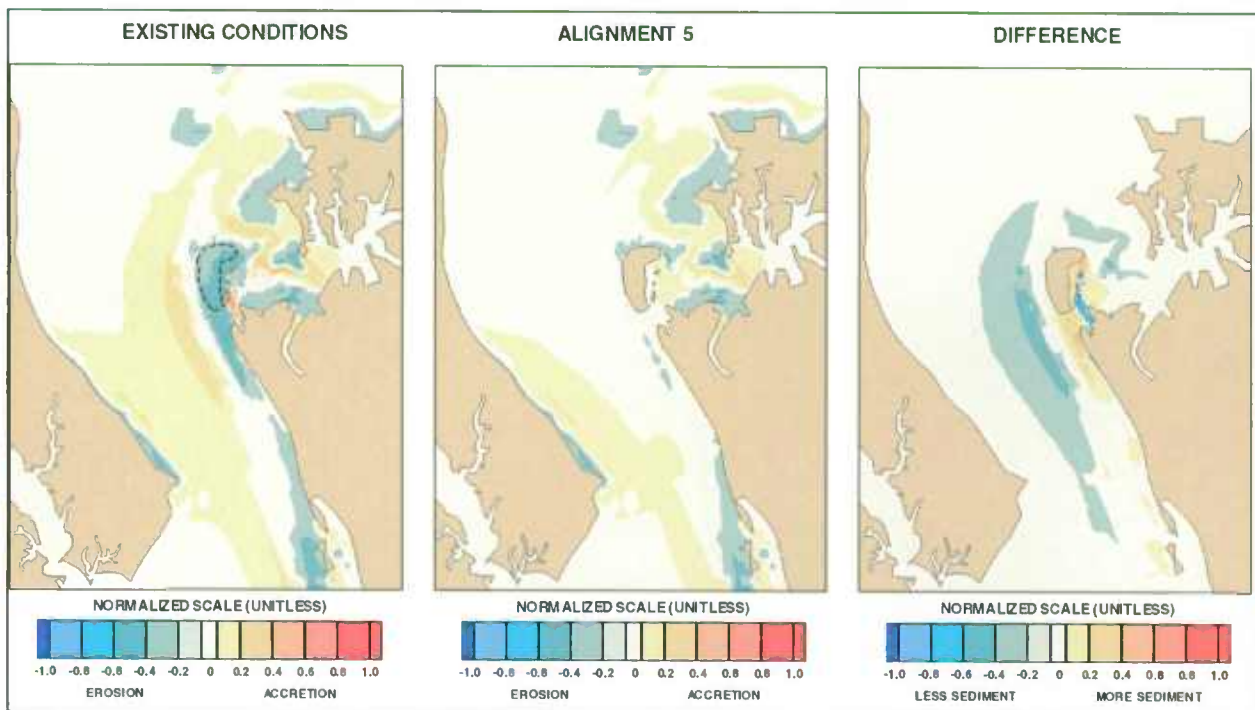
Figure 7-28: Cohesive Sediment – North-Northwest Wind 13 mph Alignment 5 vs. Existing Conditions
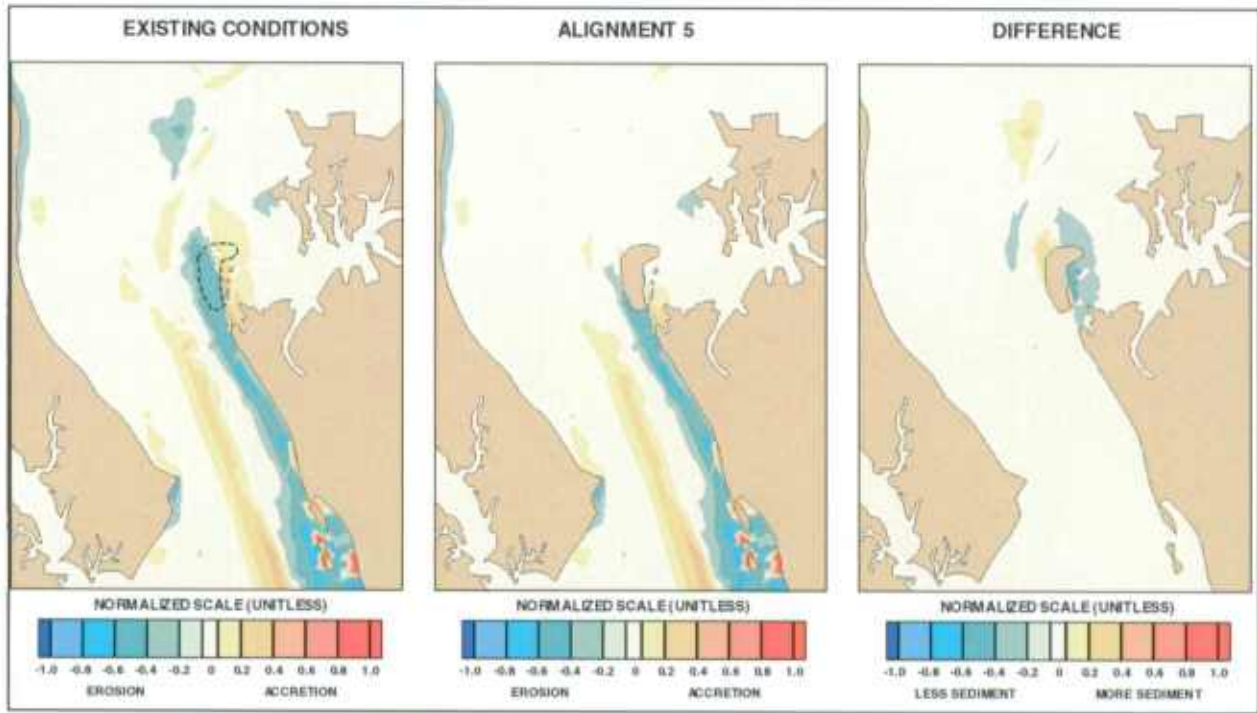
Figure 7-29: Cohesive Sediment – South-Southeast Wind 13 mph – Alignment 5 vs. Existing Conditions
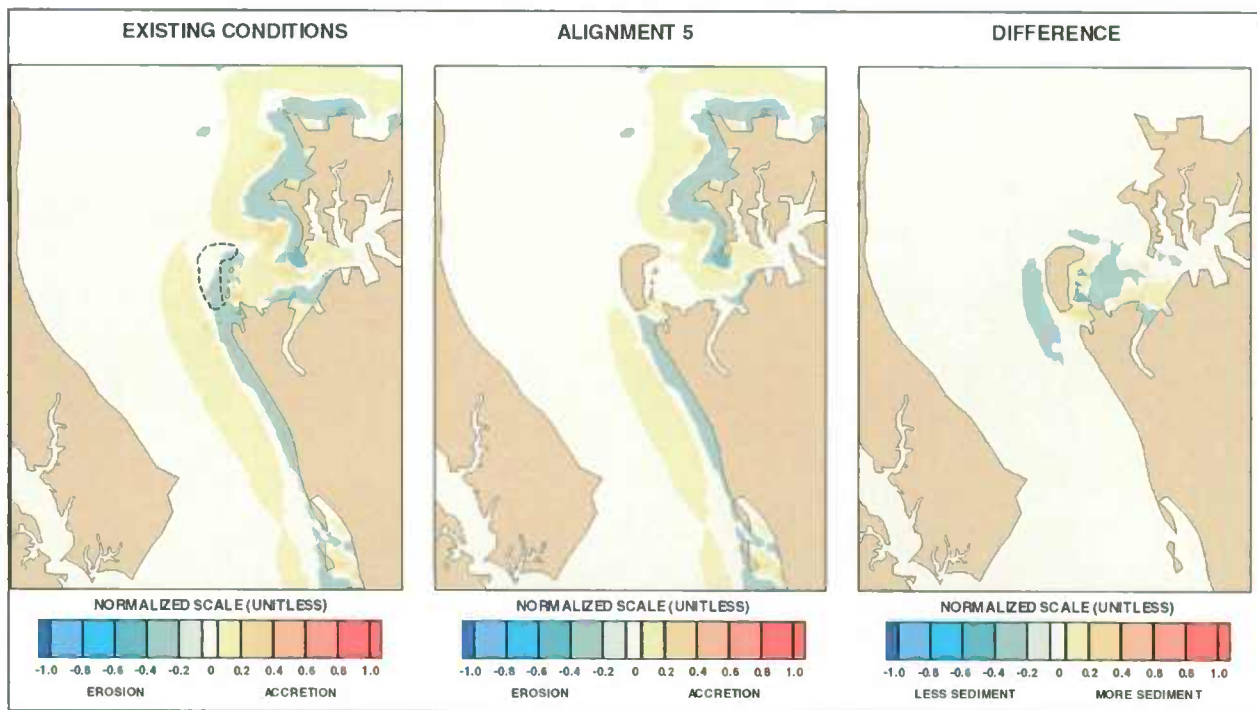
Figure 7-30: Cohesive Sediment – West-Northwest Wind 13 mph – Alignment 5 vs. Existing Conditions

8.   CONCLUSIONS AND RECOMMENDATIONS

8.1   CONCLUSIONS

Results of the Hydrodynamics and Sedimentation Numerical Modeling for the James Island Reconnaissance Study show that the restoration of the island would possibly impact local conditions, especially in the area east and south of the island, and negligible impacts in the far field. The primary impacts on local conditions include substantial reduction of shoreline erosion along James Island and portions of Taylors Island and improved water quality within the region due to creation of a quiescent area east of the project.

Current velocities around the north of James Island increase on the order of 0.1 to 0.2 ft/sec, current velocities east of the project decrease by 0.4 to 0.5 ft/sec, and current velocities south of the project increase by about 0.4 to 0.5 ft/sec. Negligible changes are seen in water surface elevations.

Potential changes in tidal current velocities, coupled with wind induced wave conditions, could cause changes in sedimentation patterns and rates. Non-cohesive sands exhibit reductions in both erosion and accretion rates following island creation. Cohesive clays have decreased sedimentation and decreased sediment movement east of James Island.

Note that reasonable assumptions, as regards input parameters, were made to perform this sedimentation modeling study. Because environmental conditions are constantly changing, the computed sedimentation rate will likely vary as new equilibrium conditions are reached. With this in mind, the results indicate that there will be localized changes in current velocities and sedimentation rates and patterns.

8.2   RECOMMENDATIONS

The following recommendations are made to achieve stated objectives if further evaluation and monitoring of the project area is considered.

Further numerical modeling performed using three-dimensional models would more accurately

---

MOFFATT & NICHOL
E N G I N E E R S

represent hydrodynamics and sedimentation in the Chesapeake Bay. A three-dimensional model would be used to simulate vertical stratification of currents and sediments due to winds and salt wedge effects. Using a three-dimensional model would allow evaluation of impacts to water quality and constituent resident times.

Additional measured data would be recommended to improve the model calibration for any further modeling studies that are considered. Data needs would include bathymetric survey, current velocity measurements, water surface elevations, and suspended sediment measurements. Water surface elevations, current velocity and sediment collection devices installed simultaneously in various locations throughout the bay and project area, and left in place for a minimum period of one month would serve to verify the model calibration. Water surface elevation and current velocities would be used to refine the hydrodynamic model; thickness of sediment and suspended sediment would be used to refine the sedimentation model.

Results obtained from the refined model could be used to examine environmental impacts including water quality as well as to optimize island alignments including fixed jetties and breakwaters.

9.   REFERENCES

Ariathurai, R.   1974.   A Finite Element Model for Sediment Transport in Estuaries, Ph. D. Thesis, Department of Civil Engineering, University of California, Davis.

Ariathurai R., MacArthur, R.C., and Krone, R.B.   1977.   Mathematical Model of Estuarial Sediment Transport, Technical Report D-77-12, US Army Engineer Waterways Experiment station (WES) Vicksburg, MS.

Brigham Young University (BYU).   1995.   FastTABS 3.1 Hydrodynamic Modeling Software. Engineering Computer Graphics Laboratory.

Earth Consultation Construction Remediation, Inc.   2002.   Final Geotechnical Repot for Preliminary Feasibility Study, James Island, Chesapeake Bay, Maryland.

Maryland Geological Survey (MGS). 1952 through 1999. Aerial Photographs.

Moffatt & Nichol Engineers. (M&N). 2000. Upper Chesapeake Bay – Finite Element Model Report.

National Climatic Data Center (NCDC).   1994.   U.S. Department of Commerce, National Oceanic and Atmospheric Administration (NOAA). Historical Fastest Mile Winds for Baltimore, Maryland. Asheville NC.

Nation Ocean Service (NOS). 1982. U.S. Department of Commerce, National Oceanic and Atmospheric Administration (NOAA). Historic Extreme Winds for the United States – Atlantic and Gulf of Mexico Coastline. Rockville, MD.

National Ocean Service (NOS). 1988. U.S. Department of Commerce, National Oceanic and Atmospheric Administration (NOAA). Tide and Tidal Currents in the Chesapeake Bay. Rockville, MD.

National Ocean Service (NOS). 1993. U.S. Department of Commerce, National Oceanic and Atmospheric Administration (NOAA). Chart Number 12230.

National Ocean Service (NOS). 1993. U.S. Department of Commerce, National Oceanic and Atmospheric Administration (NOAA). Chart Number 12263.

National Ocean Service (NOS). 1993. U.S. Department of Commerce, National Oceanic and Atmospheric Administration (NOAA). Chart Number 12264.

National Ocean Service (NOS). 1993. U.S. Department of Commerce, National Oceanic and Atmospheric Administration (NOAA). Chart Number 12266.

National Ocean Service (NOS). 1993. U.S. Department of Commerce, National Oceanic and Atmospheric Administration (NOAA). Chart Number 12268.

National Ocean Service (NOS). 1993. U.S. Department of Commerce, National Oceanic and Atmospheric Administration (NOAA). Chart Number 12270.

National Ocean Service (NOS). 1993. U.S. Department of Commerce, National Oceanic and Atmospheric Administration (NOAA). Chart Number 12272.

National Ocean Service (NOS). 1993. U.S. Department of Commerce, National Oceanic and Atmospheric Administration (NOAA). Chart Number 12273.

National Ocean Service (NOS). 1993. U.S. Department of Commerce, National Oceanic and Atmospheric Administration (NOAA). Chart Number 12274.

National Ocean Service (NOS). 1993. U.S. Department of Commerce, National Oceanic and Atmospheric Administration (NOAA). Chart Number 12278.

National Ocean Service (NOS). 1996. U.S. Department of Commerce, National Oceanic and Atmospheric Administration (NOAA). Tidal Currents 1996. Rockville, MD.

National Ocean Service (NOS). 1997. U.S. Department of Commerce, National Oceanic and Atmospheric Administration (NOAA). Tide Datums for Selected Stations.

National Ocean Service (NOS). 2000. U.S. Department of Commerce, National Oceanic and Atmospheric Administration (NOAA). Web Site: http://mapfinder.nos.noaa.gov/. Digital Elevation Models (DEMs).

Partheniades, E., 1962. *"A study of erosion and deposition of cohesive soils in salt water"*, Thesis presented to the University of California at Berkley in partial fulfillment for the degree of Doctor of Philosophy.

Schubel, J.R. and D.W. Pritchard, 1987. A brief physical description of the Chesapeake Bay, in Contaminant problems and management of living Chesapeake Bay resources, edited by S. K. Majumdar, L.W. Hall, Jr., and H. M. Austin, 1-32, Pa Acad. Sci., Philadelphia, PA.

Swart, D.H. 1976. Coastal Sediment Transport, Computation of Longshore Transport, R968, Part I, Delft Hydraulics Laboratory, The Netherlands.

Thomas, W.A., W.H. McAnally, Jr. and S.A. Adamec, Jr. 1985. A User's Manual for the Generalized Computer Program, Sediment Transport in Unsteady, 2-Dimensional Flow, Horizontal Plane (STUDH).

U.S. Army Corps of Engineers (USACE), Waterways Experiment Station (WES), Coastal Engineering Research Center (CERC). 1984. Shore Protection Manual, Volumes I and II. Fourth Edition. U.S. Government Printing Office.

U.S. Department of Agriculture (USDA), Soil Conservation Service (SCS). 1973. Soil Survey of Prince Georges County, Maryland.

U.S. Geological Survey (USGS). 2000. Web Site: http://md.water.usgs.gov/historical.html

White, W.R., Milli, H., and Crabbe, A.D. 1975. Sediment Transport Theories: An Appraisal of Available Methods. Report Int. 119 (Vols. 1 and 2), Hydraulics Research Station, Wallingford, England.

Winterwerp, Han. On the dynamics of high-concentrated mud suspensions. Delft: Delft University of Technology, Faculty of Civil Engineering and Geosciences, 1999; 1 v. (Communications on hydraulic and geotechnical engineering; rept. no. 99-3). G642 X no.99-3

10. GLOSSARY OF TECHNICAL TERMS

ACCRETION. The natural or artificial buildup of land by deposition of waterborne or airborne material or by an act of man, such as the construction of a **GROIN, BREAKWATER**, or mechanical beach fill.

ASTRONOMICAL TIDE. The tidal levels and character which would result from gravitational effects due to the Earth, Sun, and Moon, without atmospheric influences.

BAR. A submerged or emerged embankment of sand, gravel, or other unconsolidated material built on the sea floor in shallow water by waves and currents.

BATHMETRIC CHART. A topographic map of the bed of the ocean, with depths indicated by contours (isobaths) drawn at regular intervals.

BATHYMETRY. The measurement of depths of water in oceans, seas, and lakes; also information derived from such measurements.

BAY. A recess in the shore or an inlet of a sea between two capes or headlands, not so large as a gulf but larger than a cove. See also **EMBAYMENT**.

BED LOAD. Sediment transport mode in which individual particles either roll or slide along the bed as a shallow, mobile layer a few particle diameters deep; the part of the load that is not continuously in suspension.

BED SHEAR STRESS. The transfer of energy to the sea bed from waves and currents.

BENCH MARK, TIDAL. A bench mark whose elevation has been determined with respect to **MEAN SEA LEVEL** at a nearby tide gauge; the tidal bench mark is used as reference for that tide gauge.

BOUNDARY CONDITIONS. Environmental conditions such as waves, currents, water surface elevations, etc. used as boundary input to physical or numerical models

---

MOFFATT & NICHOL ENGINEERS

BREAKWATER. A structure protecting a shore area, harbor, anchorage, or basin from waves.

CAUSEWAY. A raised road across wet or marshy ground, or across water.

CLAY. A fine grained, plastic, sediment with a typical grain size less than 0.004 mm. Possesses electromagnetic properties which bind the grains together to give a bulk strength or cohesion.

CORRELATION. The state or relation of being correlated; specifically: a relation existing between phenomena or things or between mathematical or statistical variables which tend to vary, be associated, or occur together in a way not expected on the basis of chance alone; a number or function that indicates the degree of correlation between two sets of data or between two random variables and that is equal to their covariance divided by the product of their standard deviations

CO-TIDAL LINES. Lines which link all the points where the tide is at the same stage (or **PHASE**) of its cycle.

COHESIVE SEDIMENT. Sediment containing a significant proportion of clays, the electromagnetic properties of which cause the sediment to bind together

CONSOLIDATION. The gradual, slow compression of a cohesive soil due to weight acting on it, which occurs as water is driven out of the voids in the soil. Consolidation only occurs in clays or other soils of low permeability.

CORIOLIS EFFECT. Force due to the Earth's rotation, capable of generating currents. It causes moving bodies to be deflected to the right in the Northern Hemisphere and to the left in the Southern Hemisphere. The "force" is proportional to the speed and latitude of the moving object. It is zero at the equator and maximum at the poles.

CURRENT. The flowing of water, or other liquid or gas or that portion of a stream of water which is moving with a velocity much greater than the average or in which the progress of the water is principally concentrated. Ocean currents can be classified in a number of different ways. Some important types include the following: (1) Periodic - due to the effect of the tides. Such Currents may be rotating rather than having a simple back and

forth motion.   The currents accompanying tides are known as tidal currents;   (2) Temporary - due to seasonal winds. (3) Permanent or ocean - constitute a part of the general ocean circulation. (4) Nearshore - caused principally by waves breaking along a shore.

CURRENT, EBB.   The tidal current away from shore or down a tidal stream.   Usually associated with the decrease in the height of the tide.

CURRENT, FLOOD.   The tidal current toward shore or up a tidal stream. Usually associated with the increase in the height of the tide.

CURRENT, TIDAL.   The alternating horizontal movement of water associated with the rise and fall of the tide caused by the astronomical tide-producing forces.   See also **CURRENT, FLOOD** and **CURRENT, EBB**.

DATUM. Any permanent line, plane or surface used as a reference datum to which elevations are referred.

DATUM, PLANE.   The horizontal plane to which soundings, ground elevations, or water surface elevations are referred. The plane is called a **TIDAL DATUM** when defined by a certain phase of the tide.   The following **TIDAL DATUMS** are ordinarily used on hydrographic charts:

   MEAN LOW WATER - Atlantic coast (U. S.), Argentina, Sweden, and Norway.

   MEAN LOWER LOW WATER - Pacific coast (U. S.).

   MEAN LOW WATER SPRINGS -United Kingdom, Germany, Italy, Brazil, and Chile.

   LOW WATER DATUM -Great Lakes (U. S. and Canada).

   LOWEST LOW WATER SPRINGS -Portugal.

   LOW WATER INDIAN SPRINGS-India and Japan (See **INDIAN TIDE PLANE**).

> LOWEST LOW WATER - France, Spain, and Greece.

> A common datum used on United States topographic maps is **MEAN SEA LEVEL**. See also **BENCH MARK, TIDAL**.

DEPTH. The vertical distance from a specified datum to the sea floor.

DESIGN STORM. A hypothetical extreme storm whose waves are used to design coastal protection structures. The severity of the storm (i.e. return period) is chosen in view of the acceptable level of risk of damage or failure. A design storm consists of a **DESIGN WAVE** condition, a design water level and a **DURATION**.

DESIGN WAVE. In the design of **HARBORS**, harbor works, etc., the type or types of waves selected as having the characteristics against which protection is desired.

DIFFRACTION (of water waves). The phenomenon by which energy is transmitted laterally along a wave crest. When a part of a train of waves is interrupted by a barrier, such as a **BREAKWATER**, the effect of diffraction is manifested by propagation of waves into the sheltered region within the barrier's **GEOMETRIC SHADOW**.

DIURNAL. Having a period or cycle of approximately one **TIDAL DAY**.

DIURNAL INEQUALITY. The difference in height of the two high waters or of the two low waters of each **TIDAL DAY**. Also, the difference in velocity between the two daily flood or **EBB CURRENTS** of each day.

DIURNAL TIDE. A tide with one high water and one low water in a **TIDAL DAY**.

DRAINAGE BASIN. The area drained by a stream or river and its tributaries.

DREDGING. Excavation or displacement of the bottom or shoreline of a water body with mechanical or hydraulic machines. Done to maintain channel depths or berths for navigational purposes, for shellfish harvesting, for cleanup of polluted sediments, and as a source for placement of sand on beaches.

DURATION. In wave forecasting, the length of time the wind blows in nearly the same

direction over the **FETCH**.

DYNAMIC EQUILIBRIUM. Short term morphological changes that do not affect the morphology over a long period.

EBB. Period when tide level is falling; often taken to mean the ebb current which occurs during this period.

EBB CURRENT. The movement of a tidal current away from shore or down a tidal stream. The terms of maximum ebb and minimum ebb are applied to the maximum and minimum velocities of a continuously running ebb current, the velocity alternately increasing and decreasing without coming to a slack or reversing. The expression maximum ebb is also applicable to any ebb current at the time of greatest velocity.

EBB TIDE. The period of tide between high water and the succeeding low water; a falling tide.

EMBAYMENT. An indentation in the shoreline forming an open bay.

EROSION. The wearing away of land by the action of natural forces. On a beach, the carrying away of beach material by wave action, tidal currents, littoral currents, or by deflation.

ESTUARY. (1) The part of a river that is affected by tides. (2) The region near a river mouth in which the fresh water of the river mixes with the salt water of the sea and which received both fluvial and littoral sediment influx.

FETCH LENGTH. The horizontal distance (in the direction of the wind) over which a wind generates **SEAS** or creates a **WIND SETUP**.

FETCH-LIMITED. Situation in which wave energy (or wave height) is limited by the size of the wave generation area (fetch).

FLOOD. (1) Period when tide level is rising; often taken to mean the flood current which occurs during this period (2) A flow beyond the carrying capacity of a channel.

FLOOD CURRENT. The movement of a tidal current toward the shore or up a tidal stream. The terms maximum flood and minimum flood are applied to the maximum and

minimum velocities of a flood current the velocity of which alternately increases and decreases without coming to slack or reversing. The expression maximum flood is also applicable to any flood current at the time of greatest velocity.

FLOOD TIDE. The period of tide between low water and the succeeding high water; a rising tide.

FLUSHING TIME. The time required to replace all the water in an **ESTUARY, HARBOR**, etc., by action of current and tide.

GROIN (British, GROYNE). Narrow, roughly shore-normal structure, built to reduce longshore currents, and/or to trap and retain littoral material. Most groins are of timber or rock. See also **T-GROIN**.

FULLY-DEVELOPED SEA. The waves that form when wind blows for a sufficient period of time across the open ocean. The waves of a fully developed sea have the maximum height possible for a given wind speed, **FETCH** and duration of wind.

GAUGE (GAGE). Instrument for measuring the water level relative to a datum.

GEOMETRIC SHADOW. In wave diffraction theory, the area outlined by drawing straight lines paralleling the direction of wave approach through the extremities of a protective structure. It differs from the actual protected area to the extent that the diffraction and refraction effects modify the wave pattern.

HINDCASTING. In wave prediction, the retrospective forecasting of waves using measured wind information.

HISTORIC EVENT ANALYSIS. Extreme analysis based on hindcasting typically ten events over a period of 100 years.

KNOT. The unit of speed used in navigation equal to 1 nautical mile (6,076.115 ft or 1,852 m) per hour.

LEE. (1) Shelter, or the part or side sheltered or turned away from the wind or waves. (2)

(Chiefly nautical) The quarter or region toward which the wind blows.

LUNAR DAY. See **TIDAL DAY**.

MEAN HIGH WATER (MHW). The average height of the high waters over a 19-year period. For shorter periods of observations, corrections are applied to eliminate known variations and reduce the results to the equivalent of a mean 19-year value. All high water heights are included in the average where the type of tide is either semidiurnal or mixed. Only the higher high water heights are included in the average where the type of tide is diurnal. So determined, mean high water in the latter case is the same as mean higher high water.

MEAN HIGHER HIGH WATER (MHHW). The average height of the higher high waters over a 19-year period. For shorter periods of observation, corrections are applied to eliminate known variations and reduce the result to the equivalent of a mean 19-year value.

MEAN LOW WATER (MLW). The average height of the low waters over a 19-year period. For shorter periods of observations, corrections are applied to eliminate known variations and reduce the results to the equivalent of a mean 19-year value. All low water heights are included in the average where the type of tide is either semidiurnal or mixed. Only lower low water heights are included in the average where the type of tide is diurnal. So determined, mean low water in the latter case is the same as mean lower low water.

MEAN LOWER LOW WATER (MLLW). The average height of the lower low waters over a 19-year period. For shorter periods of observations, corrections are applied to eliminate known variations and reduce the results to the equivalent of a mean 19-year value. Frequently abbreviated to **LOWER LOW WATER**.

MEAN RANGE OF TIDE. The difference in height between **MEAN HIGH WATER** and **MEAN LOW WATER**.

MEAN SEA LEVEL. The average height of the surface of the sea for all stages of the tide over a 19-year period, usually determined from hourly height readings. Not necessarily equal to **MEAN TIDE LEVEL**.

MEAN TIDE LEVEL. A plane midway between **MEAN HIGH WATER** and **MEAN LOW WATER**. Not necessarily equal to **MEAN SEA LEVEL**.

NAUTICAL MILE. The length of a minute of arc, 1/21,600 of an average great circle of the Earth. Generally one minute of latitude is considered equal to one nautical mile. The accepted United States value as of 1 July 1959 is 1,852 meters (6,076.115 feet), approximately 1.15 times as long as the U.S. statute mile of 5,280 feet.

NUMERICAL MODELING. Refers to analysis of coastal processes using computational models.

PEAK PERIOD. The wave period determined by the inverse of the frequency at which the wave energy spectrum reaches its maximum.

PHASE. In surface wave motion, a point in the period to which the wave motion has advanced with respect to a given initial reference point.

SAND. Sediment particles, often largely composed of quartz, with a diameter of between 0.062 mm and 2 mm, generally classified as fine, medium, coarse or very coarse. Beach sand may sometimes be composed of organic sediments such as calcareous reef debris or shell fragments.

SCOUR. Removal of underwater material by waves and currents, especially at the base or toe of a shore structure.

SEA GRASS. Members of marine seed plants that grow chiefly on sand or sand-mud bottom. They are most abundant in water less than 9m deep. Some common types are: Eel grass (Zostera), Turtle grass (Thallasia), and Manatee grass (Syringodium).

SEA LEVEL RISE. The long-term trend in **MEAN SEA LEVEL**.

SEAS. Waves caused by wind at the place and time of observation.

SEDIMENT. (1) Loose, fragments of rocks, minerals or organic material which are transported from their source for varying distances and deposited by air, wind, ice and water. Other

sediments are precipitated from the overlying water or form chemically, in place. Sediment includes all the unconsolidated materials on the sea floor. (2) The fine grained material deposited by water or wind.

SEDIMENT TRANSPORT. The main agencies by which sedimentary materials are moved are: gravity (gravity transport); running water (rivers and streams); ice (glaciers); wind; the sea (currents). Running water and wind are the most widespread transporting agents.

SEMIDIURNAL. Having a period or cycle of approximately one-half of a tidal day (12.4 hours). The predominating type of tide throughout the world is semidiurnal, with two high waters and two low waters each tidal day. The tidal current is said to be semidiurnal when there are two flood and two ebb periods each day.

SIGNIFICANT WAVE. A statistical term relating to the one-third highest waves of a given wave group and defined by the average of their heights and periods. The composition of the higher waves depends upon the extent to which the lower waves are considered. Experience indicates that a careful observer who attempts to establish the character of the higher waves will record values which approximately fit the definition of the significant wave.

SIGNIFICANT WAVE HEIGHT. The average height of the one-third highest waves of a given wave group. Note that the composition of the highest waves depends upon the extent to which the lower waves are considered. In wave record analysis, the average height of the highest one-third of a selected number of waves, this number being determined by dividing the time of record by the significant period.

SILT. Sediment particles with a grain size between 0.004 mm and 0.062 mm, i.e. coarser than clay particles but finer than sand.

SPECTRAL PEAK PERIOD. PEAK PERIOD of the wave energy spectrum.

SUSPENDED LOAD. The material moving in suspension in a fluid, kept up by the upward components of the turbulent currents or by colloidal suspension.

TIDAL DAY. The time of the rotation of the Earth with respect to the Moon, or the interval

between two successive upper transits of the Moon over the meridian of a place, approximately 24.84 solar hours (24 hours and 50 minutes) or 1.035 times the mean solar day. Also called **LUNAR DAY**.

TIDAL RANGE. The difference in height between consecutive high and low (or higher high and lower low) waters.

TIDE. The periodic rising and falling of the water that results from gravitational attraction of the Moon and Sun and other astronomical bodies acting upon the rotating Earth. Although the accompanying horizontal movement of the water resulting from the same cause is also sometimes called the tide, it is preferable to designate the latter as **TIDAL CURRENT**, reserving the name **TIDE** for the vertical movement.

VISCOSITY (or internal friction). That molecular property of a fluid that enables it to support tangential stresses for a finite time and thus to resist deformation. Resistance to flow.

WAVE HEIGHT. The vertical distance between a crest and the preceding trough. See also **SIGNIFICANT WAVE HEIGHT**.

WAVE PERIOD. The time for a wave crest to traverse a distance equal to one wavelength. The time for two successive wave crests to pass a fixed point.

WIND WAVES. (1) Waves being formed and built up by the wind. (2) Loosely, any wave generated by wind.